KENNELLY, TERESA

A STUDY OF THE PHOTOINDUCED REDOX CHEMISTRY OF TRIS (2,2' - BIPYRIDINE) RUTHENIUM (II) IN: (I) AN EDTA / PARAQUAT SOLAR ENERGY CONVERSION SYSTEM AND (II) A POROUS GLASS MATRIX

City University of New York PH.D. 1980

A STUDY OF THE PHOTOINDUCED REDOX CHEMISTRY OF TRIS (2,2' - BIPYRIDINE) RUTHENIUM (II) IN: (I) AN EDTA / PARAQUAT SOLAR ENERGY CONVERSION SYSTEM AND (II) A POROUS GLASS MATRIX

by

TERESA KENNELLY

A dissertation submitted to the Graduate Faculty in Chemistry in partial fulfillment of the requirements for the degree of Doctor of Philosophy, the City University of New York.

1980

This manuscript has been read and accepted for the Graduate Faculty in Chemistry in satisfaction of the dissertation requirement for the degree of Doctor of Philosophy.

May 19 1980
date

Henry D. Gafney
Chairman of Examining Committee

May 19, 1980
date

David C. Lorde
Executive Officer

Henry D Gafney
Arthur D Baker
Supervisory Committee

The City University of New York

Abstract

A STUDY OF THE PHOTOINDUCED REDOX CHEMISTRY OF TRIS (2,2' - BIPYRIDINE) RUTHENIUM (II) IN : (I) AN EDTA / PARAQUAT SOLAR ENERGY CONVERSION SYSTEM AND (II) A POROUS GLASS MATRIX

by

Teresa Kennelly

Adviser: Professor Harry D. Gafney

Transition metal complexes which are capable of mediating the photolysis of water are currently under investigation. The complex tris (2,2' - bipyridine) ruthenium (II) $^{2+}$, $Ru(bpy)_3^{2+}$, has been the subject of intense study. It absorbs strongly in the visible region to form an excited state, 2.1 eV above its ground state, which has sufficient potential to oxidize and reduce water. Despite this strong driving force, however, photolysis of aqueous solutions of $Ru(bpy)_3^{2+}$ does not lead to the photodissociation of water. Redox quenching of the excited state by electron carriers, which oxidize or reduce water in the presence of

catalyst, should lead to the storage of some of the absorbed energy. A rapid back reaction of the energy rich products, however, generally prevents any net chemical change. In one photoreduction system, modification of the reactants by ion pairing the photoactive $Ru(bpy)_3^{2+}$ with an electron donor, $EDTA^{2-}$, prevented the energy-wasting back reaction. The primary photoproduct $Ru(bpy)_3^{3+}$ was reduced by $EDTA^{2-}$, and the reduced electron carrier $Pq^{+\cdot}$, paraquat radical cation, reduced water to H_2 in the presence of Pt. A quantum yield of 0.05 was measured for the formation of $Pq^{+\cdot}$.

The postulated ion pairing mechanism suggests that organization of the reactants makes the forward reaction competitive with the energy dissipating back reaction. In photosynthesis, organization of reactants in the heterogeneous environment of the chloroplast promotes the storage of radiant energy as chemical potential energy.

The $Ru(bpy)_3^{2+}$ / Pq^{2+} / EDTA reaction system was adsorbed into a glass matrix to determine if non-homogeneity would improve the efficiency of the photoreduction of water. Preliminary experiments indicated that the photochemistry of $Ru(bpy)_3^{2+}$ in the glass matrix was different than that observed in solution, and a more detailed study of the photoredox chemistry of this complex

in the glass was undertaken.

Photolysis of $Ru(bpy)_3^{2+}$ adsorbed onto porous glass induced spectral changes which were identical to those previously reported for intense flash photolysis of aqueous solutions and photolysis of micellar solutions with high $Ru(bpy)_3^{2+}$ / micelle ratios. The striking difference was that the lifetime of the photoproduct was increased from 5 seconds in fluid media to $\geq$91 days in the glass.

Lifetime measurements of the complex in the glass showed an enhancement of the radiative decay of $*Ru(bpy)_3^{2+}$ comparable to that observed in micelles. At moderate concentrations, a two component decay was observed. A fast non-exponential decay (60 nsec) was followed by an exponential decay of 680$\pm$20 nsec that was comparable to that observed in homogeneous solution. At higher concentrations, approaching the adsorption limit of the glass, only the fast decay was observed. This concentration dependence suggested that a direct disproportionation reaction was competing with

$$2*Ru(bpy)_3^{2+} \longrightarrow Ru(bpy)_3^{+} + Ru(bpy)_3^{3+}$$

the unimolecular decay pathways.

The stoichiometry of the reaction in the glass, calculated from the increase in absorbance at 510 nm and

the decrease in absorbance at 452 nm, gave a value of 0.48 ± 0.05 for the ratio of the formation of $Ru(bpy)_3^+$ to the disappearance of $Ru(bpy)_3^{2+}$ compared to the theoretical value of 0.5. ESR spectra of photolyzed glasses detected the formation of radical species which increased in proportion to the 510 nm absorbance. While formation of $Ru(bpy)_3^+$ in fluid media proceeds via an e_{aq}^- intermediate, electron scavenging experiments ruled out this mechanism in the glass. These data are in good agreement with a direct disproportionation reaction.

The disproportionation products, $Ru(bpy)_3^+$ and $Ru(bpy)_3^{3+}$, unlike the excited state, $*Ru(bpy)_3^{2+}$, react with water. Photodissociation of water via the photolysis of $Ru(bpy)_3^{2+}$ adsorbed onto the glass may be a viable conversion system. Unlike the reaction schemes in homogeneous solution, no electron donor is consumed and a truly catalytic cycle may be developed. A limiting value of 2×10^{-3} was measured for the formation of $Ru(bpy)_3^+$.

ACKNOWLEDGEMENTS

I would like to express my appreciation to my research director Dr. Harry D. Gafney for his assistance in the preparation of this thesis.

I would also like to thank the other members of the department who offered their assistance. Discussions with Dr. A. Dave Baker were helpful and so were the many times he and Dr. William Berkowitz repaired the vacuum line. Thanks to Dr. Thomas Strekas for his assistance and for the free access he granted to his instruments. To Mr. Thomas Hayden, thank-you for your generous assistance.

To my husband and best friend Tom, thanks for loving me.

TABLE OF CONTENTS

LIST OF TABLES

LIST OF FIGURES

CHAPTER 1

Introduction

A strong interest in solar energy conversion systems has developed in recent years as the search for alternative energy sources has expanded. Many areas of research are being persued and one challenging possibility is the application of the excited state chemistry of transition metal complexes to the conversion of radiant energy into chemical potential energy.

Effective conversion of solar energy first requires that a system absorb light in the range of solar emission. On absorption of the radiant energy, the system must be able to undergo an endothermic reaction with a high yield. The products of this reaction should be separable and stable enough for storage. The energy releasing back reaction should occur under controlled conditions with regeneration of the starting materials. Photolysis of water to H_2 and O_2 is seen by many as an ideal solution to the world's energy problems. The starting material is widely available and the products are non-polluting and stable. Water, however, does not absorb solar radiation which is sufficiently energetic to promote electron excitation. To develop a system capable of photocatalyzing the splitting of water, it is necessary to use photosensitizers with

absorption spectra that overlap the emission spectrum of the sun (1,2). Transition metal cations and complexes meet this requirement and their use in the mediated photolysis of water has been studied extensively.

There are two basic mechanisms for the photodissociation of water (3). The high energy monoelectronic oxidation and reduction (equations 1-3) requires light of wavelengths shorter than 250 nm. Consequently, less than 1% of solar energy can be stored by this process (2).

$$H^+ + e^- \longrightarrow H\cdot \qquad E = -2.5\ V\ (pH=7) \quad (1)$$

$$H_2O \longrightarrow {}^{\cdot}OH + H^+ + e^- \qquad E = +2.5\ V \quad (2)$$

$$H_2O \longrightarrow H\cdot + {}^{\cdot}OH \qquad G = 5V \quad (3)$$

In addition to the high energy requirements of this mechanism, the radical products are unstable and poor candidates for storage and transport. Wavelengths up to 1000 nm are theoretically sufficiently energetic for the tetraelectronic process (4) (equation 4-6).

$$2H^+ + 2e^- \longrightarrow H_2 \qquad E = -0.41\ V\ (pH=7) \quad (4)$$

$$2H_2O \longrightarrow O_2 + 4H^+ + 4e^- \qquad E = +0.82\ V \quad (5)$$

$$H_2O \longrightarrow H_2 + \tfrac{1}{2}O_2 \qquad G = 1.23\ V \quad (6)$$

Many reaction schemes involving transition metals as catalysts have been proposed for the photodissociation of water. These can be grouped into the

three major research areas outlined by Balzani which are summarized below (2) (See Schemes 1-3):

1. Simple Systems

   a and b). Water is oxidized or reduced by the catalyst producing •OH or •H radicals. Regeneration of the catalyst by reaction with water completes the cycle with the formation of molecular hydrogen or oxygen respectively.

   c). H_2 and catalyst oxide are produced in the reduction of water. This is followed by the decomposition of the oxide to catalyst and O_2.

2. Binuclear Complexes

   Molecular hydrogen, oxygen or hydrogen peroxide are photochemically released from a binuclear complex. The complex, which must remain intact, reacts with water to regenerate the catalytic form and produce molecular oxygen or hydrogen.

3. Hydrido Complexes

   a). A metal hydrido complex loses H_2 on photolysis. Reaction of the complex with water regenerates the catalyst and forms O_2.

   b). The photo-catalyzed protonation of a complex produces a mono-hydrido species which undergoes dimerization and releases H_2. The metal-metal bonded dimer reacts with water to reform the monomer and produce O_2.

Reactions in groups 1a and b require high energy photons and have very low quantum yields. The low efficiency of these reactions has been attributed to the recombination of the highly reactive •H and •OH radicals with the sensitizer (2). A look at the energetics of a photoredox reagent will illustrate this problem, which is common in solar energy conversion systems and all excited state electron transfer reactions (5).

Scheme 1: Simple Cycles

a). $Cat + H_2O \longrightarrow Cat^+ + {}^\bullet H + OH^-$

$Cat^+ + \frac{1}{2}H_2O \longrightarrow Cat + H^+ + \frac{1}{4}O_2$

$\frac{1}{2}H_2O \longrightarrow {}^\bullet H + \frac{1}{4}O_2$

b). $Cat + H_2O \longrightarrow Cat^- + H^+ + {}^\bullet OH$

$Cat^- + H_2O \longrightarrow Cat + OH^- + \frac{1}{2}H_2$

$H_2O \longrightarrow \frac{1}{2}H_2 + {}^\bullet OH$

c). $Cat + H_2O \longrightarrow [Cat\text{-}O] + H_2$

$[Cat\text{-}O] \longrightarrow Cat + \frac{1}{2}O_2$

$H_2O \longrightarrow H_2 + \frac{1}{2}O_2$

Scheme 2: Binuclear Complexes

a). $[Cat\text{-}O_2]_{ox} \longrightarrow [Cat]_{red} + O_2$

$[Cat]_{red} + 2H_2O \longrightarrow [Cat\text{-}O_2]_{ox} + 2H_2$

$2H_2O \longrightarrow 2H_2 + O_2$

b). $[Cat\text{-}(OH)_2]_{ox} \longrightarrow [Cat]_{red} + H_2O_2$

$H_2O_2 \longrightarrow H_2O + \frac{1}{2}O_2$

$[Cat]_{red} + 2H_2O \longrightarrow [Cat\text{-}(OH)_2]_{ox} + H_2$

$H_2O \longrightarrow H_2 + \frac{1}{2}O_2$

c). $[Cat\text{-}H_2]_{red} \longrightarrow [Cat]_{ox} + H_2$

$[Cat]_{ox} + H_2O \longrightarrow [Cat\text{-}H_2]_{red} + \frac{1}{2}O_2$

$H_2O \longrightarrow H_2 + \frac{1}{2}O_2$

Scheme 3: Hydrido Complexes

a). $\underline{cis}\text{-}CatH_2^{z+} \longrightarrow Cat^{z+} + H_2$

$Cat^{z+} + H_2O \longrightarrow Cat^{(z-2)+} + 2H^+ + \frac{1}{2}O_2$

$Cat^{(z-2)+} + 2H^+ \longrightarrow \underline{cis}\text{-}CatH_2^{z+}$

$H_2O \longrightarrow H_2 + \frac{1}{2}O_2$

b). $Cat + H^+ \longrightarrow CatH^+$

$CatH^+ \longrightarrow \frac{1}{2}[Cat]_2^{2+} + \frac{1}{2}H_2$

$\frac{1}{2}[Cat]_2^{2+} + \frac{1}{2}H_2O \longrightarrow Cat + H^+ + \frac{1}{4}O_2$

$\frac{1}{2}H_2O \longrightarrow \frac{1}{2}H_2 + \frac{1}{4}O_2$

Figure 1

Redox Potentials of $Ru(bpy)_3^{2+}$

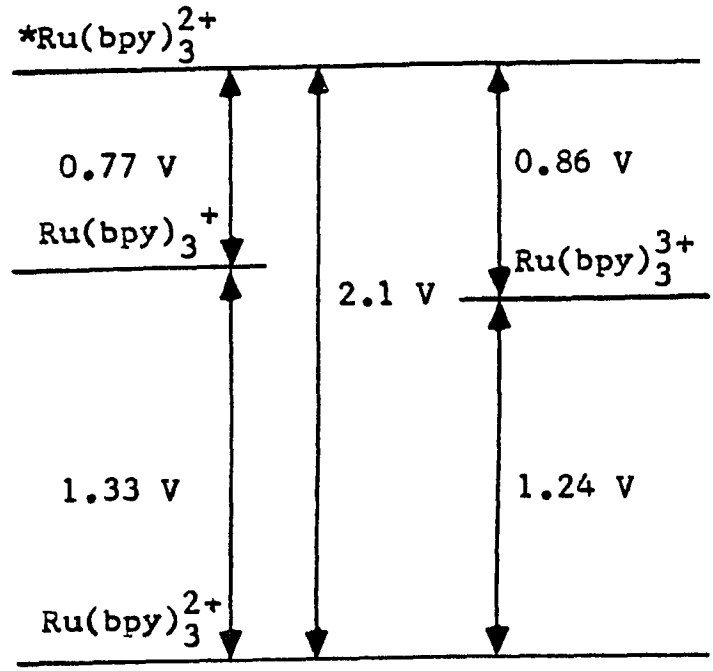

As seen in Figure 1, in the case of tris(2,2'-bipyridine) ruthenium(II)$^{2+}$, $Ru(bpy)_3^{2+}$, light absorption leads to the population of a metal to ligand charge transfer state which is 2.1 eV above the ground state (6,7). Redox quenching of this state (equation 7,8) leads to the formation of $Ru(bpy)_3^{+}$ or $Ru(bpy)_3^{3+}$, still 1.33 eV and 1.24 eV above the ground state.

$$*Ru(bpy)_3^{2+} + Q \longrightarrow Ru(bpy)_3^{+} + Q^{+} \quad (7)$$

$$*Ru(bpy)_3^{2+} + Q \longrightarrow Ru(bpy)_3^{3+} + Q^{-} \quad (8)$$

Unlike the products of thermal reactions, the products of an excited state electron transfer reaction may be stronger oxidizing and reducing agents than the ground state reactants. There is a significant driving force then for these high energy products to react and return to the ground state (equation 9,10) (10).

$$Ru(bpy)_3^{+} + Q^{+} \longrightarrow Ru(bpy)_3^{2+} + Q \quad (9)$$

$$Ru(bpy)_3^{3+} + Q^{-} \longrightarrow Ru(bpy)_3^{2+} + Q \quad (10)$$

Extensive quenching studies have shown that these reactions occur rapidly and with high yields. Flash photolysis techniques have revealed that many systems, previously considered inert, underwent electron transfer reactions which were followed by the rapid recombination of

the products within the lifetime of the quenching encounter complex (6-18). Since energy is harnessed in these systems by isolating the redox products, reaction schemes involving stable products must be developed (5).

The reaction system proposed in 1c does not involve any radical intermediates, but does highlight another serious problem with the development of conversion systems. As seen in equation 4-6, the low energy reduction of water is a multi-electron event. Spectroscopic selection rules, however, demand that an excited state reductant be a one-electron donor. The transfer of two electrons in scheme 1b is therefore forbidden. Mediation of light absorption by transition metal complexes requires that the photolysis of water occurs in a series of one-electron steps. The probability of a reaction such as equation 11 in fluid solution, however, is negligible even though it is energetically possible (19). Using binuclear complexes as photosensitzers may avoid radical formation and increase the probability of a multiple electron transfer event.

$$2^{*}Ru(bpy)_3^{2+} + 2H_2O \longrightarrow 2Ru(bpy)_3^{2+} + H_2 + \tfrac{1}{2}O_2 \quad (11)$$

However, multiple electron transfer increases the complexity of catalyst regeneration. The four electron

reduction of $[(bpy)_2MnO_2Mn(bpy)_2]^{3+}$, a potential catalyst for the photogeneration of oxygen from water, breaks the dimer apart making regeneration of the photo-active form improbable (20).

The cycles based on hydrido complexes appear simpler. Complexes which photochemically release H_2 are already known (21) and the thermal diprotonation of complexes is a well established synthetic procedure (22). Incorporating both reactions in a cyclic system, however, will require additional research.

A viable energy conversion system must overcome all these problems. It must 1). prevent or retard the thermodynamically favored back reaction, 2). be able to promote a multi-electron transfer process by synchronized one-electron steps, and 3). regenerate the catalyst. Such a system would be qualitatively similar to photosynthesis. In photosynthesis, an excited state electron transfer reaction occurs as the result of photoexcitation. Through a complex multi-photon, multi-electron process, radiant energy is stored as chemical potential energy in the form of carbohydrates and oxygen (1). While we are not interested in developing photosynthetic model systems, a closer look at photosynthesis should be profitable. After all, photosynthesis is proof that solar energy conversion of this type is possible. How does photosynthesis overcome

the obstacles discussed above? Can these features be incorporated into laboratory systems?

The most striking feature of photosynthesis is the degree of organization. Both chemical and physical barriers are employed as restraints on back electron transfer to prevent the thermodynamically favored back reaction and promote energy storage. The active sites in photosynthesis are chlorophyll dimers which are localized in intracellular membranes (23). The membrane separates the oxidant in the bulk solvent from the photoactive species with a lipid-aqueous phase boundary. There is experimental evidence that this interface acts as a potential energy barrier to the thermal back reaction (24). In addition, a series of electron carriers provide a path for the migration of an electron away from the oxidized chlorophyll. Separating these reactants decreases the probability of the unproductive back reaction. It is true that some energy is lost in these intermediate steps (5), but we are proof that enough energy is conserved to complete the process.

What features of photosynthesis increase the feasibility of a multi-electron process dependent on one-electron donors? Intuitively, we might expect the chlorophyll dimer to act as a two electron donor. Other structural features may also play a role. Chloroplasts are imbedded in the lamella, a semi-rigid

matrix. Isolation of excited states in rigid media increases their lifetime and thus increases the probability of two or more excited states occuring simultaneously or at least within the lifetime of the photoredox products.

These two features of photosynthesis, the organization of reactants in a non-homogeneous reaction medium and the use of kinetic barriers to minimize the back reaction, can be incorporated into conversion systems. Indeed, Sprintschnik, et al. reported that photolysis of a substituted $Ru(bpy)_3^{2+}$ surfactant, dispersed on water, led to the evolution of small amounts of H_2 (25). The reactants, water and the hydrophobic $Ru(bpy)_3^{2+}$ analogue, were separated by a phase boundary. Unfortunately, this work could not be repeated (26-28) but it did direct attention to the potential of heterogeneous media for solar energy conversion systems.

A comparison with homogeneous reaction systems is beneficial in evaluating the advantages of heterogeneous systems. Much research effort has been expended in the study of solution reaction systems and a summary of the developments in this area follows.

Ultra-violet irradiation of aqueous solutions containing certain transition metal complexes and cations has led to the production of H_2 (3). However, less than 5% of the sunlight reaching the earth is in the ultraviolet region, while visible light accounts

for approximately 50% of the incident radiation (1,29). An efficient conversion system, therefore, should include a photosensitizer that absorbs strongly in the visible to utilize this energy. A good catalyst should also be thermally and photochemically stable.

Because of its potential to mediate the photolysis of water, the transition metal complex $Ru(bpy)_3Cl_2$ has been the subject of intense study. $Ru(bpy)_3^{2+}$ absorbs both ultraviolet and visible light and has a strong absorbance at 452 nm ($\epsilon = 1.4 \times 10^4\ M^{-1}\ cm^{-1}$), in the range of intense solar emission. Its excited state is formed with unitary efficiency (31,32) and has a solution lifetime of 600 $\pm$20 nsec in water (33). $^*Ru(bpy)_3^{2+}$ is both a strong oxidant and reductant, permitting the development of a variety of reaction systems. $Ru(bpy)_3^{2+}$ is also thermally and photochemically stable (34-39).

As seen in Figure 1, $^*Ru(bpy)_3^{2+}$ has the potential to both oxidize and reduce water (40), and the following reaction sequence could be proposed for a cyclic system:

$$^*Ru(bpy)_3^{2+} + H_2O \longrightarrow Ru(bpy)_3^{3+} + OH^- + \tfrac{1}{2}H_2 \qquad (12)$$

$$Ru(bpy)_3^{3+} + OH^- \longrightarrow Ru(bpy)_3^{2+} + \tfrac{1}{4}O_2 + \tfrac{1}{2}H_2O \qquad (13)$$

$$^*Ru(bpy)_3^{2+} + H_2O \longrightarrow Ru(bpy)_3^{2+} + \tfrac{1}{2}H_2 + \tfrac{1}{4}O_2 + \tfrac{1}{2}H_2O \qquad (14)$$

Photolysis of aqueous solutions of $Ru(bpy)_3^{2+}$, however,

does not lead to the formation of H_2 and O_2. While the oxidation step (equation 13) is known (40), the reduction step, equation 12, has not been observed. $^*Ru(bpy)_3^{2+}$ does not transfer an electron directly to water, but the photoreduction of water in the presence of an electron carrier species has been reported (37,41-44).

Quinones (3), hydrido complexes (3,41), and paraquat (1,1'-dimethyl-4,4'-bipyridinium dication, Pq^{2+}) (42,43) have been used as electron carriers in homogeneous conversion systems. When an excited state can not react directly with substrate for mechanistic reasons (3,25), electron carriers may facilitate the reaction by permitting the migration of an electron away from the excited donor via the reduced form of the carrier. While some energy is lost in the formation of this intermediate, most of the energy of the photo-excited complex, which would be lost when the unreacted complex relaxed, is conserved for reaction with the substrate. The reduced electron carrier may also promote multiple electron transfer in conjunction with redox catalysts. The reports of H_2 evolution mentioned above were based on the photolysis of solutions containing both electron carriers and redox catalyst.

The most commonly employed electron carrier has been Pq^{2+}, which can act as an electron acceptor in biological conversion systems (45). The facile reduction of this compound ($Pq^{2+}/Pq^{+\cdot}$, E=0.44eV) is accompanied

by a dramatic color change and it has been widely used as a reversible redox indicator (45-49). Colorless Pq^{2+} readily accepts an electron to form the bright blue cation radical ($\lambda = 605$ nm, $\epsilon = 1.2 \times 10^4$ M^{-1} cm^{-1}) (46,50), shown in Figure 2, which reduces water in the presence of a redox catalyst (42,51).

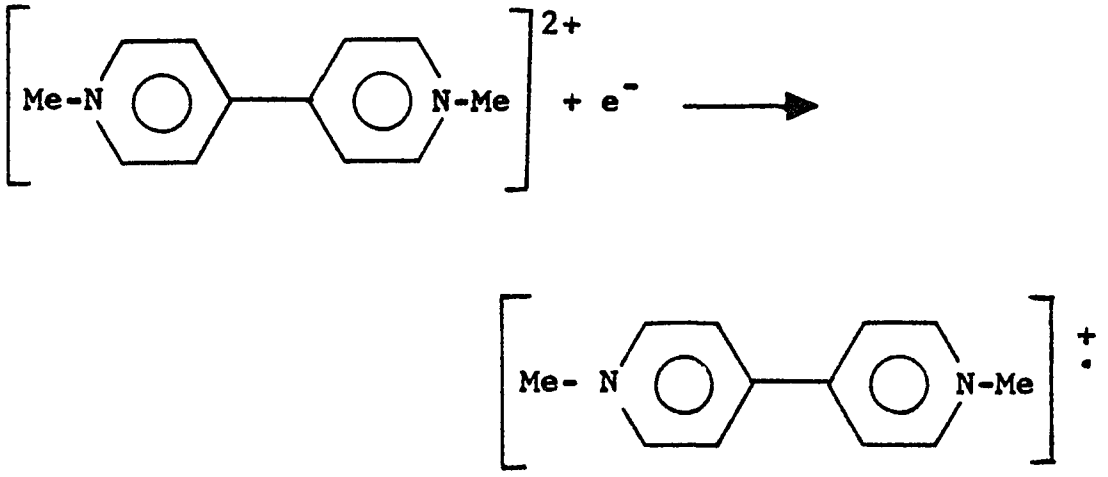

Figure 2

The ease with which paraquat can be oxidized and reduced make it a good electron carrier, but it also creates experimental problems. $Pq^{+\cdot}$ is very sensitive to O_2 and has even been used as a colorimetric indicator for the detection of O_2 (52). Exclusion of O_2 by careful degassing of all solvents and equipment is necessary to minimize loss of energy by oxidation of this species. For the same reason, other reactants must be carefully selected to minimize loss of $Pq^{+\cdot}$ through

competitive side reactions. Unlike photosynthesis, in which an array of useful products are formed through side reactions (1), we are aiming for the maximum yield of one product, H_2, which is dependent on the formation of $Pq^{+\cdot}$.

$Pq^{+\cdot}$ is generated by the reductive quenching of $*Ru(bpy)_3^{2+}$ by Pq^{2+} (11), which has a rate constant of 5×10^8 M^{-1} s^{-1} (equation 15) (42). We have already stated that $Pq^{+\cdot}$ reduces water in the presence of a suitable catalyst, yet photolysis of solutions of $Ru(bpy)_3^{2+}$, Pq^{2+} and catalyst does not lead to hydrogen production. The back reaction of primary redox products is very rapid, $k_{16} = 2.4 \times 10^9$ M^{-1} s^{-1} (equation 16) (42).

$$*Ru(bpy)_3^{2+} + Pq^{2+} \longrightarrow Ru(bpy)_3^{3+} + Pq^{+\cdot} \qquad (15)$$

$$Ru(bpy)_3^{3+} + Pq^{+\cdot} \longrightarrow Ru(bpy)_3^{2+} + Pq^{2+} \qquad (16)$$

Efforts to improve the overall reaction yield, therefore, have concentrated on retarding the energy dissipating back reaction.

Modification of the ligand periphery has been used successfully by Whitten to slow the rate of the back reaction (7,14,16). It was found, however, that the differences in the relative rates of the forward and back reactions were not sufficient to induce any net chemical change. Frequently the forward reaction was decreased to a greater extent than the back reaction.

Other attempts to impede the back reaction have focused on the separation of the primary redox products. Bock and coworkers (13) have studied the effect of charge on the probability of the separation of the redox couple before geminate recombination can occur. If the encounter pair is repulsive, separation is more likely to occur. The $Ru(bpy)_3^{2+}$: Pq^{2+} encounter pair is repulsive and so are the redox products, $Ru(bpy)_3^{3+}$: $Pq^{+\cdot}$, but the back reaction proceeds with high efficiency. Separation of the ions can only be observed on a microsecond time scale. Larger charge densities might be more effective but they would also alter the rate of the forward reaction (53). A novel approach to this problem was reported by Grätzel (54). The quencher, Pq^{2+}, was modified by replacing one of the CH_3 groups with a 14-carbon chain. Quenching of $*Ru(bpy)_3^{2+}$ was not significantly affected, but the back reaction was slowed by a factor of 100. The $C_{14}Pq^{+\cdot}$ analogue was more hydrophobic than the dication and rapidly formed micelles. The increased charge density at the micellar surface repeled the $Ru(bpy)_3^{3+}$ and inhibited recombination.

Secondary reactions can retard the back reaction by removing one of the reactants. Many workers have found that the addition of an electron donor to the system promotes the accumulation of stable $Pq^{+\cdot}$ in the absence of O_2 and catalyst (42,55,56). The

electron donor may quench $*Ru(bpy)_3^{2+}$ or reduce $Ru(bpy)_3^{3+}$ but effective stabilization of $Pq^{+\bullet}$ requires that the oxidized donor undergo secondary reactions to form non-oxidizing species (42,55). A great deal of the work on conversion systems has focused on these reactions, but they are not cyclic. Electron donor is consumed and the oxidation pathway is blocked.

Ideally, the ultimate source of electrons in the photolysis of water should be water itself with the metal sensitizer and the quencher acting as catalysts. Recombination of H_2 and O_2 to release the stored energy would complete the cycle. The recent report by Grätzel on the photodissociation of water with coupled redox catalysts proves that the development of cyclic systems is possible (57). The optimum conditions for the reduction and oxidation of water, however, are not the same. While hydrogen is evolved from nuetral solutions (3,58), the oxidation of hydroxide ion with regeneration of the catalyst (equation 17) peaks at pH = 9 (40).

$$Ru(bpy)_3^{3+} + OH^- \longrightarrow Ru(bpy)_3^{2+} + \tfrac{1}{4}O_2 + \tfrac{1}{2}H_2O \qquad (17)$$

Sutin has demonstrated that this reaction is strongly pH dependent and the yield of O_2 and $Ru(bpy)_3^{2+}$ drops sharply and is less than 5% below pH = 8, and $\lesssim$ 0.5%

when the pH$\leq$6.8. The efficient oxidation and reduction of water may best be carried out at separate sites as the analogy to photosynthesis suggests. This would also facilitate separation of the gaseous products.

Most research efforts have been based on simplified systems which focus on only one aspect of the photodissociation of water. These modified systems require an electron donor. This work is concerned with the photoreduction of water. A review of the work in this area follows.

Sweetser reported that photolysis of buffered solutions of EDTA, Pq^{2+} and proflavine, a photosensitizer, produced $Pq^{+\cdot}$ with a quantum yield of 0.6 but when no EDTA was present, the bright blue $Pq^{+\cdot}$ could not be detected (52). Photolysis of an aqueous solution of $Ru(bpy)_3^{2+}$, Pq^{2+}, $Rh(bpy)_3^{2+}$, and Pt resulted in the production of H_2 when TEOA (triethanol amine), a mild reducing agent, was present (41). What was the role of the electron donors in these reactions? Lehn and Sauvage (41) speculate that in the case of TEOA, the electron donor quenches $*Ru(bpy)_3^{2+}$. They based this on previous reports that other mild reducing agents, such as N,N'-dimethyl aniline, reduce $*Ru(bpy)_3^{2+}$. The $Ru(bpy)_3^{+}$ which is formed is a strong reductant capable of reducing water to H_2.

The two possible mechanisms for the redox

quenching of $*Ru(bpy)_3^{2+}$ are depicted in equations 18-21. The first mechanism predicts quenching by the electron carrier or substrate (S) followed by the reduction of $Ru(bpy)_3^{3+}$ by the electron donor (D). The second predicts

$$*Ru(bpy)_3^{2+} + S \longrightarrow Ru(bpy)_3^{3+} + S- \quad (18)$$

$$Ru(bpy)_3^{3+} + D \longrightarrow Ru(bpy)_3^{2+} + D^+ \quad (19)$$

$$*Ru(bpy)_3^{2+} + D \longrightarrow Ru(bpy)_3^{+} + D^+ \quad (20)$$

$$Ru(bpy)_3^{+} + S \longrightarrow Ru(bpy)_3^{2+} + S^- \quad (21)$$

reductive quenching of $*Ru(bpy)_3^{2+}$ followed by reduction of the substrate. The proposal of Lehn and Sauvage would fall into the second category.

Moradpour and coworkers ruled out this possibility in their work on aqueous solutions containing $Ru(bpy)_3^{2+}$, EDTA or TEOA, Pq^{2+} and Pt^o or Au^o (43). Flash photolysis studies revealed no luminescence quenching by the electron donor species. The electron donor then, must reduce $Ru(bpy)_3^{3+}$ after the excited state electron transfer to Pq^{2+} (59). Using laser flash photolysis, Kalyanasundaram confirmed that TEOA operates according to reactions 18 and 19 (42).

Determining that EDTA operates according to reaction 18 and 19 does not explain how it manages to compete with the rapid recombination of the geminate ion pair following the electron transfer. Matsuo has

suggested that EDTA only reduces free $Ru(bpy)_3^{3+}$ which has escaped the reaction sphere of $Pq^{+\cdot}$ (56). The rapid rate of the back reaction, however, suggests that the thermal redox reaction occurs before the encounter pair can dissociate (13). This explains the previous failure to detect any permanent net chemical change in these systems in the absence of EDTA, but it can not account for quantum yield of $Pq^{+\cdot}$ in the presence of a donor or for its stability.

Whitten and coworkers (55) competitively scavenged $Ru(bpy)_3^{3+}$ produced in the photolysis of acetonitrile solutions of $Ru(bpy)_3^{2+}$, Pq^{2+} and one of the following donors: 2,6-lutidine, N,N-dimethylformamide or triethylamine. The back reaction (equation 21) proceeds at a rate of $k_{21} = 8.1 \times 10^9\ M^{-1}\ s^{-1}$ in this solvent.

$$Ru(bpy)_3^{3+} + Pq^{+} \longrightarrow Ru(bpy)_3^{2+} + Pq^{2+} \qquad (21)$$

The reduction of $Ru(bpy)_3^{3+}$ by the donor and the subsequent hydrogen abstraction reaction between the solvent and the oxidized donor are competitive with this rapid reaction, and these workers commented on the striking nature of these results.

How EDTA (59a) is effective as an electron donor in scavenging the $Ru(bpy)_3^{3+}$ species is still uncertain. An understanding of this mechanism could provide insight

into how to manipulate this part of the reaction system to optimize the rate of the forward reaction. Examination of this subject was undertaken as part of this thesis work.

In the absence of a suitable noble metal redox catalyst, no hydrogen is generated in any of these systems. Even when an electron donor is present and significant accumulations of $Pq^{+\cdot}$ are formed, no evolution of H_2 occurs (42). The formation of H_2 is a two electron event but $Pq^{+\cdot}$ is a one electron donor. Heterogeneous catalysis provides a pathway for the coordination of two one-electron transfers to yield product.

PtO_2, Pt, Pd, and Au (37,42,43,60) have all been used in these systems to catalyze H_2 evolution. Experiments performed by Kiwi and Grätzel (60) have indicated that particle size and the nature of the catalyst support, if any is used, affect the yield of H_2. Colloidal dispersions (43,60), particulates generated in situ (41), and treated asbestos (51) have been used by different workers. The mechanism of catalysis is uncertain, but the efficiency of hydrogen production varies for the different forms (60). This is consistent with the idea that surface effects are very important (61). Some attempts to achieve more uniform catalysis results were made as part of this thesis project.

The evolution of hydrogen from these systems has been shown to be dependent on the combination of a light absorber, an electron carrier, an electron donor, and a redox catalyst (3). If any one element is missing, the reaction will not proceed despite the favorable energetics. What opportunities for optimizing the efficiency of these reactions do heterogeneous systems offer? A review of the results obtained with monolayers, micelles, and vesicles will illustrate the alterations in reactivity which can be achieved by incorporating reagents into non-homogeneous systems (62).

Photosynthesis is a two-photon, two-electron process (63). The reactions in photosystem I (PS I) and photosystem II (PS II) occur simultaneously but in different environments. The pigments involved in these photoprocesses are localized in a membrane, the lamellar. It is thought that the two photosystems are on opposite sides of the membrane and that PS II transfers its excited electron across the membrane to PS I (64,65). The membrane could act as a barrier to the thermal back electron transfer (24). Some researchers believe that this effect of the membrane, a phase boundary, may be the single most important feature of photosynthesis in the control of the back reaction (66). The phase boundary in photosynthesis is a complex biological membrane, which we will not try to duplicate. Rather

we will work from simple phase boundaries, monolayers, to more complex systems, micelles and vesicles, and note the effect these different media have on the chemistry of certain systems.

As stated earlier, Sprintschnik and coworkers (25) reported that they had successfully photodissociated water by irradiating a surfactant $Ru(bpy)_3^{2+}$ complex dispersed as a monolayer on water. They postulated that the order of the monolayer either lowered the barrier to electron transfer, as evidenced by the emission quenching of the surfactant $Ru(bpy)_3^{2+}$ by water (25,28), or acted as a barrier to the geminate recombination of the donor and quencher (25). Attempts to repeat the work were unsuccessful and it was later determined that impurities in the prepared surfactant were probably responsible for the observed reaction (28).

This report was an incentive to additional monolayer research. The accumulated data have demonstrated the powerful influence that the structure of a monolayer exerts on the reactivity of molecules. Hopf and Whitten (67) noted that Ru(II) carbonyl porphyrins, effectively isolated by limited diffusion in a monolayer, readily formed coordinatively unsaturated monomers which were unstable in solution. In other cases, porphyrins in the hydrophyllic portions of monolayers preferentially stacked as dimers (68), reminiscent of the chlorophyll

dimer in photosynthesis. Quina and Whitten (69) found a similar effect when they packed surfactant olefins and dienes in monolayers. The photochemical formation of dimers and excimers, which was not observed in solution, was favored by this arrangement of the molecules.

Further study of monolayers may reveal new methods for controlling chemical reactivity, but there are serious drawbacks to their application in conversion systems. The light absorption of a monolayer is inherently low, even when complexes with large extinction coefficients ($\epsilon = 10^4\ M^{-1}\ cm^{-1}$), such as $Ru(bpy)_3^{2+}$, are used (28). Efficient use of sunlight would require an enormous surface area but the large scale use of liquid dispersed monolayers is impractical. Depositing samples on solids for use in multi-surface reactors could overcome this problem; however samples prepared on solids do not exhibit uniform absorption or emission characteristics (26,70).

Micelles can be used in bulk quantities to overcome one of the major drawbacks of monolayer systems, low absorption. Their three dimensional structure creates more options for the dispersal of reagents (they can be in the bulk solvent, adsorbed to the surface, solubilized in the interface, or contained within the micelles) and thus for tailoring the reaction system (71-73). These advantages have led to considerable work on micellar

solutions.

Grätzel and coworkers (74) demonstrated that incorporation of phenothiazine or tetramethylbenzidene into anionic micelles greatly increased the rate of monophotonic photo-ionization of these compounds. Electron transfer to acceptors adsorbed at the micellar surface proceeds at rates faster that those obtained in homogeneous solution. The lifetimes of the cation radicals produced by these processes were much longer than the solution lifetimes. Similar results were obtained by Thomas and Piciulo (75) in their work on the visible photolysis (λ = 530 nm) of 3-aminoperylene in anionic and cationic micelles. The rapid rate of electron transfer from the molecule within the micelle to the adsorbed acceptor ions, at the concentrations used in these experiments, suggests that the transfer occurs via an electron tunnelling mechanism. It has been established that photo-ejected electrons can tunnel through lipid monolayers for 10 Å distances (74). If this mechanism is operative in these micellar systems, then the surface charge of the micelle would affect the rates and thus provide a means of rate controll (76,77). Cationic micelles did not promote ionization or electron transfer. The potential for photoionization in cationic micelles is a few hundred millivolts higher than in water, while potentials in anionic micelles are lower (75,77).

The variation in effective local concentration attainable in micelles can affect the rate of a reaction (78-80). Matsuo (81) noted that the electron transfer quenching of $Ru(bpy)_3^{2+}$ by benzyl viologen (BV^{2+}) progressed at a rate 3.5 times faster when the Ru(II) complex was solubilized in anionic micelles than in solution. He attributed this to the high concentration of quencher, BV^{2+}, adsorbed to the anionic surface. When $Ru(bpy)_3^{2+}$ was incorporated into cationic micelles which would repel BV^{2+}, the quenching rate was very slow. Dissolving both the $Ru(bpy)_3^{2+}$ and the quencher Pq^{2+} in cationic micelles improved the quenching efficiency to the point that a quantitative yield of stable, reduced quencher was obtained (76).

Rabani and coworkers (82) found that variation of the $Ru(bpy)_3^{2+}$ concentration within the micelle had a dramatic effect on the lifetime of the excited state. When $Ru(bpy)_3^{2+}$ was incorporated into SDS (sodium dodecyl sulphate) micelles and irradiated, a two component luminescent decay was observed. The slower exponential component was comparable to the solution decay and predominated at low $Ru(bpy)_3^{2+}$/micelle ratios. The fast, nonexponential decay, dominant at higher $Ru(bpy)_3^{2+}$/micelle ratios, suggested a triplet-triplet annihilation reaction. This reaction, though it is thermodynamically favored by $\sim$ 1.7 V (83,84), had not been observed previously

in fluid media.

$$2^*Ru(bpy)_3^{2+} \longrightarrow Ru(bpy)_3^{+} + Ru(bpy)_3^{3+} \qquad (22)$$

Micelles can be used to retard or accelerate reactions observed in solution or to promote reactions not detected in solutions (e.g. triplet-triplet annihilation of $^*Ru(bpy)_3^{2+}$). Experimentally, micelles are versatile. They may be arranged with the hydrophobic portion of the component molecules at the surface (85) or the interior. This permits the use of a wide range of solvents. Micelles are dynamic structures, however, and this is a serious handicap. It is difficult to regulate their size or to controll the concentration of incorporated compounds (66). In addition, they are only stable for $\sim$ 1 week, and therefore are not suitable for use in solar energy conversion systems.

Vesicles are more representative of membranes than monolayers or micelles (66,86). They have two surfaces and a reaction system could be built on both sides. The interface between the surfaces has been the main focus of research. An electron conduction system built into the oil-aqueous interface could transfer an excited electron from one reaction center across the phase boundary to another reaction site mimicking photosynthesis. Work with porphyrins in phospholipid

vesicles demonstrated that electron transfer from the photo-excited porphyrin to anthraquinone proceeded at rates 10^4-10^5 times faster than in homogeneous solution (66).

Stabilization of the photoredox products should improve the efficiency of electron transfer by allowing the reduced quencher more time to diffuse to the secondary reaction site. Vesicles can separate the electron donor and acceptor species and have been shown to have a stabilizing effect on the ionic products of redox reactions (87). Fendler, et al. (88) reported that cationic radicals,formed by the quenching of tris (2,2'-bipyridine) Ru(II) intercalated in DODAC (dioctadecyldimethyl ammonium chloride) vesicles,were very long lived. When the $Ru(bpy)_3^{2+}/EDTA/Pq^{2+}$ system was incorporated into vesicles, high concentrations of stable $Pq^{+\cdot}$ radical were generated.

Unlike micelles, vesicles are static entities. They are readily formed by sonication of solutions and can contain many guest molecules (89). Compounds can be solubilized in the bilayer, adsorbed to the surfaces, or reside in the inner or bulk portions of the solvent. The electrostatic fields at the vesicle surface can be manipulated to promote the separation of redox products and thereby enhance the forward reaction. Unfortunately, the useful lifetime of vesicles is short-only about one week. A more stable system is necessary

if these reaction systems are to have practical value. Polymers have been studied for the structural stability they offer.

Meisel (90) has examined the reactivity of $Ru(bpy)_3^{2+}$ in aqueous solutions of PVS, poly(vinyl sulfate). Emission and absorption spectra indicated that the coordination sphere of the Ru(II) was intact when the complex was adsorbed and that PVS does not act as a quencher. Stern-Volmer constants for quenching by Cu^{2+} in these systems were 10^2 to 10^3 times larger than those measured in aqueous solution. How does the polymer facilitate the quenching encounter of these like charged species? Meisel suggests that the quenching mechanism is still dynamic, but that the negatively charged polyelectrolyte enhanced the effective local concentration of the reactants (91). The unusual reversal in quenching efficiency at high concentrations of Cu^{2+} provided a clue to the mechanism. Quenching increases with $[Cu^{2+}]$ until, at high concentrations when the ratio of $Ru(bpy)_3^{2+}/Cu^{2+}$ adsorbed on the polymer is small, there is a decrease in the quenching. At high $[Cu^{2+}]$, $Ru(bpy)_3^{2+}$ was displaced into the bulk solvent where it was less readily quenched due to electrostatic repulsion. The negative charge of the polymer surface also minimized the repulsive nature of the encounter between the two dications (92). The surface charge of the polymer may be utilized to further

increase the reaction efficiency. Monovalent cations are more loosely bound than dications. The formation of a reduced quencher with a lower positive charge, or one that is neutral, will promote desorption of that species and thus inhibit the back reaction (91).

Calvin (66) has been working on the development of a crosslinked styrene-butadiene-acrylic acid copolymer with bound porphyrin groups for study of their electron-transfer properties.

Kelly and coworkers (93) are experimenting with the synthesis of polymer-bound photoactive complexes. They prepared $Ru(bpy)_2PVPCl^+$ and $Ru(bpy)_2(PVP)_2^{2+}$, where PVP represents poly(vinyl pyridine), and compared their reactivity with non-polymeric species of similar structure, $Ru(bpy)_2(py)_2^{2+}$ and $Ru(bpy)_2pyCl^+$. The thermal and photo chemistry of these compounds, which are dominated by substitution reactions, are very similar, differing only in their rates. It is hoped that a study of these compounds will help to determine what portion of the altered reactivity of heterogeneous systems is due to physical order rather than to chemical modification of the reagents. These workers are presently developing a synthesis of $Ru(bpy)_3^{2+}$-bound polymers for use in conversion systems.

Researchers in this laboratory have done some work involving poly(methyl methacrylate) supports (94).

$Ru(bpy)_3Cl_2$ was dissolved in the liquid monomer and the solution was hardened. The plastic exhibited the strong luminescence characteristic of $*Ru(bpy)_3^{2+}$. To perform any redox chemistry in these plastics, however, it would be necessary to dope them with electron carriers (e.g. quinones) to improve their poor conductive quality. It soon became apparent that this medium was not practical. High concentrations of guest molecules inhibited the polymerization process but the low concentrations of $Ru(bpy)_3Cl_2$ in hardened samples made light absorption inefficient. In addition irradiation at $\lambda \geq 300$ nm eventually made the plastic opaque and further inhibited absorption by the ruthenium complex. Most importantly, the matrix isolation of the $Ru(bpy)_3^{2+}$ made it inaccessible to other reagents and inhibited the cyclic redox chemistry required for the maintenance of photocatalytic activity.

Each of these heterogeneous systems met some of the criteria, outlined above, for efficient conversion systems. Different media enhanced the rates of electron transfer, stabilization of the redox products, and product separation. None of these systems, however, had all the characteristics necessary for practical application. Another heterogeneous medium which offers both chemical and structural stability is Thirsty Glass.

Corning's code 7930 controlled pore glass,

referred to as Thirsty Glass, is an intermediate in the production of Vycor. The product of the acid leaching of borosilicate glass, it contains a matrix of randomly distributed, interconnected cavities (95,96). Pore size is precisely controlled and ranges in size from 40 to 2500 Å diameters; deviation within a size category is less than 30% (96,97,98). The larger pore sizes scatter light making the samples opaque and unsuitable for photochemical study, but the 70 Å cavities employed in this work are transparent and readily adapt to photolyses and spectral analysis. In addition, the extended array of cavities in Thirsty Glass creates a surface area of 130 m^2/g glass (97b). This makes it an ideal substitute support for further investigation of surface phenomena and the role they play in reaction control.

Burwell (99) has suggested that one might "heterogenize homogeneous catalysis" by bonding homogeneous catalysts to silica gel. The heterogeneous systems produced would facilitate separation of catalyst and reactants, allow greater flexibility in the choice of solvent, and be adaptable to flow systems. We would like to apply this suggestion to Thirsty Glass. The chemistry of the two materials are similar, both are covered with Si-OH groups (96,97a,99). This group is mildly acidic and when these materials are immersed

in water, the loss of protons creates an anionic SiO^- surface to which cations are readily adsorbed. For a more stable arrangement, synthetic techniques already developed for modification of silica gel (100) could be used to chemically bond compounds to the surface of Thirsty Glass. Large quantities of reagents could be incorporated by either method. The inherent low absorption of monolayers is not a problem with this medium. Indeed it is necessary to limit the concentration of reagents to facilitate spectroscopic monitoring.

We should expect that incorporation of a compound into this porous glass matrix will affect its reactivity. Rigid media sometimes increase the lifetimes of transient species (e.g. the lifetime of $*Ru(bpy)_3^{2+}$ is 600 nsec in solution and 5.21μ sec in an EtOH glass (32)) and reports by several workers indicate that some unstable species are longer lived in Thirsty Glass. Melamud and coworkers (101) have observed that UV photolysis of alkylated glasses produced methyl radicals with unusual stabilities. Some species had half-lives $\geq$ 5 months. Sutherland and Piciulo (102) noted a substantial increase in the lifetime of triplet pyrene adsorbed to the glass. This stabilizing influence may affect the overall efficiency of conversion systems in two ways: 1) longer excited state lifetimes increase the probability of two excited states occuring simultaneously or within the

lifetime of the photoredox products; 2) stabilization of the products slows down the back reaction and thus increases the probability of the secondary reaction.

There are two basic approaches which can be taken in designing a conversion system utilizing this support. One would be to separate the primary redox products and the other would be to construct a reaction site which would promote the secondary reaction.

In the first case, some reagents could be adsorbed into the cavities while others were restricted to the external environment. $Ru(bpy)_3^{2+}$ adsorbed into the glass could transfer electrons through an electron transport system built into the cavities of the glass to Pq^{2+} and catalyst in the bulk aqueous solution. In conjuction with the imposition of a phase boundary at the glass surface, back electron transfer could be strongly curtailed.

The second approach involves the physical organization of the light absorber, quencher, catalyst, and substrate, water, within a reaction volume. Under these conditions, the rate of the reaction of reduced quencher and catalyst would not be limited by diffusion. If in addition, the excited state, $*Ru(bpy)_3^{2+}$, or the redox products, $Ru(bpy)_3^{3+}$ and $Pq^{+\cdot}$, are stabilized by the matrix and several reaction units can be incorporated into the same cavity, then the two electron reduction

of water may be strongly favored. Both of these approaches have been persued, but the later has been the focus of this work.

This thesis is a report of the experiments performed to explore: 1) the photophysical, photochemical, and chemical properties of reagents adsorbed to the glass, 2) the procedures for assembly of a tailored reaction site within a cavity, and 3) incorporation of specific water reduction systems into the glass.

CHAPTER 2

Experimental

I. Materials

A. All compounds were reagent grade and were used without further purification. $H_2PtCl_6 \cdot 6H_2O$ was obtained as a 10% solution in water from Baker and Adamson, General Chemical Division of Allied Chemical Corporation. Elmer and Amend were the suppliers of the 5% platinized asbestos. D_2O (99.8 atom% D) was purchased from Aldrich. Corning provided the porous glass, code #7930, "Thirsty Glass".

B. Preparation of $Ru(bpy)_3Cl_2$

$Ru(bpy)_3Cl_2$ was prepared according to the method of Palmer and Piper (103). $RuCl_3 \cdot 1\text{-}3\ H_2O$, purchased from Ventron, was refluxed in 95% ethanol with three equivalents of bipyridine and 0.5 equivalents of $Na_2C_2O_4$ (104) for 48 hours. The volume was reduced to approximately 10 ml, the solution was cooled, and the product filtered on a glass frit and dried by aspiration.

C. Preparation of $Ru(bpy)_3(ClO_4)_3$

$Ru(bpy)_3(ClO_4)_3$ was prepared according to the method of Creutz and Sutin (40). 0.3135 g of $Ru(bpy)_3Cl_2 \cdot 3H_2O$ was dissolved in 10 ml of 1 N H_2SO_4 and bubbled with Cl_2 until the solution was dark green. 10 ml of a $NaClO_4$ saturated solution and some solid $NaClO_4$ were added to the reaction mixture, which was bubbled with Cl_2 again and

then sealed under a Cl_2 atmosphere. The flask was cooled in an ice bath for two hours and the contents were then filtered through a cold sintered glass filter. The solid was partially air dried by aspiration and then transfered to a vacuum line where the drying was completed in the dark. The product was recrystalized from warm 1 N H_2SO_4 and stored in the dark under refrigeration.

II. Instrumentation

Visible and ultraviolet absorption spectra were recorded using a Cary 14 or a Techtron 635 spectrophotometer. Raman spectra were obtained with a Spectra-Physics model 164-08 Argon Ion laser equipped with a Spectra-Physics 265 exciter, a Spex Industries 1408 spectrophotometer, a Pacific Precision Instruments model 126 photometer and a Beckman recorder. NMR spectra were recorded on a 60 MHz Varian EM 360. Luminescence measurements were made on a Perkin-Elmer Hitachi MPF-2A flourescence spectrophotometer equipped with a red sensitive Hamamatsu R928 photomultiplier. Gas samples were analyzed on a Gow-Mac model 69-100 gas chromatograph equipped with a Poropak-Q column and rhenium-tungsten filaments. The GC detector response was displayed on a Varian A-25 recorder. Conductivity studies were performed with a Yellow Springs Instrument Company, Inc. model 31 conductivity bridge. EPR spectra were recorded on a Varian EM 500 or Varian E-9 spectrometer. The vacuum

line was equipped with a CVC Products, Inc. VMF-10 oil diffusion pump and Welch Duo-Seal pumps and could be pumped down to a pressure of $\leq 10^{-3}$ torr. Gas samples were isolated with a Toepler pump. pH measurements were made with a Corning semi-micro combination electrode and a Beckman Expandomatic SS-2 pH meter. Chloride ion concentration was monitored with an Orion Research combination chloride electrode, #96-17, made by Corning.

III. Photolysis Apparatus

White light sources included a 350 W Hg-Xe high-pressure arc lamp from Illuminations Industries and a 100 W high-Pressure Xe arc lamp with a Sola Electric Co. filtered DC power supply. These light sources were passed through Bausch and Lomb grating monochromators, models 33-86-79 and 33-86-76, with 1350 grooves/mm to obtain monochromatic light. Other monochromatic light sources were the Spectra-Physics model 132 He-Ne and model 164-08 ionized argon lasers. The photomutliplier tube was an RCA 31034 powered by a Pacific Photometric Instruments regulated negative high-voltage power supply, model 203. The change in voltage as a function of time was displayed on a Varian 25-A recorder.

A. Continuous Photolysis of Solutions

1. As seen in Figure 3, the light from a 350 W Hg-Xe arc was focused onto the slits of a monochromator and a

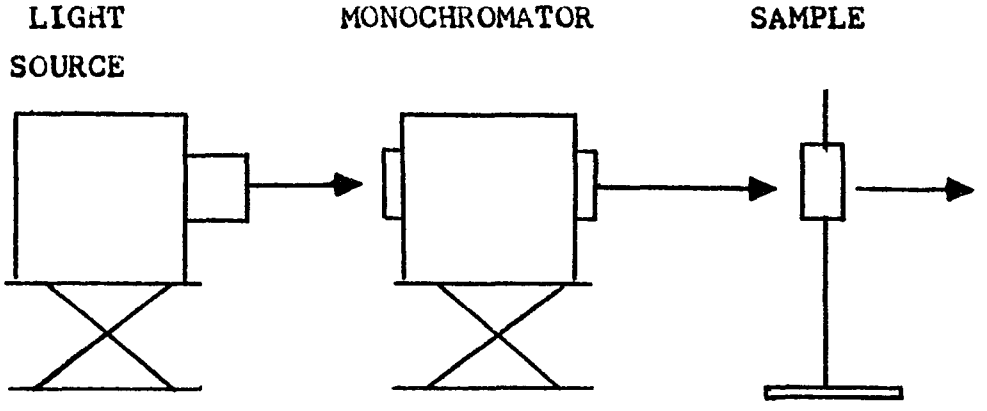

Figure 3

Apparatus for Continuos Photolysis of Solutions

selected wavelength was passed through the sample.

2. Simultaneous photolysis and product analysis were achieved using the apparatus shown in Figure 4. The photolyzing radiation (λ =457.9 nm from an Argon Ion laser) was dispersed with a lens and passed through the sample. The analyzing beam (λ =634 nm from a He-Ne laser) was coaxial to the photolyzing beam. Approximately 9% of the transmitted analyzing light was reflected by a glass slide through a red filter ($\lambda \geq$ 600 nm) and onto the slits of a monochromator. The change in the intensity of the analyzing beam was monitored by a RCA 31034 PM tube and recorded as a function of time.

B. Continuous Photolysis of Glasses

1. As seen in Figure 5, monochromatic light was a) reflected directly onto the sample; b) passed through a neutral density filter and then reflected onto the sample, or c) 9% of the light was reflected from a glass slide onto the sample. The visible absorption spectrum of the sample was recorded periodically.

2. Continuous photolysis with simultaneous monitoring of product formation was achieved using the optical train depicted in Figure 6. After passing through a water filled 12 cm quartz cell and a 3 mm plexiglass sheet to eliminate UV and IR wavelengths, white light from a 350 W Hg-Xe arc was focused onto the sample. Neutral density filters were placed in front of the sample holder when used. Transmitted

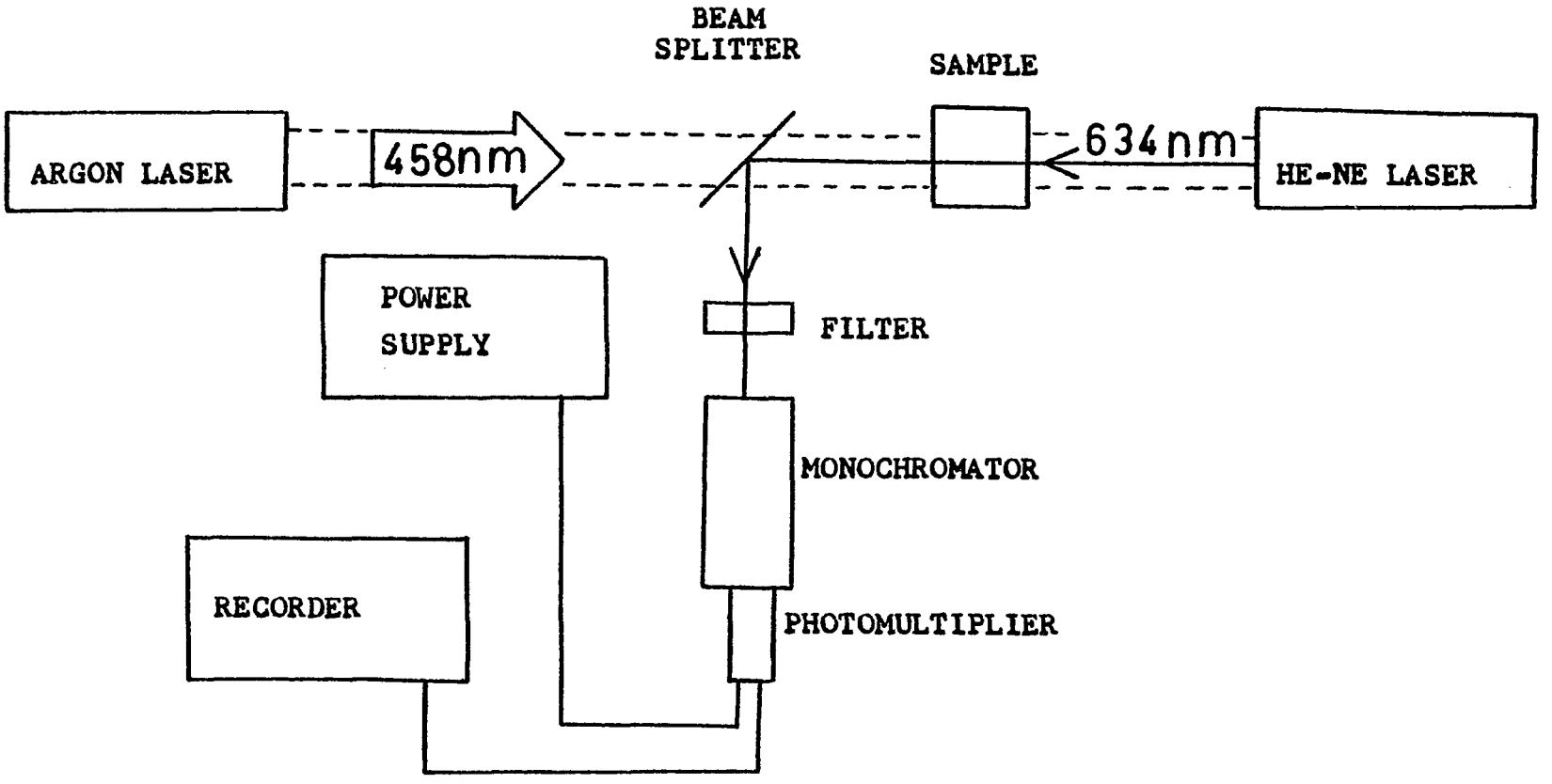

Figure 4

Apparatus for Simultaneous Contiuous Photolysis and Product Analysis of Solutions

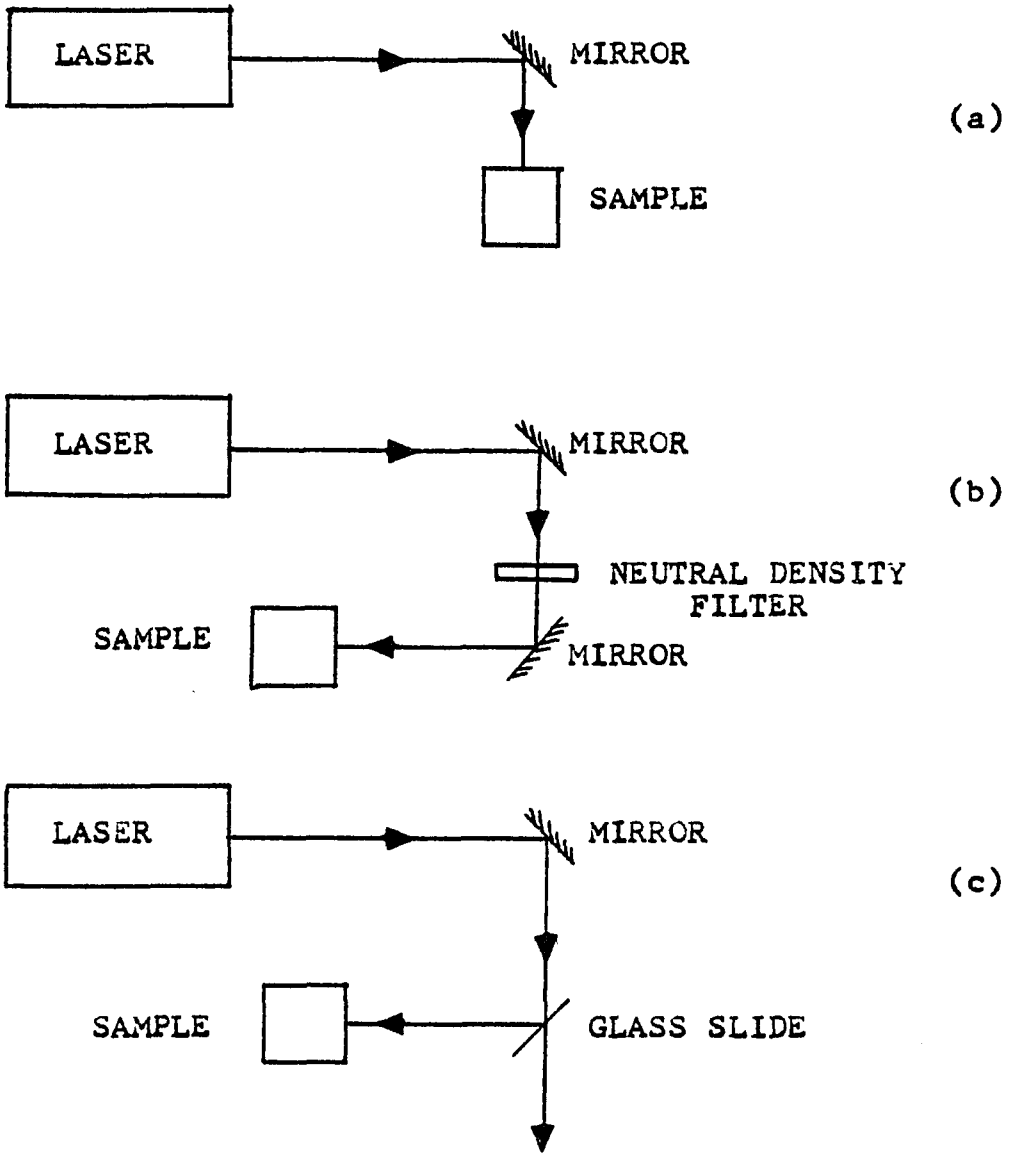

Figure 5
Apparatus for Continuous Photolysis of Glasses

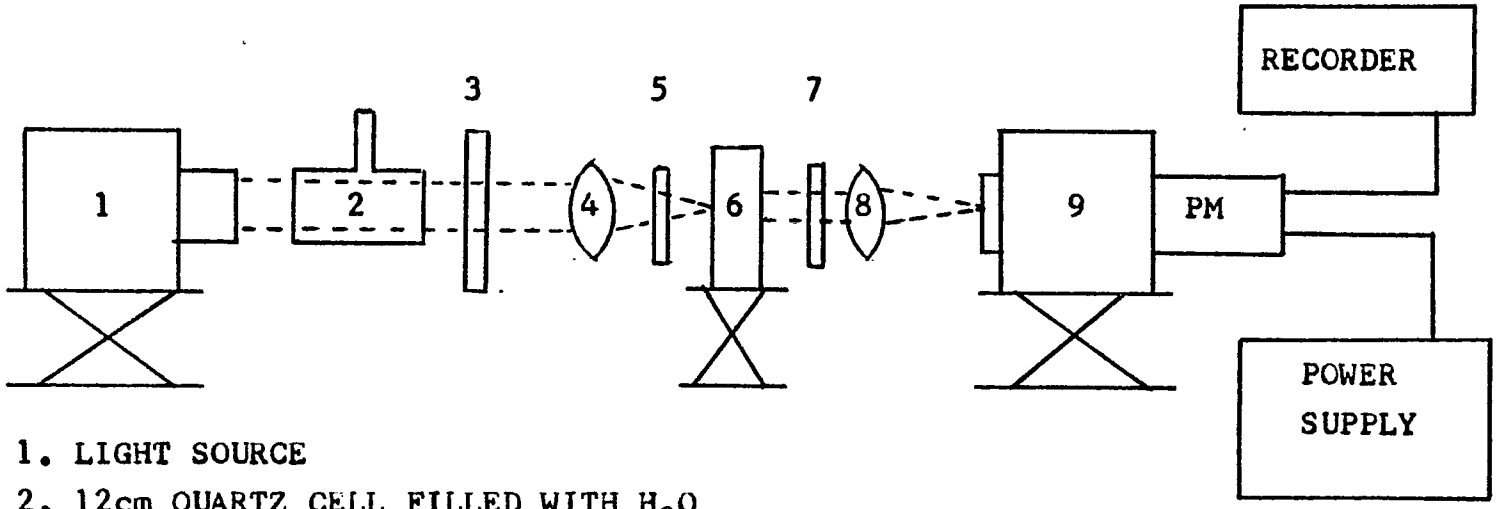

1. LIGHT SOURCE
2. 12cm QUARTZ CELL FILLED WITH H_2O
3. 3mm PLEXIGLASS SHEET
4. LENS
5. NEUTRAL DENSITY FILTER
6. SAMPLE
7. CUT-OFF FILTER
8. LENS
9. MONOCHROMATOR

Figure 6

Apparatus for Simultaneous Continuous
Photolysis and Product Analysis of Glasses

light was passed through a Klinger Scientific Corporation cut-off filter (GG475) and focused onto the slits of a monochromator. The change in the intensity of the analyzing wavelength was monitored with the RCA 31034 photomultiplier tube and recorded as a function of time.

C. Flash Apparatus

The coaxial flash (Candella Corporation) was charged by a high-voltage power supply (Walden Electronics Corporation model 545A, 10-30 KV). Coumarin 450 dye (Exciton) in 100% ethanol was circulated through the unit with a pump (Manostat Varistalltic). The photolyzing flash (λ=446 nm) was triggered externally and had a 150 nsec half-peak duration. The power could be varied by regulation of the capacitor with an upper limit of 0.6 joules/pulse. Following the flash, the intensity of an analyzing beam was monitored to detect any changes in the sample. This analyzing beam could be focused with a lens (Dolmeyer Telephoto, 12", F/4.5) onto the sample. To prevent the excitation pulse from reaching the detector, the light transmitted through the sample was passed through a Klinger cut-off filter ($\lambda \geq 500$ nm) and onto the slits of a monochromator. Changes in intensity were monitored by a RCA 31034 PM tube and displayed on a Hewlett-Packard model 175A oscilloscope. The oscilloscope sweep was triggered by inductive coupling with the photolyzing flash. The time resolution of this apparatus is $\sim$5 nsec (see Figure 7).

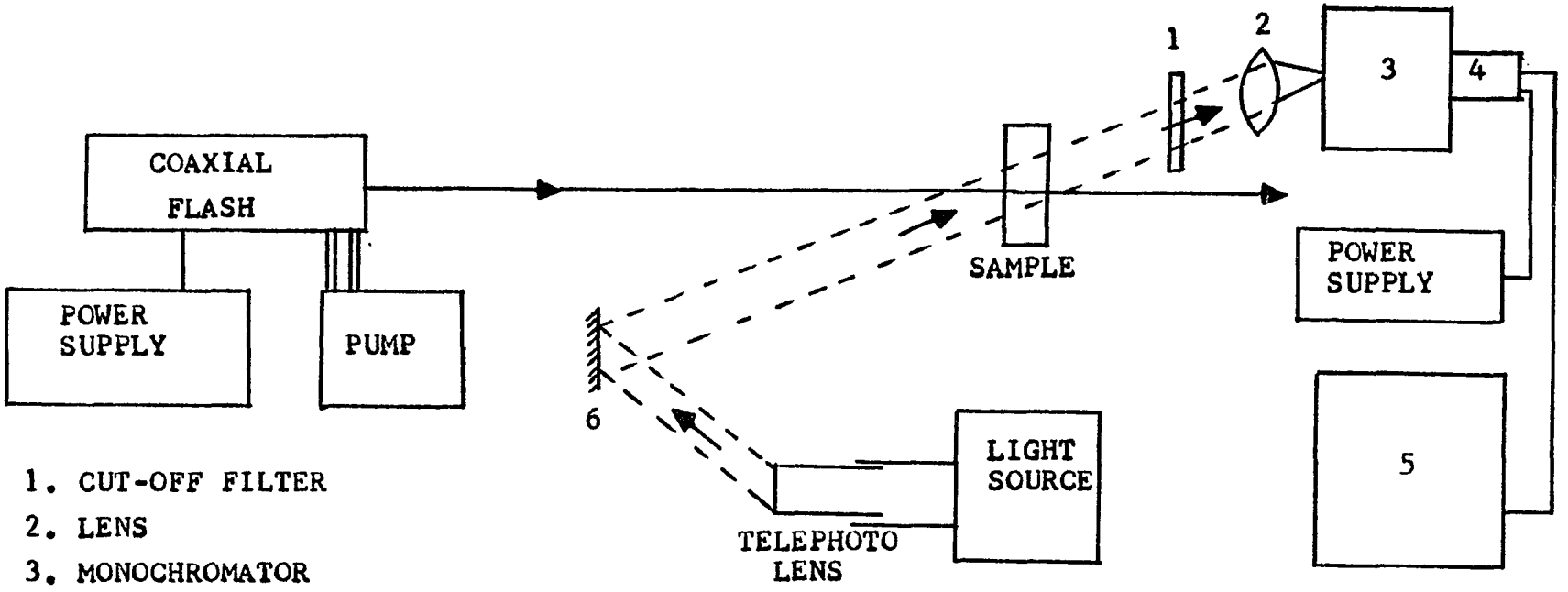

1. CUT-OFF FILTER
2. LENS
3. MONOCHROMATOR
4. PHOTOMULTIPLIER TUBE
5. OSCILLOSCOPE
6. MIRROR

Figure 7

Flash Photolysis Apparatus

IV. Procedures

A. Solutions

1. Quenching of $*Ru(bpy)_3^{2+}$

Samples were prepared by pipetting 1.0 ml of 10^{-3} M $Ru(bpy)_3Cl_2$ stock solution, 1.0 ml of 1 M KCl, and aliquots of quencher (1 M- 10^{-4} M) into a 10 ml volumetric flask and diluting to volume with water. An aliquot of this solution was transfered to a 10x10x40 mm fused quartz cell which was joined through a graded seal to a 14/20 outer joint. This sample cell was fitted to an upper section which had a sidearm, a vacuum stopcock, and a 10/30 joint for connection to a vacuum line (Figure 8). Solutions were degassed by successive freeze-thaw cycles or deaerated by He-bubbling for 15 min (He : Union Carbide, high purity grade). Emission intensity measurements, made at 600 nm, were used to construct Stern-Volmer plots.

2. Quantum Yield Determinations

Quantum yields were determined by measuring the rate of product formation at a constant light intensity. Ferric oxalate actinometry was used to measure the light intensity; measurements were made before and after photolysis using a 0.15 M solution with the Hg-Xe arc and an $8.8x10^{-6}$ M solution with the laser. All measurements were made at ambient temperature (22-25°C). Solutions containing 10^{-4} M $Ru(bpy)_3^{2+}$, 10^{-2} M Na_2EDTA, and Pq^{2+}

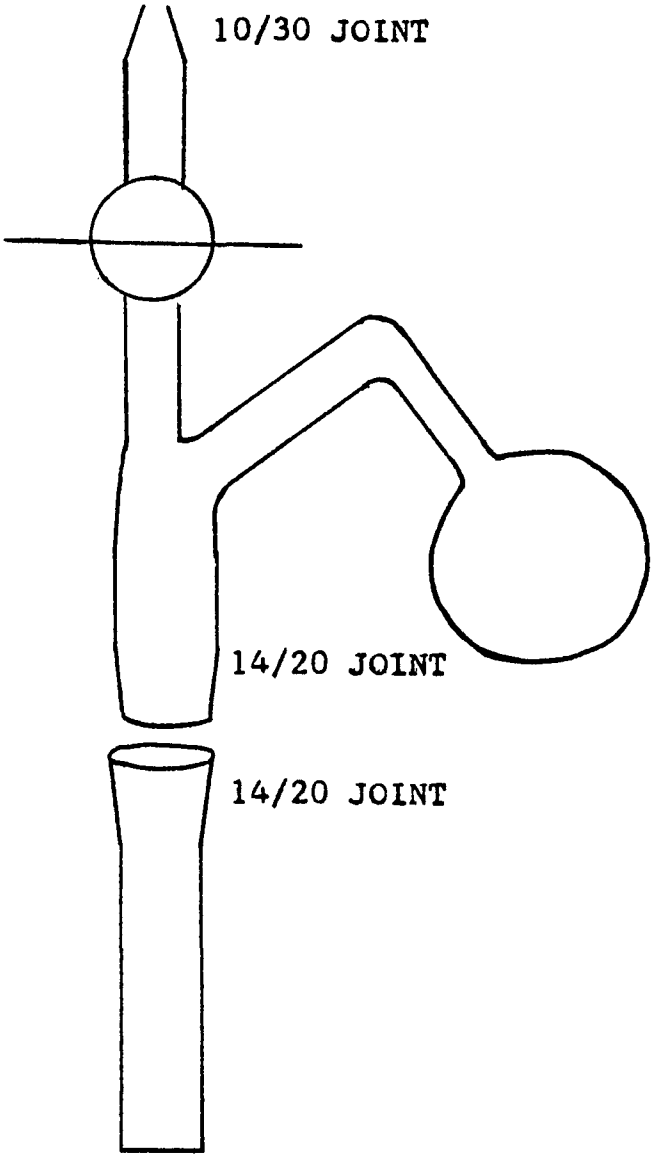

Figure 8
10 x 10 x 40 mm Cell and Upper Section

ranging from 10^{-4} M to 10^{-2} M at a constant ionic strength of 0.1 M (KCl) were degassed by three successive freeze-thaw cycles at liquid nitrogen temperature and irradiated. Product formation was monitored by periodically recording the visible absorption spectrum or by measuring the change in the intensity of an analyzing beam. A plot of $1/\phi_{Pq^{+\cdot}}$ against $1/[Pq^{2+}]$ was made and extrapolated to obtain a limiting yield for $Pq^{+\cdot}$.

3. Ion-Pairing Experiments

a). Conductivity Experiments

Blank titrations were performed on aqueous 10^{-3} M solutions of $Ru(bpy)_3^{2+}$, Pq^{2+} and Na_2EDTA. Glass distilled water was added from a burette calibrated to 0.10 ml. After stirring, the change in the solution's resistance was measured with a dipping cell. Fresh 10^{-3} M $Ru(bpy)_3^{2+}$ and 10^{-3} M Pq^{2+} solutions and water were then titrated with 10^{-1} M Na_2EDTA. To check the influence of ionic strength on the data, solutions $2x10^{-2}$ M in KCl and 10^{-3} M in Pq^{2+} or $Ru(bpy)_3^{2+}$ were also titrated. Plots of conductance (1/R) against the volume of titrant were constructed.

b). Job's Plots

Ultra-violet and visible absorption spectra were run on the following combinations of reactants: 1) $Ru(bpy)_3^{2+}$ and Pq^{2+}; 2) $Ru(bpy)_3^{2+}$ and Na_2EDTA; 3) Pq^{2+} and Na_2EDTA. The total concentration was kept constant at 10^{-4} M.

c). Quenching of $*Ru(bpy)_3^{2+}$

Emission intensity measurements were made using the

procedure described in IV-A-1 with the modification that Na_2EDTA was present. Stern-Volmer plots were constructed for each data set of Na_2EDTA concentration (10^{-1}-10^{-3} M).

d). NMR Experiments

All solutions were prepared in D_2O with 4% DSS (3-Trimethylsilyl-1-propanesulfonic acid, sodium salt hydrate) as an internal standard. First, spectra of 10^{-1} M solutions of $Ru(bpy)_3^{2+}$, Pq^{2+}, and Na_2EDTA were recorded individually and then the spectra of reagent pairs were run to detect any change in the chemical shift, δ . The pair showing frequency shifts, $Ru(bpy)_3^{2+}$ and $EDTA^{2-}$, was examined further. While the concentration of one reagent was held constant, the other was varied and the chemical shift of the components was measured as a function of the mole ratio and plotted. The effect of ionic strength on these values was examined by the addition of KCl (0.3 M-1 M).

e). Inhibition of Na_2EDTA

In the first set of experiments, solutions 0.1 N in H_2SO_4 containing 10^{-4} M $Ru(bpy)_3^{2+}$, 10^{-2} M Pq^{2+}, 10^{-2} M Na_2EDTA and 0.1 M KCl were degassed by the freeze-thaw techniques described above and irradiated. In the second set of experiments, aqueous solutions containing 10^{-4} M $Ru(bpy)_3^{2+}$, 10^{-2} M Pq^{2+}, 10^{-2} M Na_2EDTA, 10^{-1} M KCl and 0 or 10^{-2} M Fe^{2+} were buffered at pH=7, degassed and irradiated. An iron free solution of the reactants and $6x10^{-3}$ M Na_2EDTA was also degassed and irradiated. The

formation of $Pq^{+\cdot}$ was monitored spectrally at 605 nm in all cases.

4. Extraction Experiments

Aqueous solutions containing 10^{-3} M $Ru(bpy)_3^{2+}$, 10^{-2} M Na_2EDTA, and 10^{-2} M Pq^{2+} were stirred with an equal volume, 10 ml, of $CHCl_3$ in a 50 ml round bottom flask and irradiated with 436 nm light from a Hg-Xe arc. Identical reaction mixtures were stirred in the dark for the same time ($\sim$20 hr). The spectrum of each solvent layer was recorded to determine the concentration of bipyridine and the decomposition of the complex. To calibrate the extraction procedure, reaction solutions containing 10^{-4} M bipyridine were treated in the same manner as the light and dark reactions. This calibration gave an extraction efficiency of 76% of the added bipyridine.

5. Gas Sampling

Sample cells were attached to the vacuum line and liquid phase components were frozen in the sidearm with liquid nitrogen. The gas phase was allowed to expand through a trap, cooled with liquid nitrogen or a dry ice/acetone slush, into the evacuated upper chamber of a Toepler pump seen in Figure 9. Stopcocks B and D were closed and air was let into the bottom chamber through E. The mercury displaced the gas in the upper chamber forcing it through C and F into the sample loop. F was shut and the pump evacuated through E. The sample was pumped three times

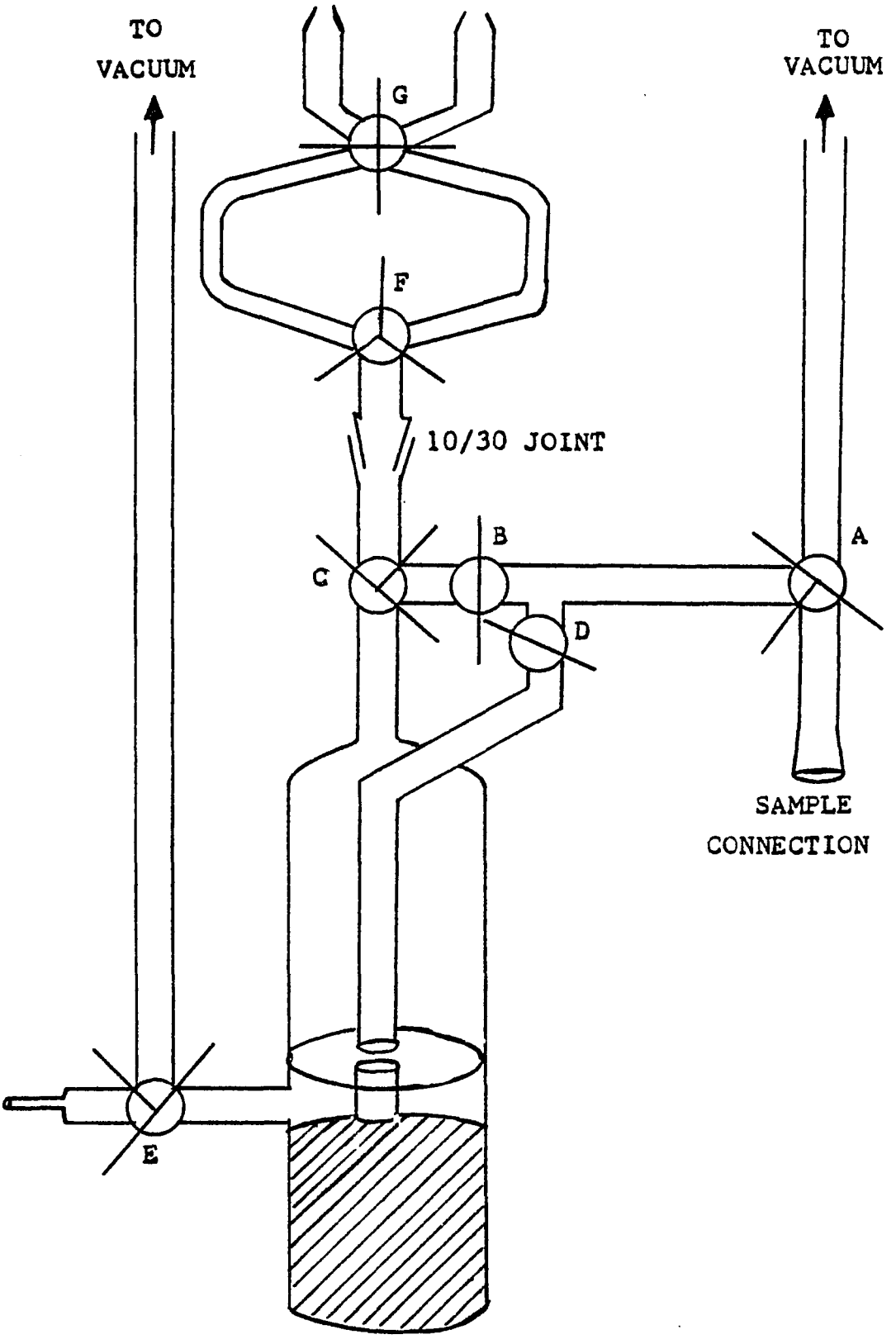

Figure 9
Gas Sampling Apparatus

in this manner until > 97% of the gas was in the sample loop. The loop was then transferred to the gas chromatograph and connected to the carrier gas stream as seen in Figure 10. This arrangement allowed the system to be purged before the sample was introduced. This instrument was calibrated by determining the volume of the sample cell and sealing it under a known pressure of the gas being analyzed. This calibration sample was then pumped in the manner described above and run through the gas chromatograph. All measurements were made at room temperature. A plot of moles of gas against signal intensity was made and used for analysis of sample data.

a). H_2

5 ml aliquiots of solutions containing 2.5×10^{-3} M $Ru(bpy)_3^{2+}$, 10^{-2} M Pq^{2+} and 10^{-2} M Na_2EDTA or 50 ml samples of solutions containing 10^{-1} M KCl, 10^{-2} M Na_2EDTA, 10^{-4} M $Ru(bpy)_3^{2+}$ and 10^{-2} M Pq^{2+} were degassed by the freeze-thaw method and irradiated at room temperature with 457.9 nm light from an Argon Ion laser or photolyzed in a water/ice slurry with the light from a Hg-Xe arc lamp. The visible spectrum was recorded and the samples were then mixed with 5% platinized asbestos, platinized platinum gauze (105) or H_2PtCl_6 from a sidearm. When the sample had lost its blue color, the cell was attached to the vacuum line and frozen with liquid nitrogen. The gas was allowed to expand through a liquid nitrogen trap into the Toepler pump and

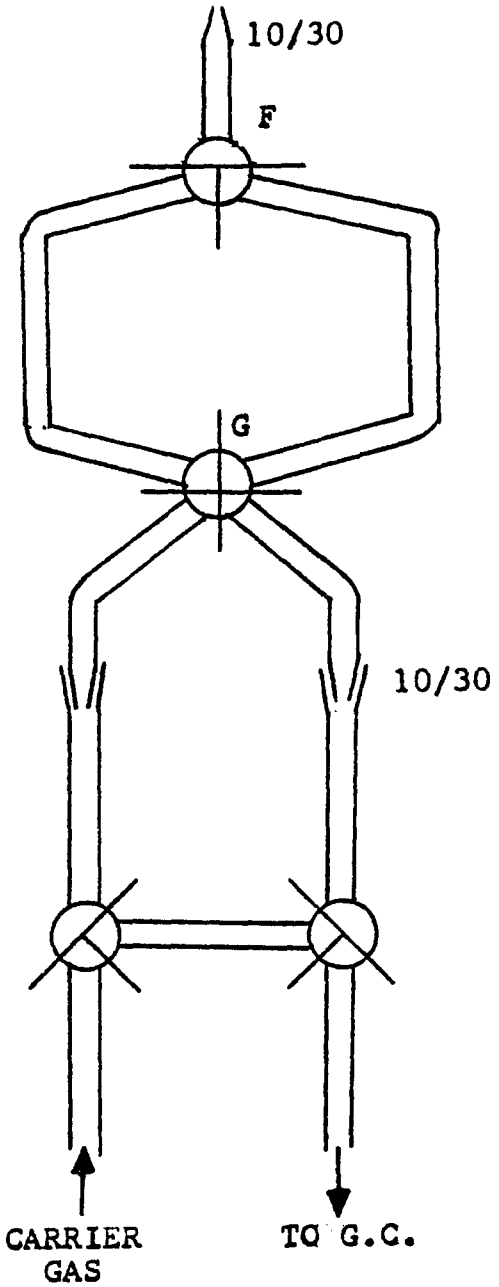

Figure 10

Connection of Gas Sampling Loop to G.C.

was sampled in the manner described above. Nitrogen was the carrier gas for all H_2 analyses.

b). CO_2

A 10 ml aliquot of a 10^{-2} M Na_2EDTA solution was freeze-thawed in a 25 ml round bottom flask fitted to an upper section with a sidearm, containing varied amounts of solid $Ru(bpy)_3(ClO_4)_3$. The cell was tilted to mix the reactants. When all effervescence stopped, the sample was frozen with a dry ice/acetone slush and allowed to expand through a trap cooled with the same slurry into the pump. The sampling technique was the same as described above except that the carrier gas was He. These sample solutions were saved for the formaldehyde analysis described below.

6. Colorimetric Determination of H_2CO

Following the procedure described by Bricker and Vail (106), 0.1 g of chromotropic acid was dissolved in a 1.0 ml aliquot of each sample in 5b and in 1.0 ml of a series of formaldehyde standards. The samples were evaporated to dryness on a hot plate, 5 ml of concentrated H_2SO_4 was added, and they were heated in a boiling water bath for 30 min. After cooling, the samples were quantitatively transfered to 50 ml volumetrics and diluted to volume with H_2O. The optical densities of all solutions were recorded at 570 nm. A calibration plot was constructed from the standard data and used to analyze the other samples.

B. Glasses

1. Cleaning

Glasses were soaked in dilute HCl and then rinsed several times with glass distilled water. The glasses were vacuum dried at 45° C until they were clear and then transferred to a muffle furnace. The temperature was raised slowly and then held at 500° C for a minimum of 48 hr. The furnace was shut off and allowed to cool to room temperature. Cleaned glasses were stored in a vacuum oven or vacuum dessicator.

2. Adsorption

a). Determination of the average number of cavities per gram of glass

A series of $\sim$40 pieces of clean dry glasses were weighed and then soaked in distilled water for 1 hr (experiments over a 24 hr period have shown that $>$ 99% of the water was adsorbed within the first hour). The pieces were removed from the water, the surface water quickly removed with Kimwipes, and reweighed. They were returned to the vacuum oven, dried overnight at 45° C, and weighed again. From the difference in weight and the density of water, the total pore volume was calculated. Assuming the average pore is spherical with a 70 Å diameter, the average number of cavities/gram of glass was determined.

b). Adsorption of reagents

The adsorption of reagents was monitored primarily by UV-vis spectroscopy. The exception was Cl^- ion, which was monitored by a specific ion electrode. Clean, dry glasses were weighed and immersed in solutions of known concentration and volume. The change in the concentration of the solution were monitored and the total number of moles adsorbed were calculated. The effect of ionic strength on the adsorption of some reagents was studied by making the soaking solutions 0.1 M in KCl. Vacuum drying at 45° C to remove the solvent was the final step.

c). Distribution and Concentration

An average value for the concentration of reagents in the glass was determined using the procedures described above. The number of cavities in a piece of glass was calculated from the sample weight and the constant determined in (a). The number of adsorbed molecules was determined by spectral analysis of the soaking solution as described in (b). A ratio of these two values gives the average number of reagent molecules in a cavity. When glasses containing colored compounds were broken and examined, however, it was obvious that this average concentration was not an accurate representation. Most of the adsorbed reagent was near the surface with little or no reagent adsorbed near the middle of the glass. To obtain a more accurate value for the concentration in these glasses, the distribution of the reagents across the sample thickness

was examined.

The dimensions of several pieces of glass were determined with a caliper. These samples were then fitted into the vertical supports of a thin layer chromatography tank to guarantee exposure of both surfaces. A measured volume of adsorbate solution was added to cover the glasses. The glasses were left to soak in the closed tank until adsorption was completed, then rinsed and vacuum dried. The moles of reagent adsorbed were determined spectrally as described above.

An absorption spectrum of the glass immersed in chlorobenzene was recorded. The sample was removed from the solvent and ground on sandpaper to remove a layer of measured thickness from one surface. The glass was re-immersed in chlorobenzene and another spectrum was recorded. This process was repeated several times, then the sample was turned and the other face was treated in the same manner. A plot of absorbance as a function of sample thickness was constructed from this data. The number of reagent molecules/cavity was determined from this data as illustrated in the following example.

Example 1:

A 25x25x4 mm glass containing 10^{-5} moles of reagent shows a 50% decrease in absorbance when a 1 mm layer is removed from the front surface. 50% of the adsorbed molecules are contained in that layer. From the

volume of the layer (0.625 cm^3) and the density of the glass (1.393 g/cm^3) the mass of the layer is calculated to be 0.870 g. Using the constant determined in (a), the number of cavities in that layer is determined:

$$0.870\ g \times 2\times10^{-6}\ \text{moles of cavities/g} = 1.74\times10^{-6}\ \text{moles of cavities}$$

A ratio of the adsorbed molecules (5×10^{6} moles) to cavities (1.74×10^{-6} moles) shows that there are an average of 2.8 reagent molecules in the cavities near the surface.

d). Pt Black

The incorporation of Pt black into the glass was achieved by minor modification of a synthetic procedure for the catalyst (107). Aqueous solutions of varied concentrations of H_2PtCl_6 were made slightly alkaline with NaOH and an excess of NaHCOO was added. Clean dry glasses were either immersed in this solution to soak at 0° C or were repeatedly dipped and dried with an air gun to limit adsorption to the surface sites. When the desired amount of Pt had been adsorbed, the samples were vacuum dried to remove all the water and then transferred to a muffle furnace. The temperature was raised slowly to 300° C and held constant for 24 hr. The furnace was shut off and allowed to cool slowly to room temperature. The samples were thoroughly rinsed with water to remove any salts and then dried again in a vacuum oven. Additional reagents could then be adsorbed as detailed in 2b above.

3. Photochemical Experiments

a). Sample Cells

The sample cell depicted in Figure 8 was also used for the 4x8x30 mm glasses. Larger glasses were handled in the pyrex cell pictured in Figure 11. These cells could be adapted with standard ground glassware to degassing bulbs when required. Cells used for ESR work are depicted in Figure 12.

b). Quenching of $*Ru(bpy)_3^{2+}$ in the Glass

Quenching of $*Ru(bpy)_3^{2+}$ in the glass was studied in dry glasses and in two phase systems. In the first case, the quencher was adsorbed into the glass with the $Ru(bpy)_3^{2+}$ and the sample was vacuum dried. In the second case, the $Ru(bpy)_3^{2+}$ is adsorbed into a glass which is then immersed in a solution of the quencher or sealed under a gaseous quencher atmosphere. Samples were degassed on a vacuum line or purged with He during preparation. Emission intensity and absorption measurements were made, the sample was irradiated, and the visible spectrum recorded again.

c). Reversibility of Photolysis

Dry glasses containing $Ru(bpy)_3^{2+}$ were degassed and their absorption spectra were recorded. Samples were irradiated and another spectrum was obtained. The photolyzed samples were then treated with either an oxidizing or reducing medium by 1). tipping the cell and immersing the glass in a degassed solution from the sidearm, or 2). purging the cell with a gas. Spectra were recorded

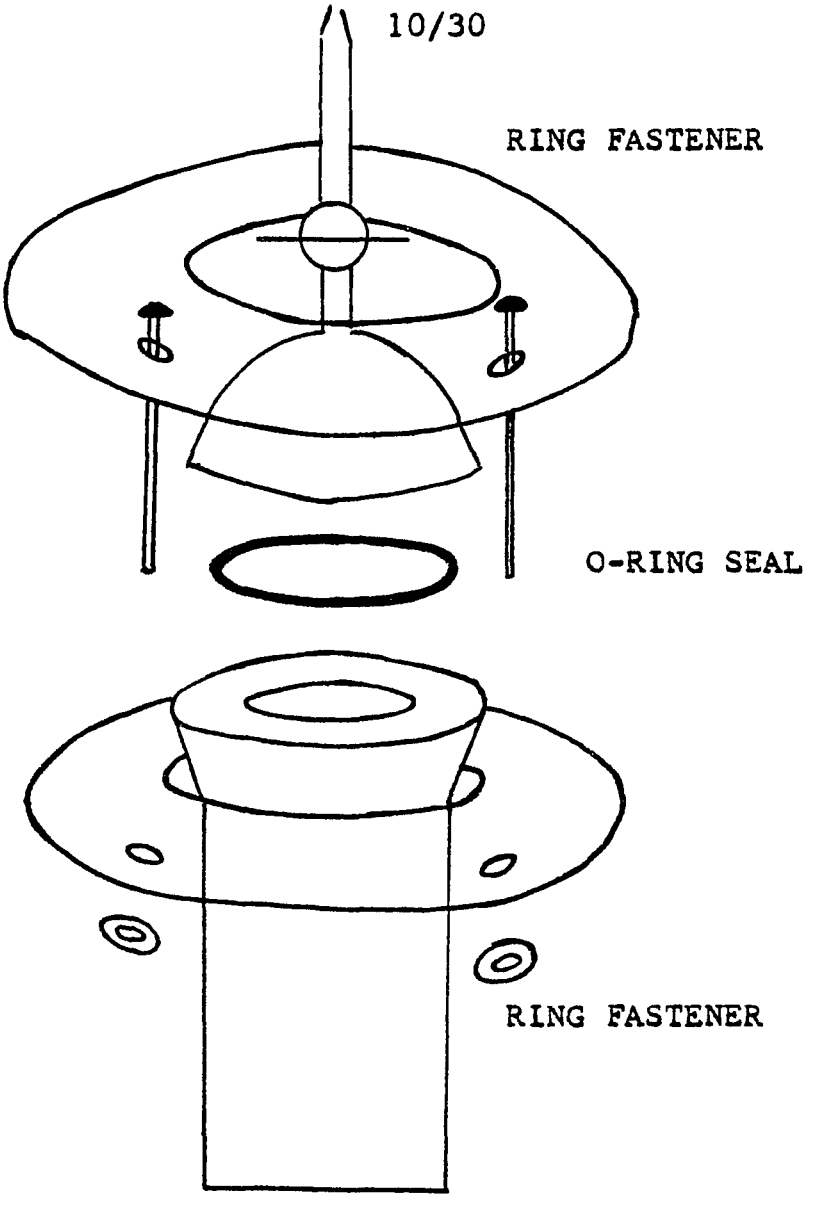

Figure 11
Large Glass Sample Cell

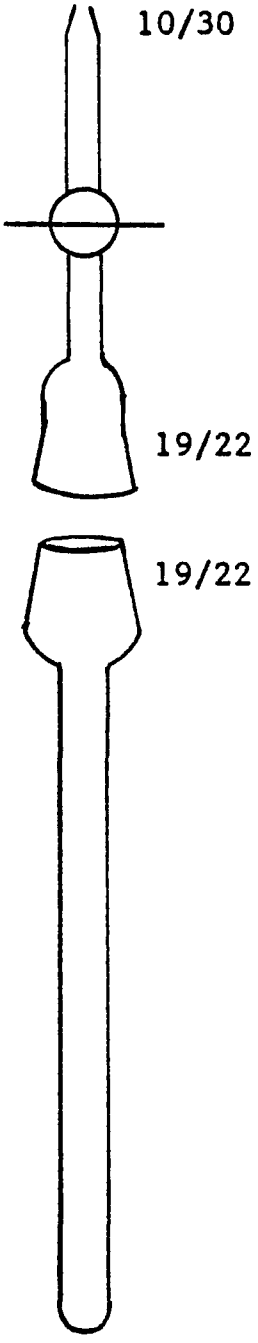

Figure 12
ESR Glass Sample Tube

periodically.

d). ESR

Dry 3x3x15 mm glasses containing $Ru(bpy)_3^{2+}$ or $Ru(bpy)_3^{2+}$ and Pq^{2+} were degassed in the pyrex tubes depicted in Figure 12. The sample was 1) irradiated with a 350 W Hg-Xe lamp or the 457.9 nm line of an Argon Ion laser and then transferred to the spectrometer, or 2) irradiated within a modified sample cavity by a 1 KW Hg-Xe arc lamp. Spectra were recorded intermittently. 2,2'-Diphenyl-1-pycrylhydrazyl was used as a standard.

e). Quantum Yields

Quantum yield data on the formation of $Ru(bpy)_3^{+}$ was abtained using the apparatus described in II-B. Ferric oxalate actinometry was employed to determine light intensities. Dry 25x25x4 mm glasses containing $Ru(bpy)_3^{2+}$ were degassed and irradiated. Product formation was followed by monitoring the change in the transmittance of 510 nm light.

f). Gas Chromatography

Platinized 25x25x4 mm glasses containing $Ru(bpy)_3^{2+}$ were placed in the large cells described above. These were adapted to include a 100 ml degassing bulb containing water. The unit was connected to a vacuum line and the liquid was degassed by repetitive freeze-thaw cycles while the entire assembly was degassed. The unit was then tilted so that the glass was immersed in the water.

After allowing time for the adsorption of water, the air cooled sample was photolyzed by a 350 W Hg-Xe arc for several hours. The assembly was tipped to return the liquid to the sidearm and the system was reconnected to a vacuum line. The contents of the degassing bulb were frozen with liquid nitrogen and a hot air gun was used to drive the water from the glass sample and the walls of the unit into the sidearm. The gas in the unit was then sampled in the manner described in IV-5-a.

CHAPTER 3

Results

I. Solution Studies

A. Quenching of $Ru(bpy)_3^{2+}$

1. Absorption and Emission Spectra

The absorption and emission spectra of aqueous $Ru(bpy)_3^{2+}$ (10^{-4} M) are shown in Figures 13 and 14. The visible absorption spectrum is dominated by an intense metal to ligand charge transfer band at 452 nm (108-111). Absorption at this wavelength leads to the population of three closely spaced electronic states (A_1, E, and A_2 in D_3 symmetry) which are in rapid thermal equilibrium at room temperature (112). Emission from these triplet states is responsible for the luminescence of this complex (113). The energy of the luminescent excited state at room temperature has been calculated from the low temperature emission spectrum to be 18.0 kK (7,30 f).

2. Intensity Quenching of $*Ru(bpy)_3^{2+}$

The luminescence quenching of $*Ru(bpy)_3^{2+}$ can be expressed by the simple equation

$$*Ru(bpy)_3^{2+} + Q \longrightarrow Ru(bpy)_3^{3+/1+} + Q^{-/+} \qquad (23)$$

where Q represents the quencher species. Steady state analysis of a reaction scheme including excitation,

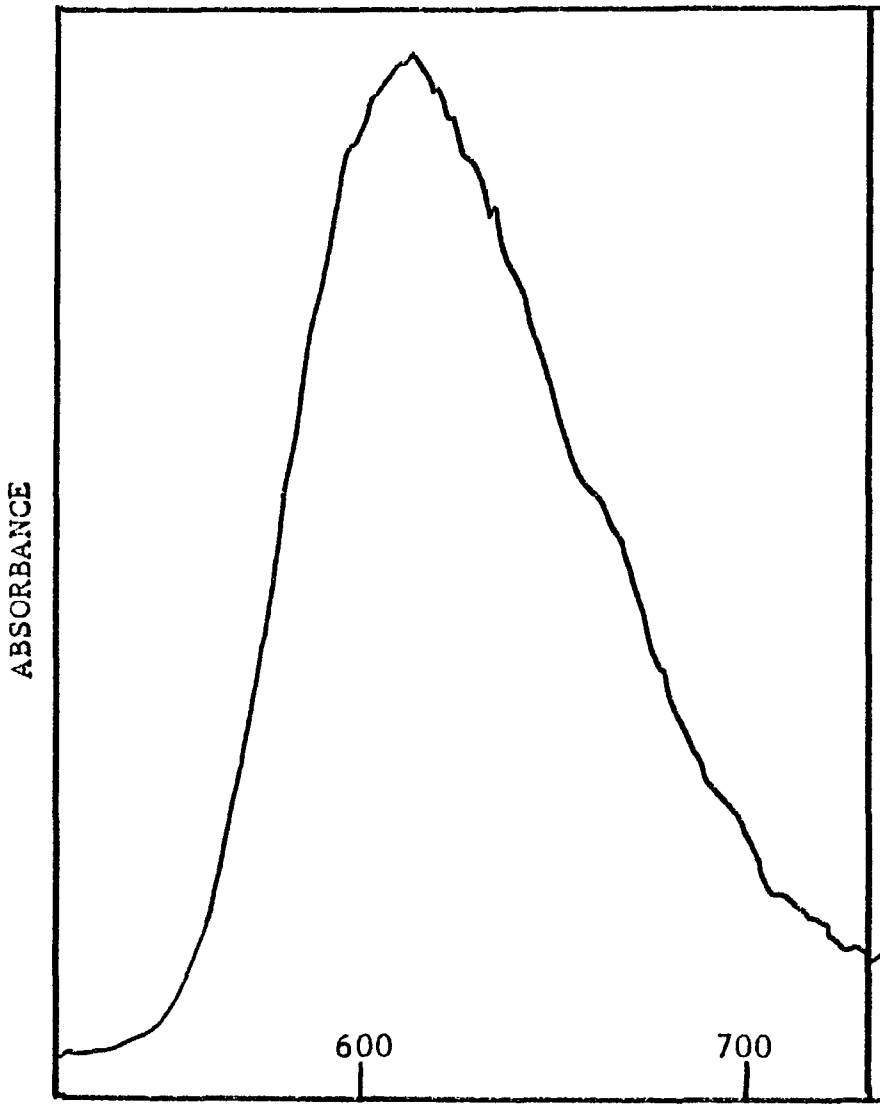

Figure 13. Emission Spectrum of 10^{-4}M $Ru(bpy)_3^{2+}$ in Water.

Figure 14. Absorption Spectrum of 10^{-4}M $Ru(bpy)_3^{2+}$ in Water.

radiative and nonradiative relaxation, and bimolecular quenching leads to the Stern-Volmer expression

$$I_o/I = 1 + K_{sv}\,[Q] \qquad (24)$$

where I_o and I are the emission intensities in the absence and presence of quencher, respectively, and K_{sv} is the Stern-Volmer quenching constant. K_{sv} is related to k_f by

$$K_{sv} = k_f \tau_o \qquad (25)$$

where τ_o is the radiative lifetime of $*Ru(bpy)_3^{2+}$ measured in the absence of quencher; $\tau_o = 600 \pm 20$ nsec in aqueous solution (33). The plots of I_o/I vs $[Q]$ in Figures 15 and 16, are representative of dynamic, not static, quenching. Dynamic quenching results from the collision of donor and quencher and is limited by diffusion, while static quenching occurs within a preformed donor : quencher pair. Stern-Volmer plots of static quenching data are not linear; they curve upward sharply. Increasing ionic strength and $EDTA^{2-}$ both increased K_{sv}. It should be noted that $EDTA^{2-}$ does not quench $*Ru(bpy)_3^{2+}$ (Figure 17) and that Pq^{2+} quenches by a dynamic mechanism when $EDTA^{2-}$ is present (Figure 16).

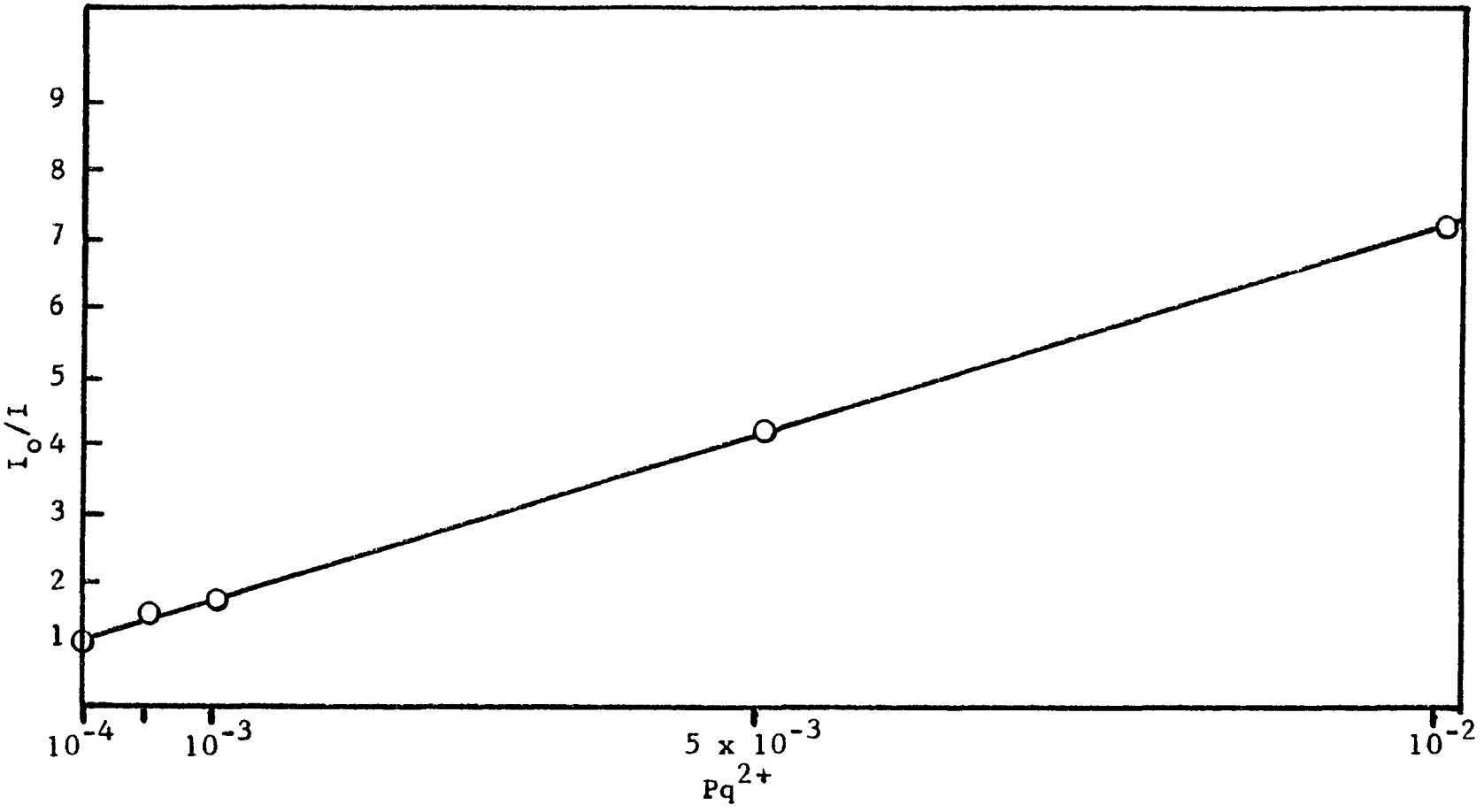

Figure 15. Stern - Volmer Plot of the Quenching of $^{*}Ru(bpy)_3^{2+}$ by Pq^{2+} (0.1M KCl).

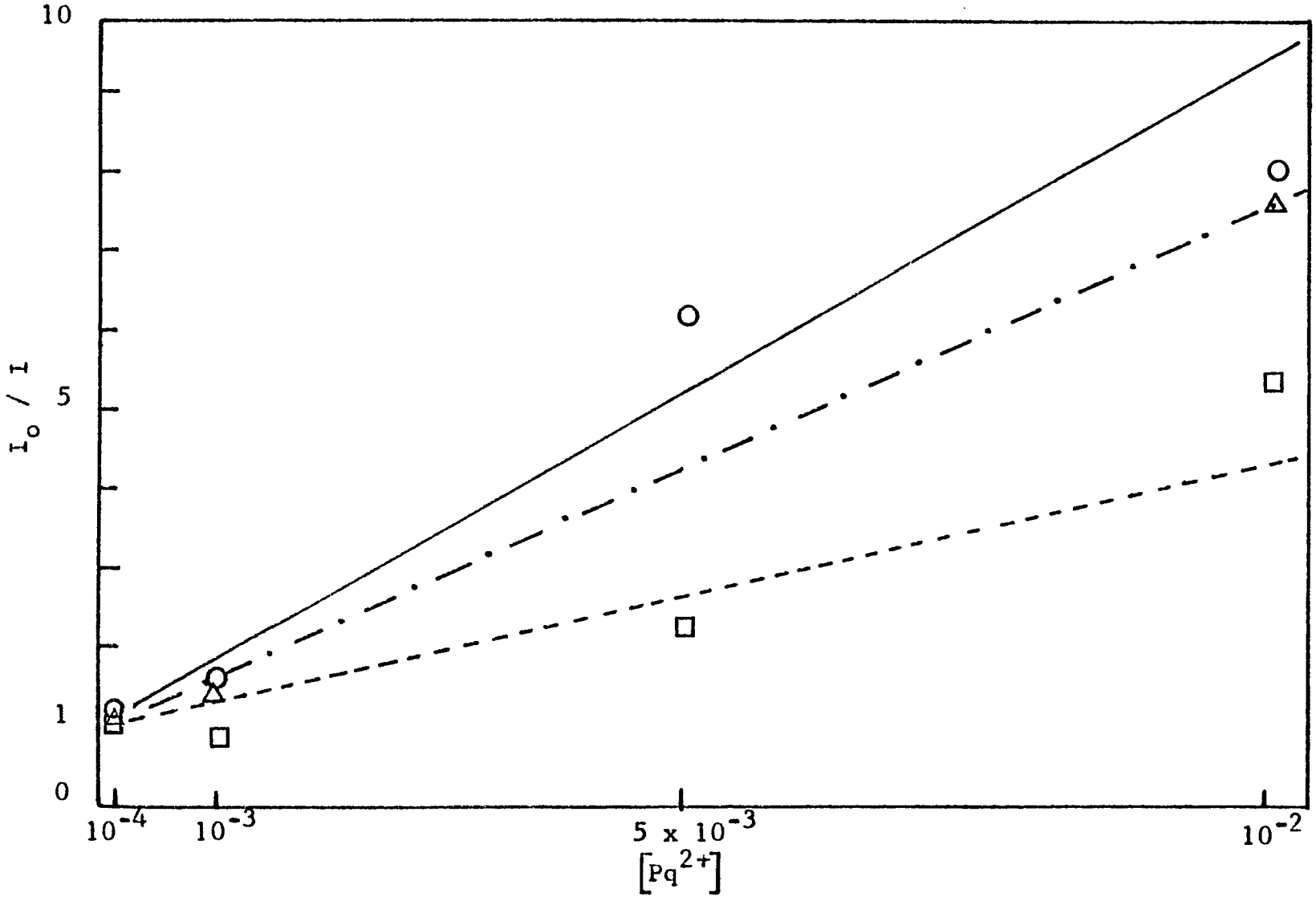

Figure 16. Effect of EDTA and Ionic Strength(KCl) on the Rate of Quenching of*$Ru(bpy)_3^{2+}$ by Pq^{2+}. 0.1M KCl(- - - -); 0.01M EDTA(-·-·-); 0.1M KCl and 0.01M EDTA(———).

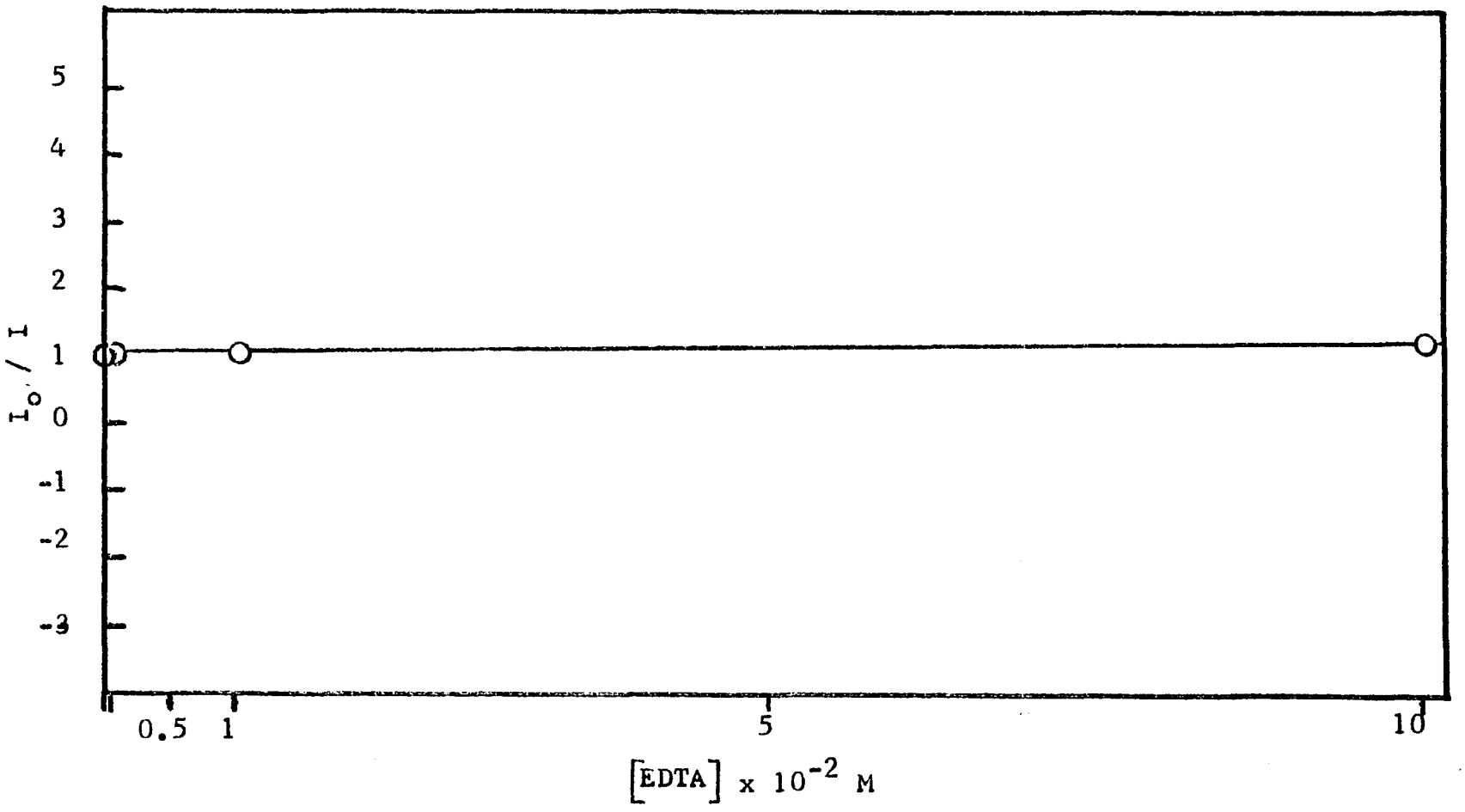

Figure 17. Stern - Volmer Plot of the Quenching of *$Ru(bpy)_3^{2+}$ by EDTA (0.1M KCl).

3. Determination of ϕ_{Pq^+}

It has been demonstrated that Pq^+ reduces water in the presence of a catalyst. An accurate value of ϕ_{Pq^+} therefore, should be a good indicator of the potential efficiency of a particular system. Values of ϕ_{Pq^+} were determined over a range of Pq^{2+} concentrations using the apparatus depicted in Figure 3. Extrapolation of a plot ot $1/\phi_{Pq^+}$ against $1/[Pq^{2+}]$, Figure 18, gives a limiting yield of 4×10^{-3} for the aqueous $Ru(bpy)_3^{2+}$ / $EDTA^{2-}$ / Pq^{2+} system. An induction period of up to several minutes was observed in these experiments (41). The Pq^+ formed during this period was not stable. A second determination of ϕ_{Pq^+} was made using the apparatus described in Figure 4. A representative recorder trace, Figure 19, shows the rapid increase in absorbance at 634 nm. A steady state is reached and when the exciting light is shut off, a partial loss of absorbance occurs. The rate of Pq^+ formation was calculated from the initial increase in absorbance. Extrapolation of the plot in Figure 20 gave a limiting yield of 0.05 using the same concentrations employed in the previous experiments.

B. Role of EDTA

There is no net chemical change in the $Ru(bpy)_3^{2+}$ / Pq^{2+} system in the absence of EDTA. Photolysis of an $Ru(bpy)_3^{2+}$ / Pq^{2+} / EDTA sample produces no Pq^+. If the sample is opened to the air, the blue color

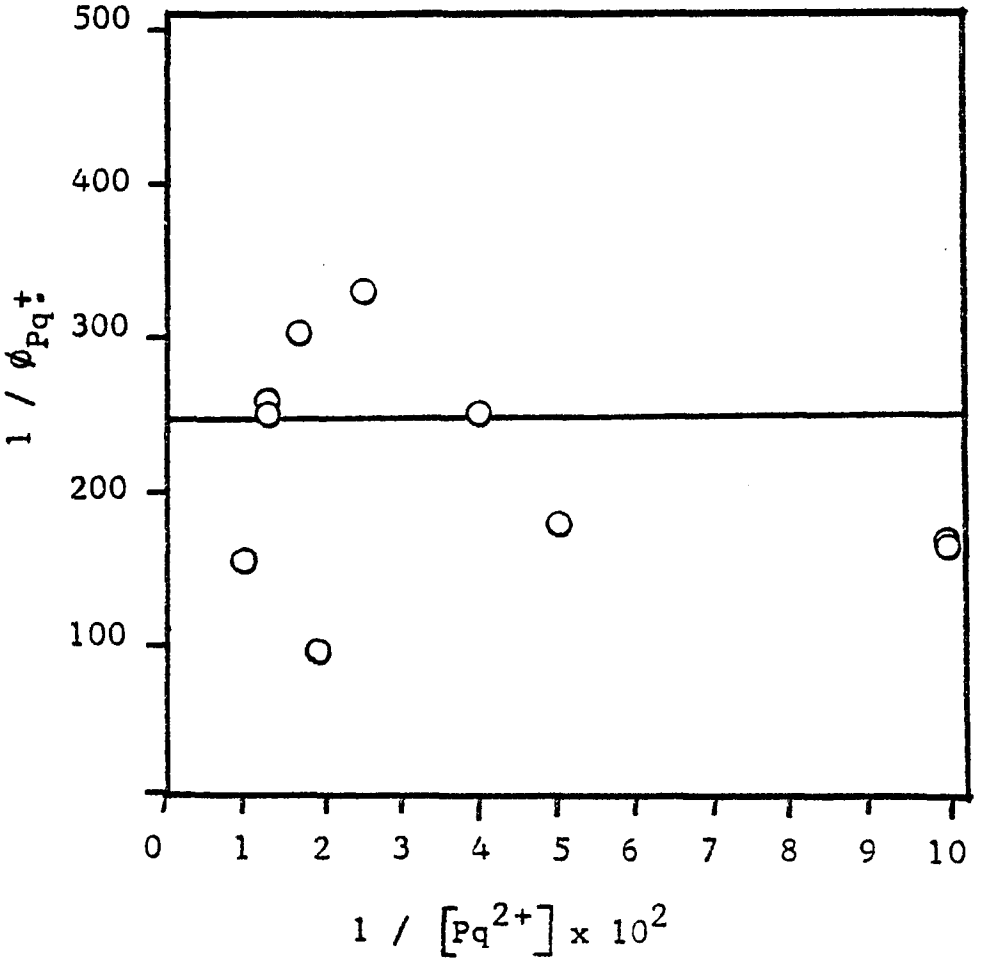

Figure 18. 1 / $\phi_{Pq^{2+}}$ as a Function of 1 / $[Pq^{2+}]$. Data obtained using the apparatus described in Figure 3. $\phi_{limit} = 4 \times 10^{-3}$.

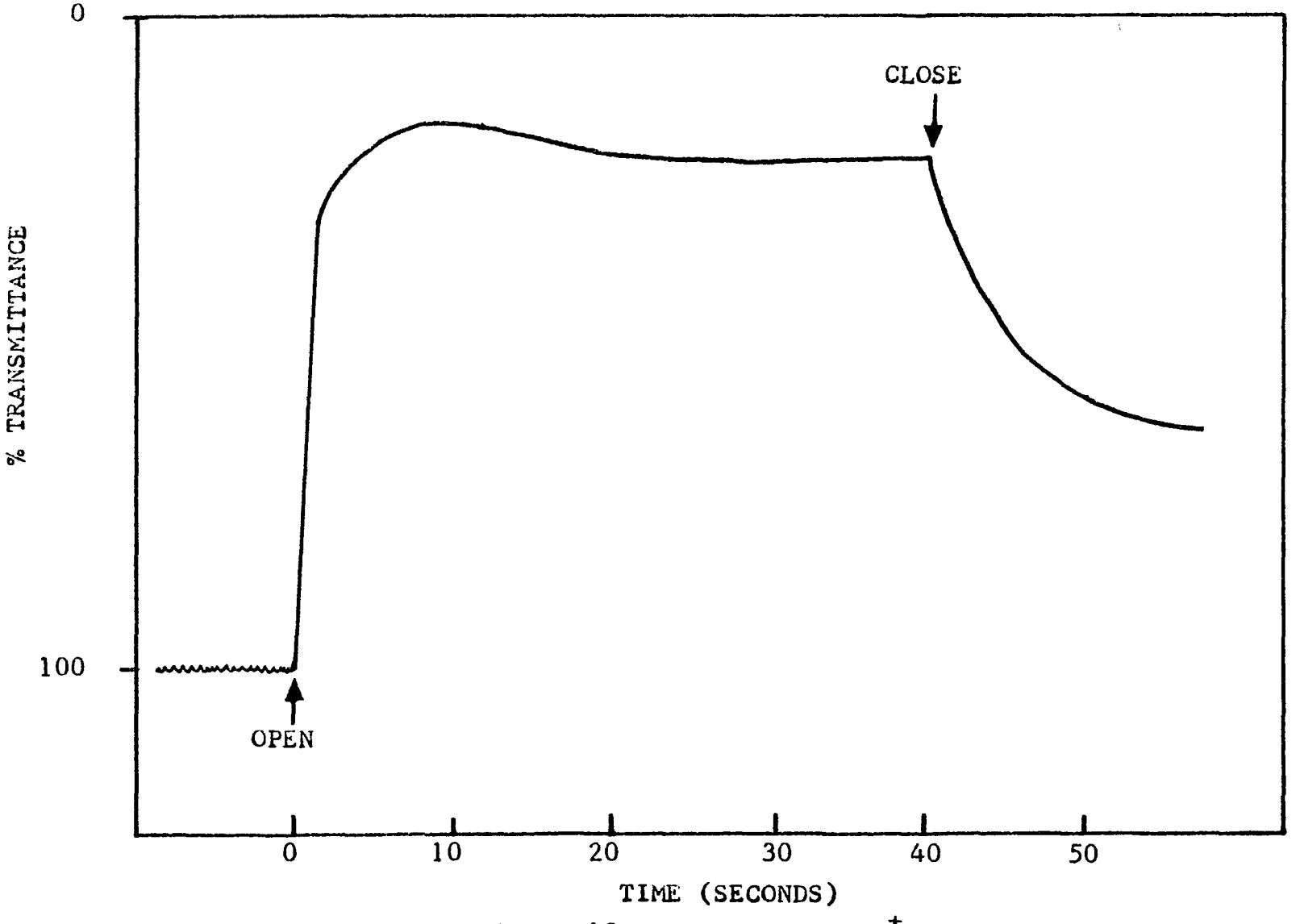

Figure 19. Formation of Pq^{+}

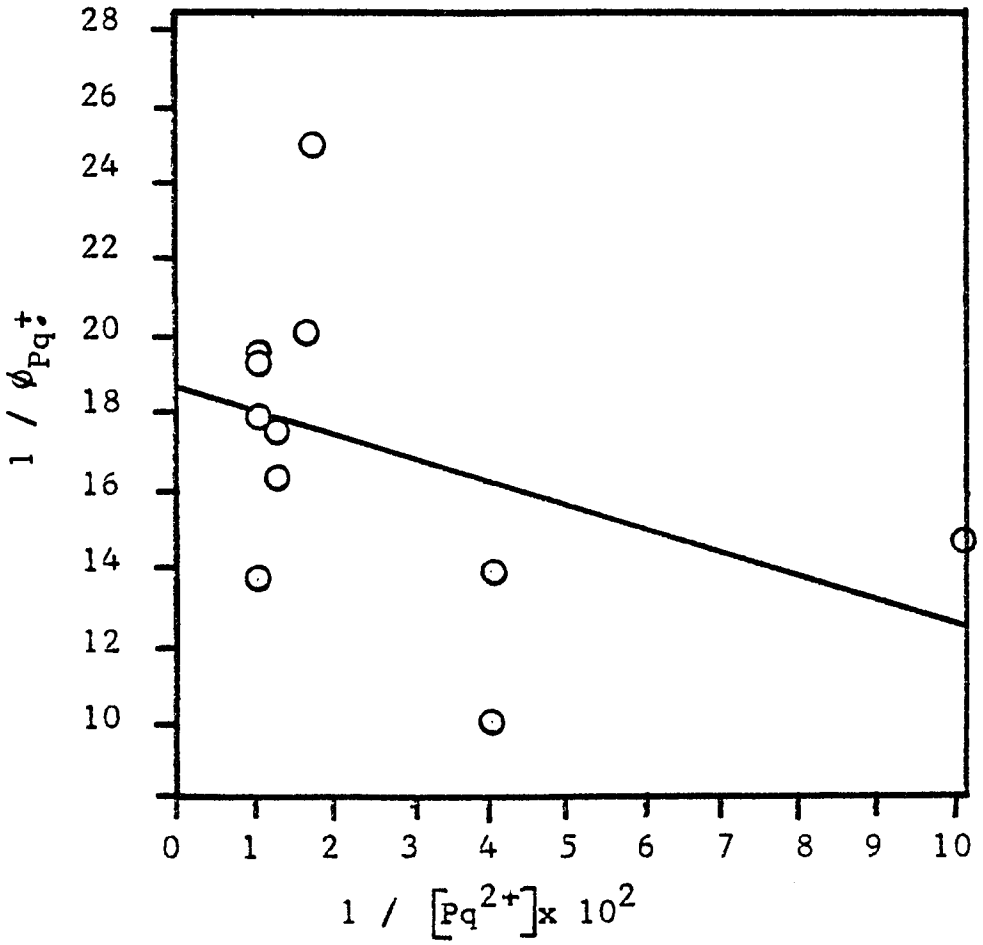

Figure 20. 1 / $\phi_{Pq^{2+}}$ as a Function of 1 / $[Pq^{2+}]$. Data obtained using the apparatus described in Figure 4. $\phi_{limit} = 5 \times 10^{-2}$.

disappears due to the reaction in equation 26 (52). After repeated photolysis and oxidation by air, a system loses its ability to photochemically produce $Pq^{+\cdot}$. Addition of fresh EDTA regenerates the system.

$$Pq^{+\cdot} + O_2 \longrightarrow Pq^{2+} + O_2^- \qquad (26)$$

It appears then that EDTA is consumed in the production of $Pq^{+\cdot}$. According to Whitten's hypothesis, the oxidized form of the electron donor must decompose to stable products if this scavenging reaction is to be competitive with the reoxidation of the catalyst or $Pq^{+\cdot}$. $Ru(bpy)_3^{3+}$ and EDTA were reacted in a sealed, evacuated system and the mixture was analyzed for the decomposition products of EDTA. CO_2 was identified by G.C. (Figure 21) and the liquid phase was tested with chromotropic acid for H_2CO (Figure 22) (106). These two compounds, CO_2 and H_2CO, present in a 1:7 ratio in these systems (Table I), and ethylenediaminetriacetic acid have been identified by other workers (51) as oxidation products of EDTA.

EDTA does not quench $^*Ru(bpy)_3^{2+}$, but as stated earlier, it alters the rate at which Pq^{2+} quenches. This data may offer an insight into the mechanism by which EDTA effectively competes with the rapid back reaction of $Ru(bpy)_3^{3+}$ and $Pq^{+\cdot}$. Table II summarizes the

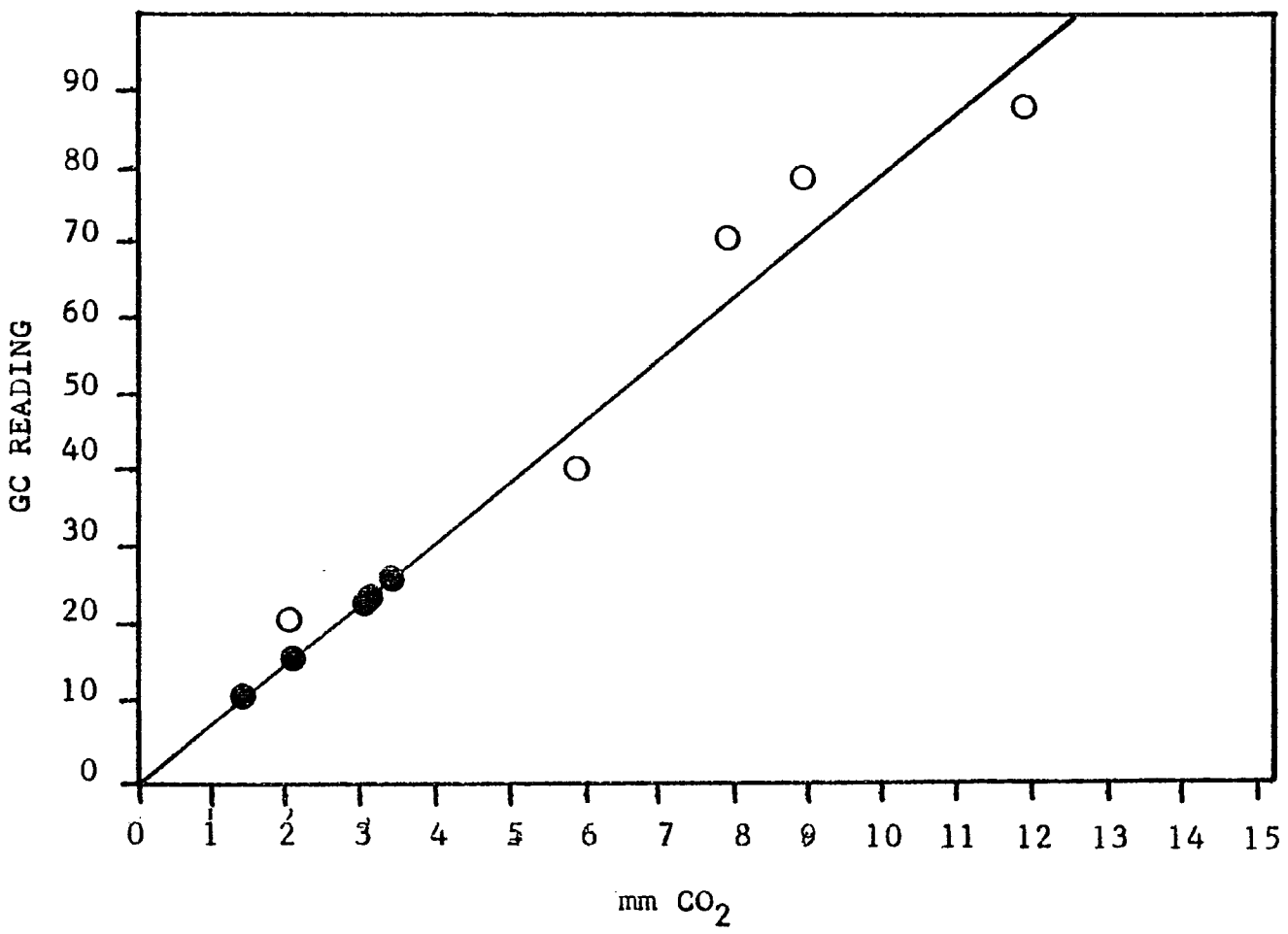

Figure 21. Moles of CO_2 Evolved on Decomposition of EDTA

Calibration plot (O): T=294°K, V=82ml, P= mm Hg; experimental data(●)

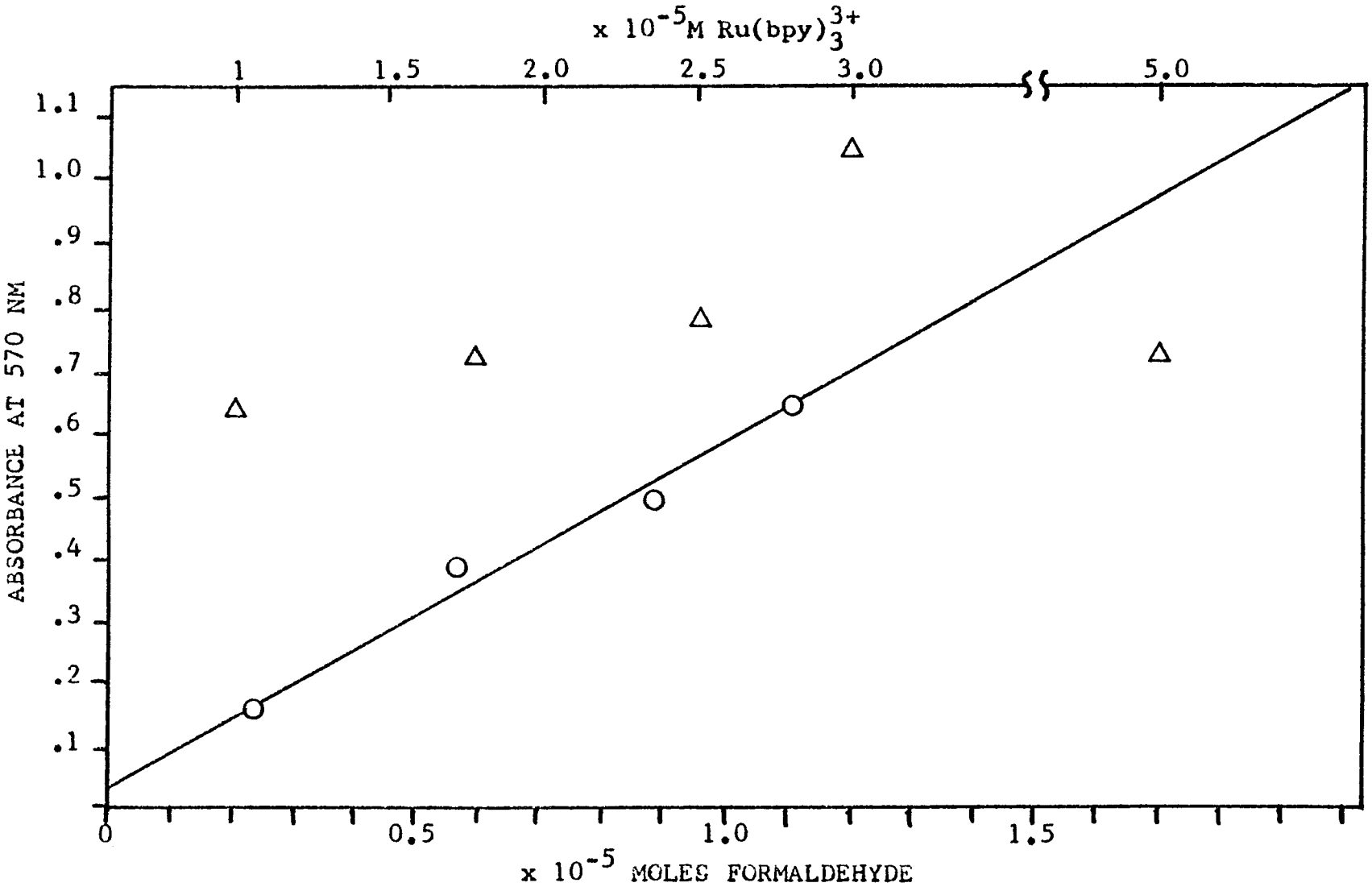

Figure 22. Chromotropic Acid Analysis for Formaldehyde. Calibration data(O), experimental data(△)based on $\left[Ru(bpy)_3^{3+}\right]$.

Table I. Decomposition Products of EDTA.

moles $Ru(bpy)_3^{3+}$	moles CO_2	moles H_2CO
4.2×10^{-5}	1.41×10^{-5}	1.1×10^{-4}
1.04×10^{-5}	0.68×10^{-5}	1.25×10^{-4}
2.63×10^{-5}	1.53×10^{-5}	1.38×10^{-4}
3.17×10^{-5}	1.52×10^{-5}	1.85×10^{-4}
1.86×10^{-5}	0.94×10^{-5}	1.27×10^{-4}

Table II. The Effect of $EDTA^{2-}$ on the Quenching of $^*Ru(bpy)_3^{2+}$ (10^{-4}M) by Pq^{2+} (10^{-4} - 10^{-2}M).

[KCl]	$[EDTA^{2-}]$	μ [a]	K_{SV} (M^{-1})	k_f ($M^{-1}s^{-1}$)
0.10M	0	0.1	$.67 \times 10^3$	1.1×10^9
0	0.01M	0.03	1.3×10^3	2.16×10^9
0.1 M	0.01M	0.13	1.7×10^3	2.8×10^9
1.0 M	0.01M	1.03	2.3×10^3	3.88×10^9

[a]This μ is a relative value based only on the KCl and Na_2EDTA contributions.

quenching data. This data suggests that EDTA acts in a specific way; it is not exerting a simple ionic strength effect. This increase in the quenching rate may be attributed to a decrease in the repulsion of the donor and quencher dications. Therefore, a series of experiments were performed to determine whether EDTA altered the nature of the reactants in solution.

Absorption spectra did not indicate any complex formation between EDTA and $Ru(bpy)_3^{2+}$ or Pq^{2+} (114). Conductiometric titrations, plotted in Figures 23-26, did not reveal the presence of any new solution species, but the large number of multiply charged ions present made this experiment inconclusive.

To probe the possibility that EDTA reacts with a dissociated Ru species, solutions of $Ru(bpy)_3^{2+}$ were photolyzed and extracted with $CHCl_3$ to analyze for free ligand (see Section IV-4). Decomposition of only 0.8% of the starting complex was detected in both photolyzed and dark reactions. This degree of dissociation corresponds to a change in absorbance of 0.01 at 452 nm. Such a change would be difficult to detect due to the experimental error of the measurement. This observation is in agreement with that of other workers that under normal conditions, photolysis causes no appreciable change in the concentration of $Ru(bpy)_3^{2+}$ (34,35).

The possibility that $EDTA^{2-}$ formed an ion pair

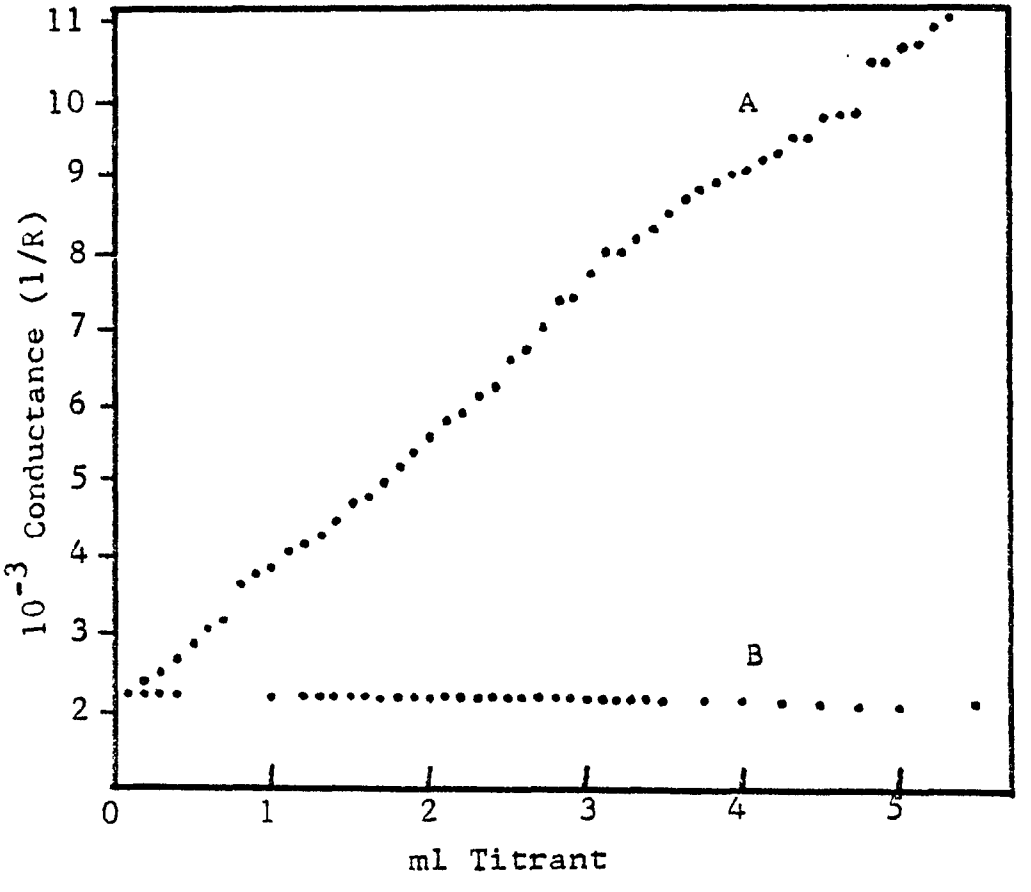

Figure 23. Conductiometric Titration of 10^{-3}M Pq^{2+} with (A) 10^{-1}M $EDTA^{2-}$ and (B) water.

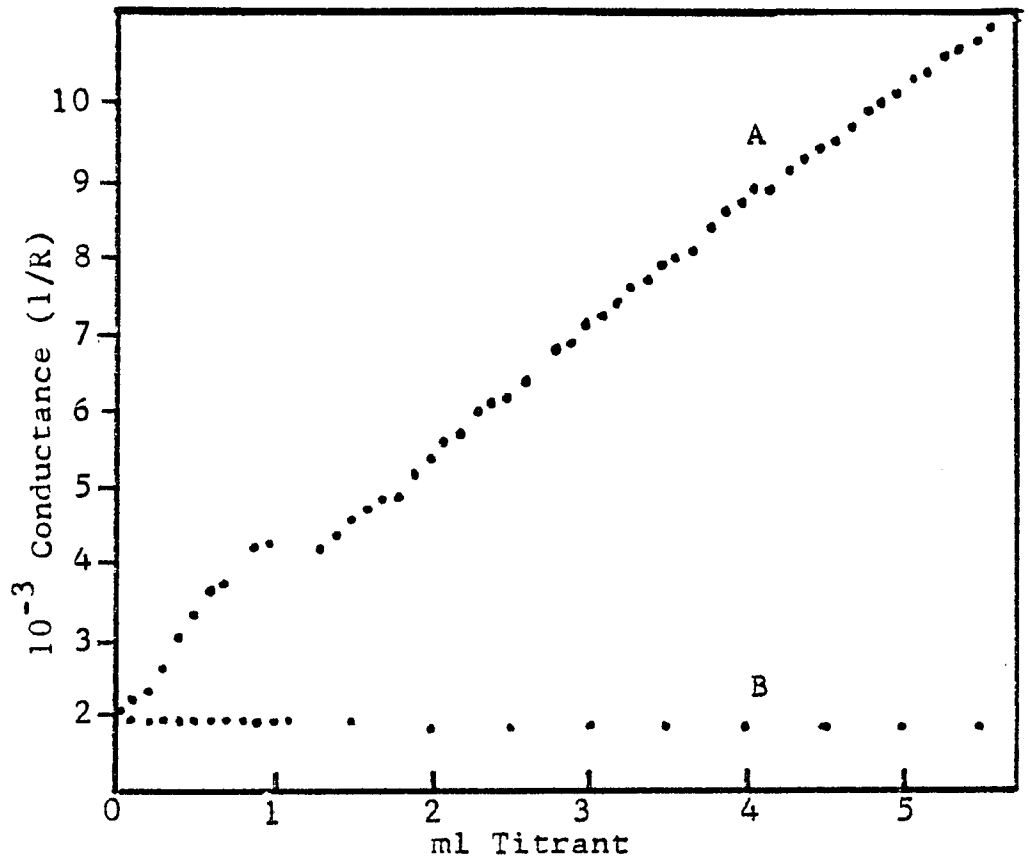

Figure 24. Conductiometric Titration of 10^{-3}M $Ru(bpy)_3^{2+}$ with (A) 10^{-1}M $EDTA^{2-}$ and (B) water.

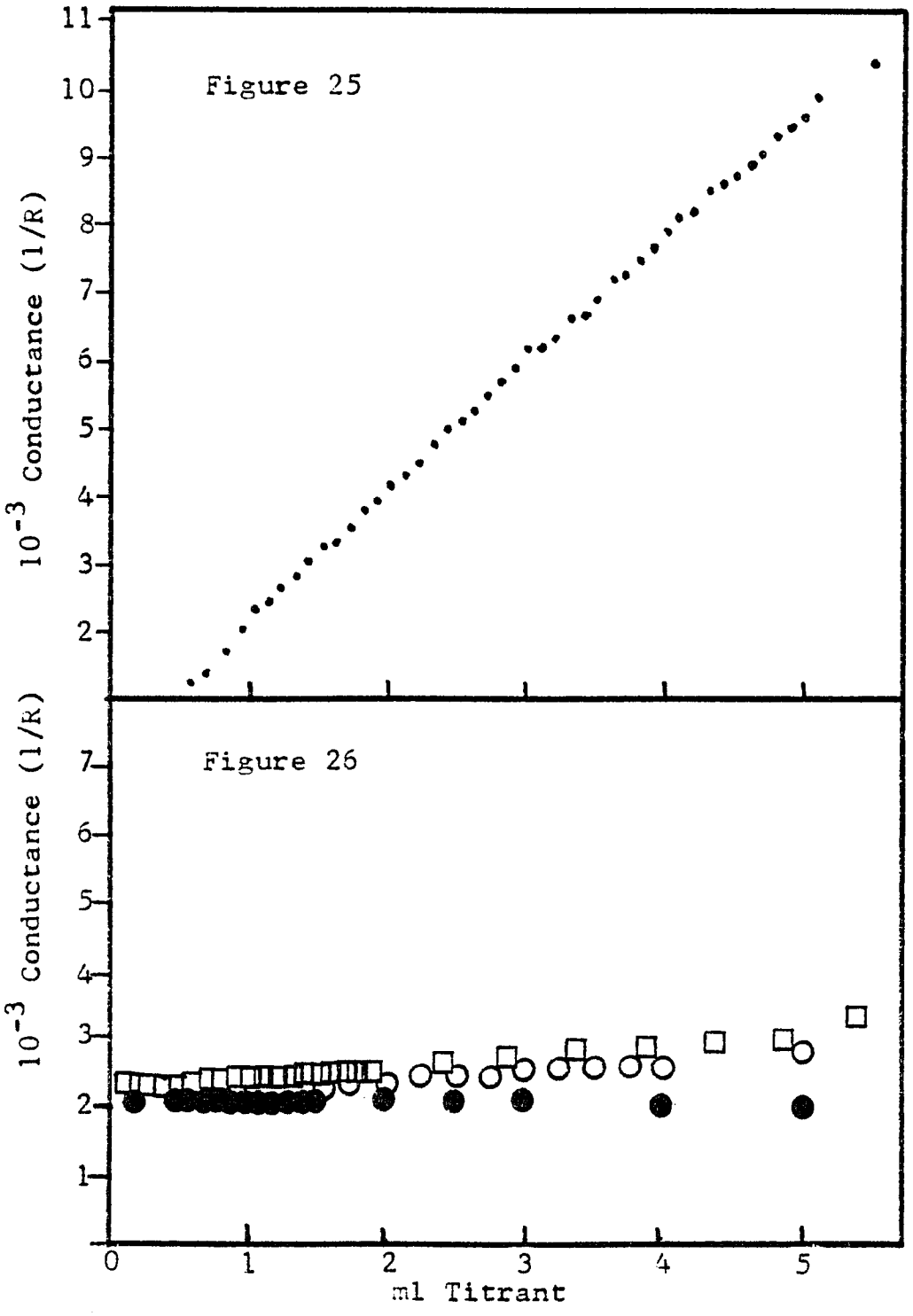

Figure 25. Blank Titration of Water with 10^{-1}M $EDTA^{2-}$.

Figure 26. Conductiometric Titration of a) 10^{-2}M Pq^{2+} with water (●), b) 10^{-2}M Pq^{2+} with 10^{-1}M EDTA (○), and c) 2 x 10^{-2}M KCl with 10^{-1}M EDTA (□).

with one of the dicationic reactants was examined by NMR. NMR spectra of each component in D_2O were recorded individually (Figures 27-29) and then the three possible combinations of reactants were examined. Spectra of $Ru(bpy)_3^{2+}$ / Pq^{2+} and $EDTA^{2-}$ / Pq^{2+} solutions were the same as those of the pure compounds. On addition of $Ru(bpy)_3^{2+}$ to $EDTA^{2-}$, however, the $EDTA^{2-}$ protons shift downfield in direct proportion to the concentration of $Ru(bpy)_3^{2+}$ (Figure 30). Tables III and IV summarize the frequency shifts as a function of concentration. Again we see that the effect of $Ru(bpy)_3^{2+}$ on $EDTA^{2-}$ is not simply due to ionic strength. These results are consistent with the formation of an ion pair. A plot of the frequency shift, $\Delta\delta$, versus the $Ru(bpy)_3^{2+}$: $EDTA^{2-}$ mole ratio suggests that a 1:1 ion pair exists when the two reactants are present in equal concentrations (see Figure 31). Based on this assumption an equilibrium constant, $K_{eq} \geq 78$, was calculated from these data using equation 27 (115), where N_A and N_B are the mole fraction of free and ion-paired EDTA, δ_A = 3.88 ppm and δ_B = 4.13 ppm.

$$\delta_{AVERAGE} = N_A \delta_A + N_B \delta_B \qquad (27)$$

While formation of an ion pair between a dication and a dianion is intuitively acceptable (116),

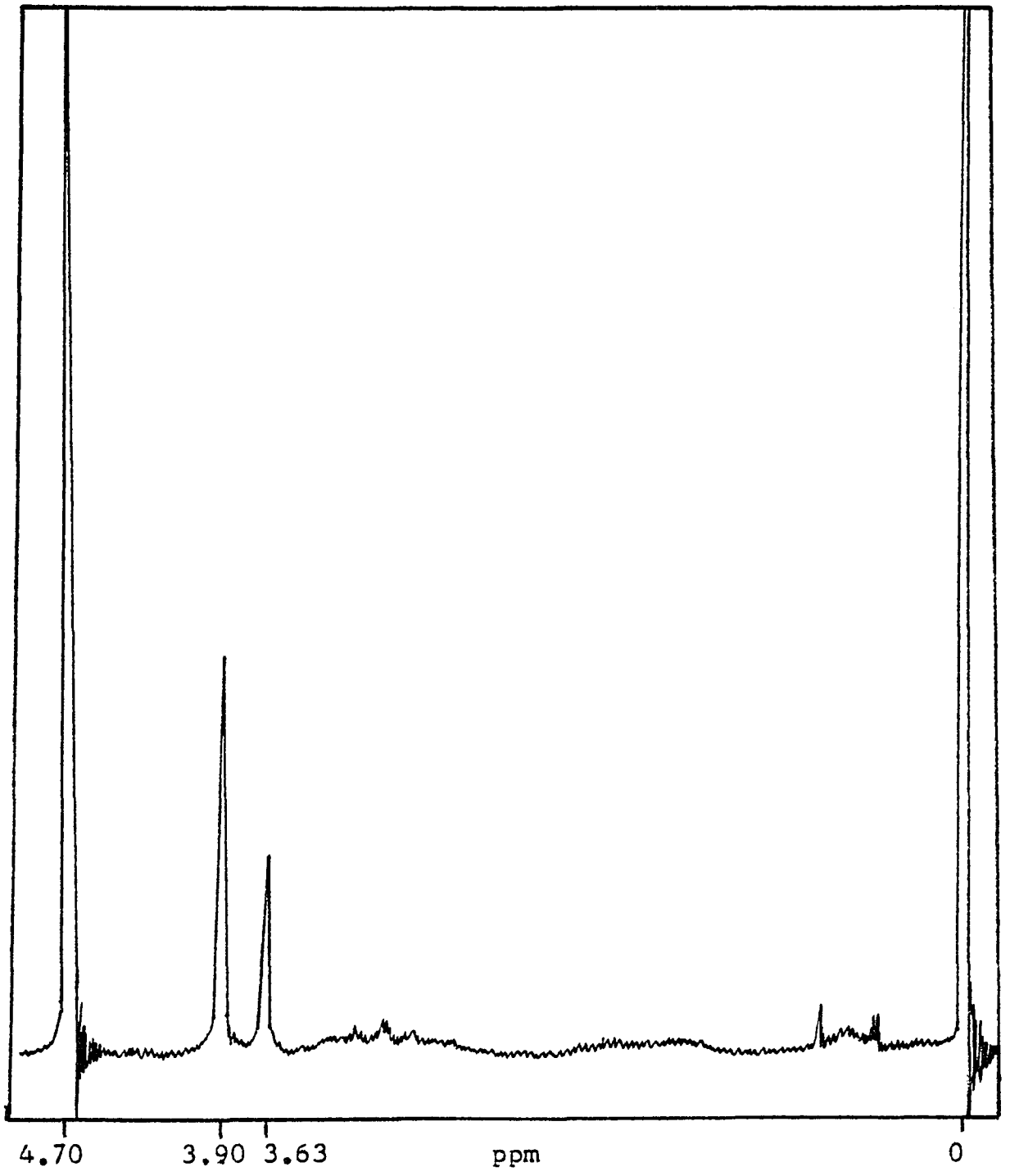

Figure 27. NMR Spectrum of 0.1M Na_2EDTA in D_2O, 4% DSS.

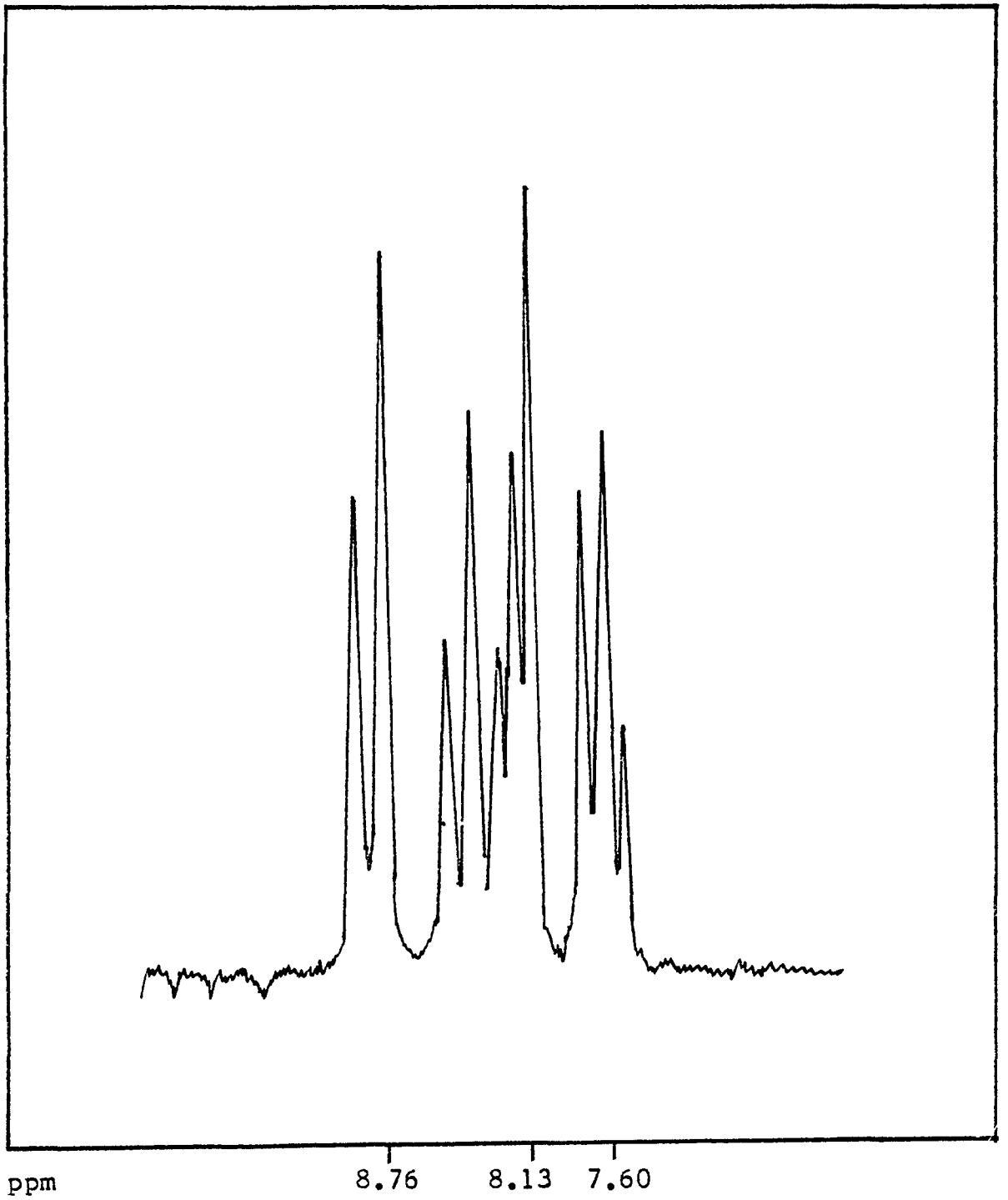

Figure 28. NMR Spectrum of 0.1M $Ru(bpy)_3Cl_2$ $3H_2O$ in D_2O, 4% DSS.

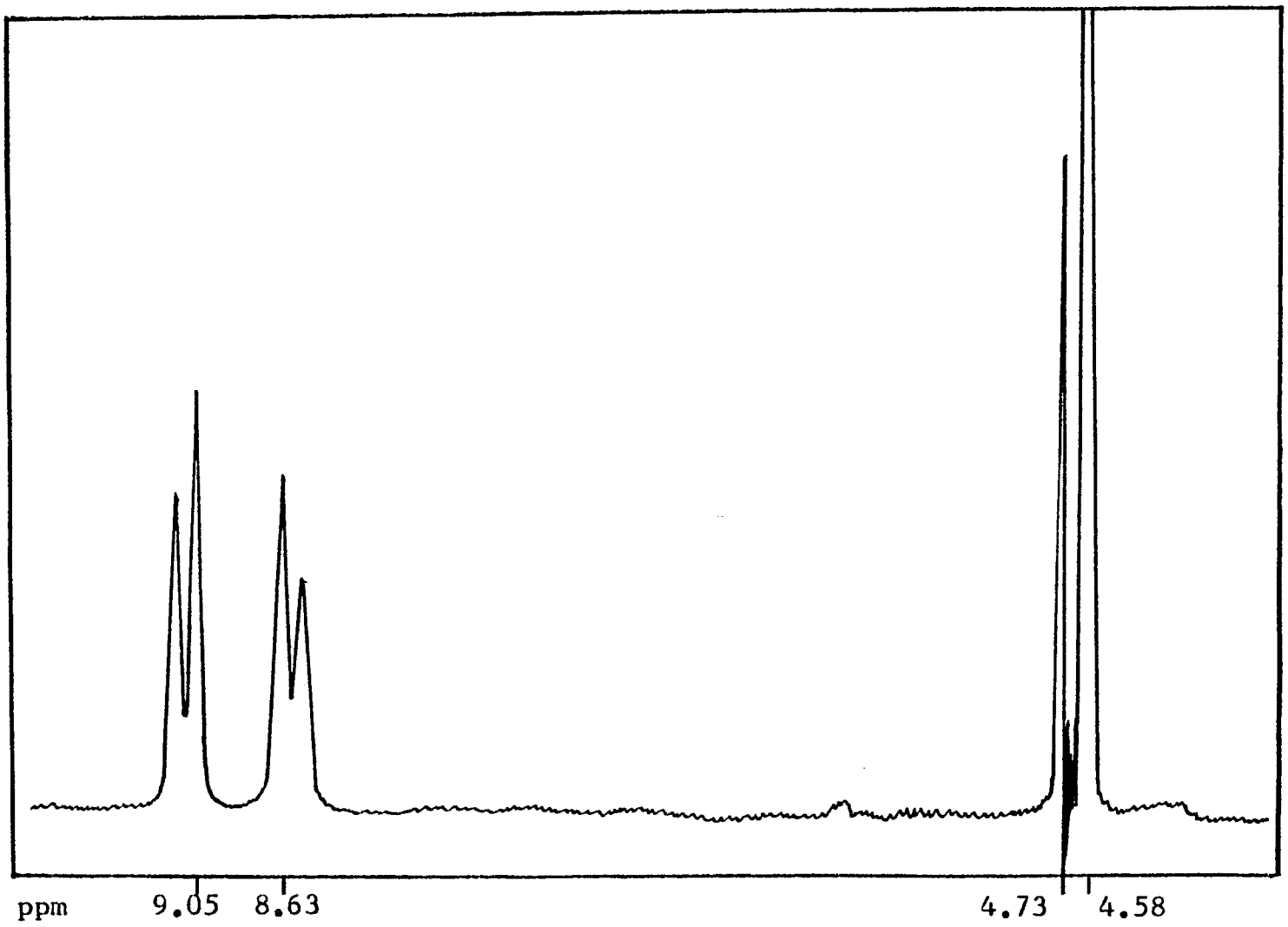

Figure 29. NMR Spectrum of $PqCl_2 \cdot x\ H_2O$ (0.1M) in D_2O, 4% DSS.

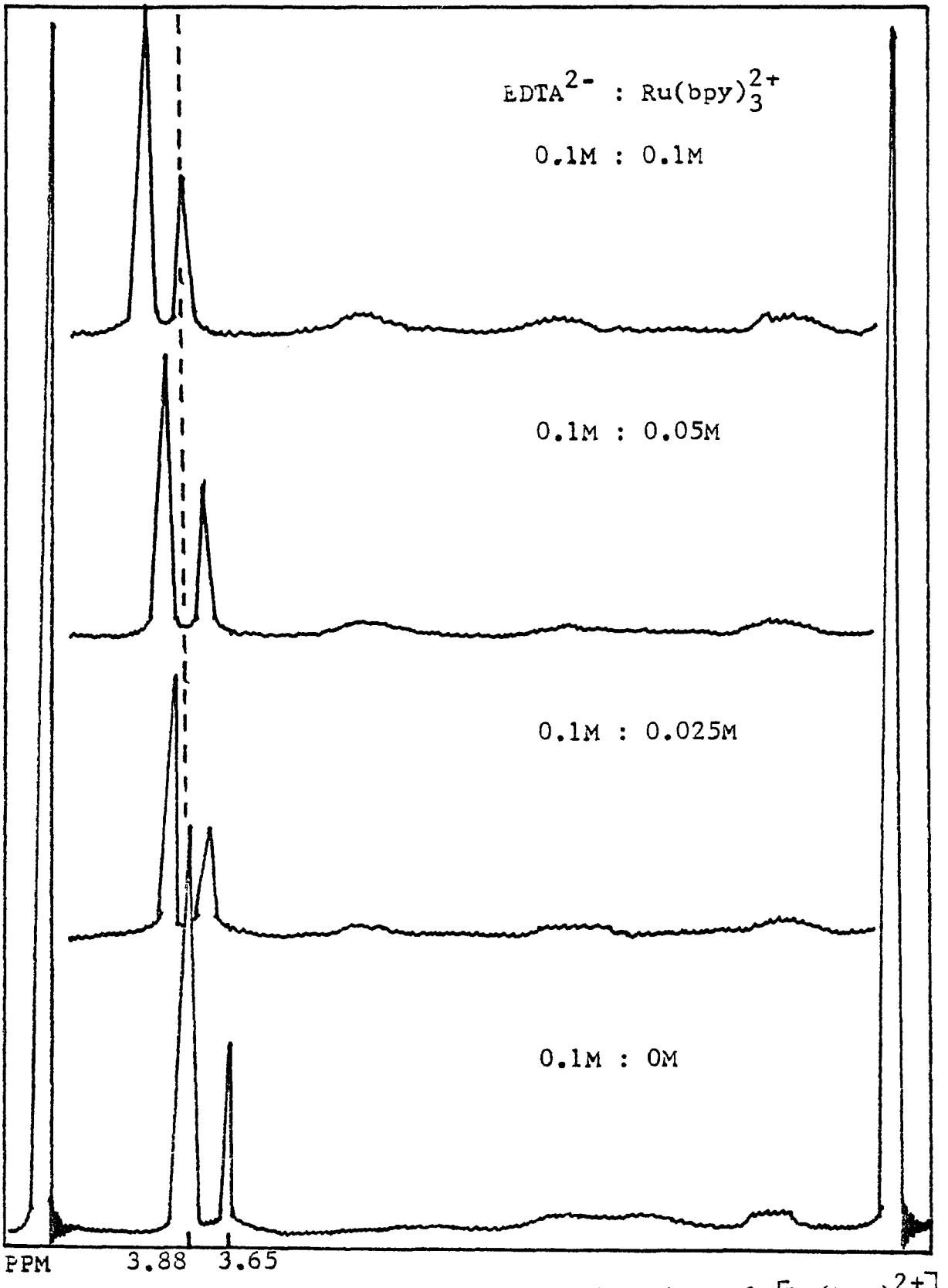

Figure 30. Shift of EDTA Protons as a Function of $[Ru(bpy)_3^{2+}]$

Table III. The Effect of Varied Ionic Strength on the NMR Spectrum of 0.1M Na_2EDTA (D_2O, DSS).

KCl	ppm ($\Delta\delta$)	ppm ($\Delta\delta$)
0	3.88	3.65
0.3 M	3.90 (0.02)	3.66 (0.01)
1.0 M	3.90 (0.02)	3.68 (0.03)

Table IV. The Effect of $Ru(bpy)_3^{2+}$ on the NMR Spectrum of Na_2EDTA (D_2O, DSS).

$Ru(bpy)_3^{2+}$	$EDTA^{2-}$	ppm ($\Delta\delta$)	ppm ($\Delta\delta$)
0	0.05 M	3.90	3.63
0.0125 M	"	3.93 (0.03)	3.72 (0.09)
0.025 M	"	3.98 (0.08)	3.77 (0.14)
0.05 M	"	4.05 (0.15)	3.83 (0.20)
0.075 M	"	4.07 (0.17)	3.85 (0.22)
0.1 M	"	4.13 (0.23)	3.92 (0.29)
0	0.1 M	3.88	3.65
0.025 M	"	3.97 (0.09)	3.73 (0.08)
0.05 M	"	4.03 (0.15)	3.80 (0.15)
0.1 M	"	4.15 (0.27)	3.93 (0.28)
0.1 M	"	4.13 (0.25)	3.90 (0.25)

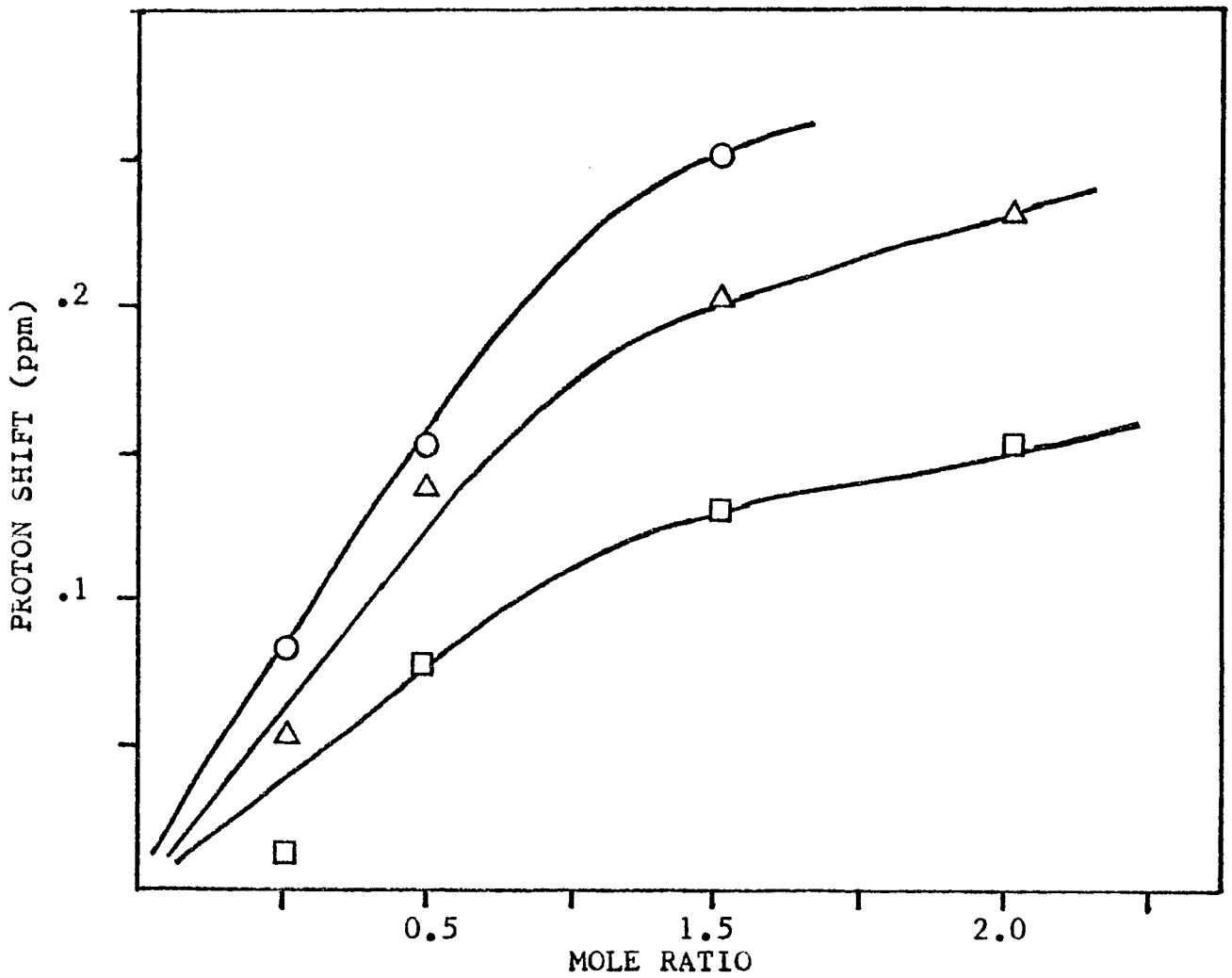

Figure 31. Downfield Shift of EDTA Proton Resonances as a Function of the Mole Ratio $Ru(bpy)_3^{2+}$: EDTA. 0.1M EDTA and 0 - 0.1M $Ru(bpy)_3^{2+}$, (○) 3.9 ppm, (□) 3.65 ppm; 5 x 10^{-2}M EDTA and 0 - 7.5 x 10^{-2}M $Ru(bpy)_3^{2+}$, (△) 3.9 ppm.

it must be demonstrated that the formation of this species is necessary in these systems. Inhibition of ion pair formation should affect the reaction rate if this is the case. A number of experiments were performed in 0.1 N H_2SO_4; under these conditions EDTA is protonated and neutral. Coulombic attraction is negligible and ion pairing would be minimal. When these acidic solutions (10^{-4} M $Ru(bpy)_3^{2+}$, 10^{-2} M Pq^{2+}, 10^{-2} M EDTA) were irradiated for prolonged periods of time, no net formation of $Pq^{+\cdot}$ was observed. While EDTA is readily oxidized by $Ru(bpy)_3^{3+}$ even in 1.0 N H_2SO_4, the pH dependence of its potential has to be considered. Additional experiments were performed at pH=7, with the EDTA tied up in an Fe(II) complex. This complex has a potential of 0.117 V from pH 2-10 (117) and is readily oxidized by $Ru(bpy)_3^{3+}$.

$$FeEDTA^{2-} \longrightarrow FeEDTA^{-} + e^{-}$$

$$E = {}^{-}0.117 \text{ V (pH 2-10)} \qquad (28)$$

$$Ru(bpy)_3^{3+} + e^{-} \longrightarrow Ru(bpy)_3^{2+}$$

$$E = 1.3 \text{ V} \qquad (29)$$

Iron free solutions containing 10^{-1} M KCl, 10^{-2} M EDTA, 10^{-2} M Pq^{2+} and 10^{-4} M $Ru(bpy)_3^{2+}$ were buffered at pH=7, degassed and irradiated. The formation of $Pq^{+\cdot}$ was immediately apparent. The same reaction solution

also containing 10^{-2} M Fe^{2+} was photolyzed but there was no net reaction. Using published equilibria data (118), it can be calculated that only 9.6×10^{-6} M Fe^{2+} and EDTA are left free in solution. Therefore, ion pairing between $Ru(bpy)_3^{2+}$ and free EDTA would be minimal and the yield of $Pq^{+\cdot}$ should decline.

C. Determination of the Yield of H_2

Interest in these reaction systems is based on their potential for H_2 production. Experiments were performed to determine the quantum yield of H_2 indirectly. Solutions of known volume and measured $Pq^{+\cdot}$ concentration were mixed with catalyst, 5% Pt on asbestos, and the gaseous products were analyzed. ϕ_{H_2} could be calculated from $\phi_{Pq^{+\cdot}}$ and the H_2 yield. These experiments were unsuccessful. There were two major, interdependent problems: 1) reproducibility was poor and 2) low yields required the use of large samples to facilitate detection of products.

The first problem had some obvious causes which we attempted to eliminate. The nature and quantity of the catalyst seemed to play a key role in the consistency of the results. $Pq^{+\cdot}$ once generated did not always lead to H_2 production. Although the same mass of catalyst, 5% Pt on asbestos, was used, in some experiments the rate of oxidation of $Pq^{+\cdot}$ was rapid while in others the ratio were markedly slower. The distribution of Pt^{o}

on the asbestos is so varied that mass was not a good measure of the catalyst. A more uniform catalyst was sought. Pt gauze was electrolytically blackened (105) and the pieces were reused within a set of trials, but again reproducibility was poor. One observation made in these experiments was that Pt^{o} dispersed on asbestos is a more facile catalyst than the particulate metal on platinum gauze.

Another facet of this problem is the inconsistency in results caused by solvent vapor. The capacity of the sampling loop was $\leq 5x10^{-5}$ moles at ambient temperature and pressure (Figure 32). Increased sample pressure due to solvent molecules resulted in the incomplete transfer of H_2 to the gas chromatograph. To eliminate this problem, traps were used between the sample cell and the Toepler pump, Figure 9, to freeze out the solvent vapor. However, this did not overcome the difficulty.

The problem of low yields was two fold. Poor catalysis required large initial concentrations of $Pq^{\cdot+}$ to obtain measureable quantities of H_2. An accurate measurement of $Pq^{\cdot+}$, necessary for data evaluation, is not possible at high concentrations of $Pq^{\cdot+}$. $Pq^{\cdot+}$ does not follow Beer's law in water solution (119). At high concentrations, dimer formation complicates the quantitative measurement of $Pq^{\cdot+}$. Large volumes of

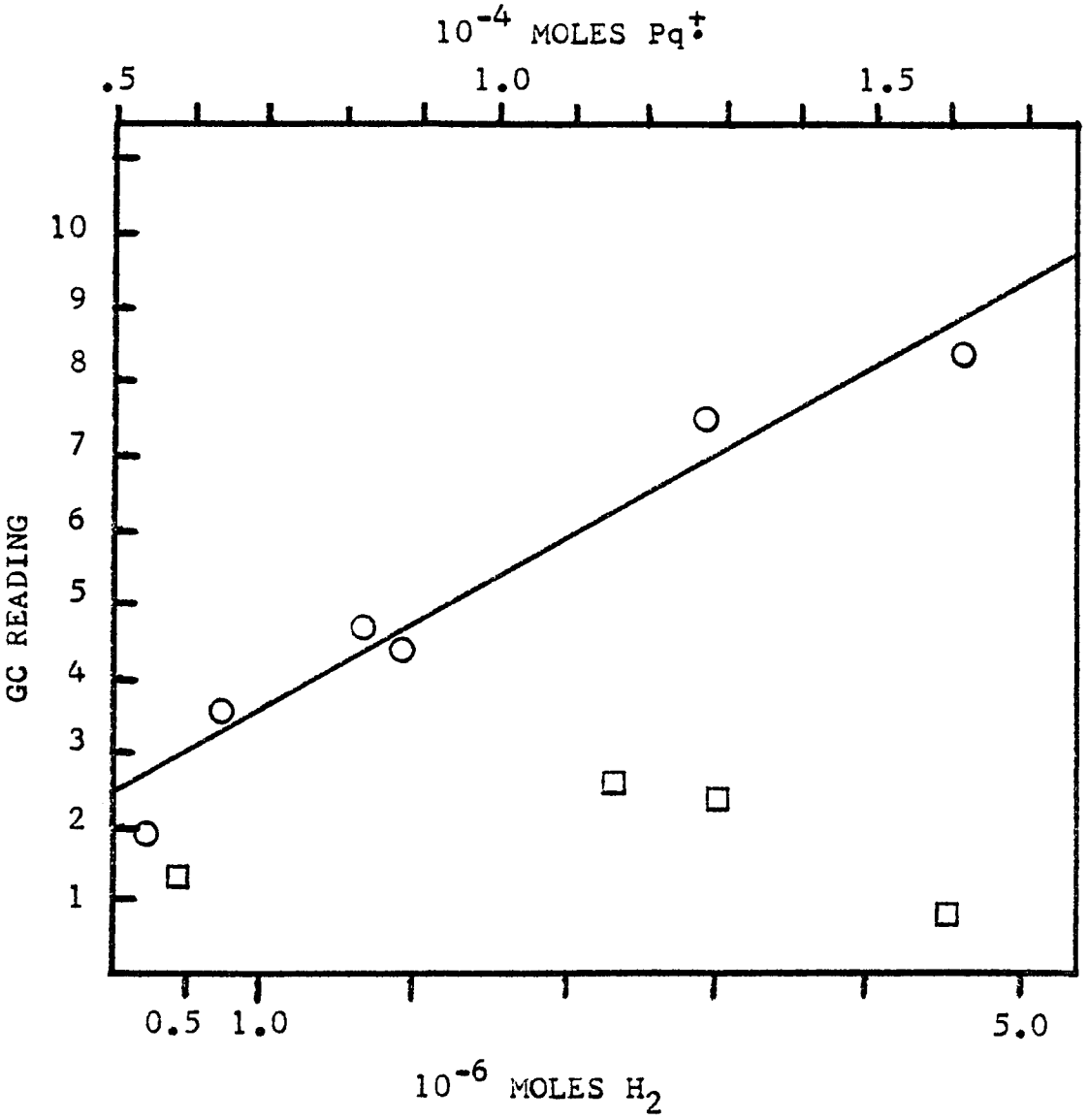

Figure 32. Calibration Plot for the GC Detection of H_2 (○)and Moles of H_2 Detected when x Moles of Pq^{+} Were Mixed with Catalyst (□).

moderate concentration would be a possibility if it weren't for the problem already discussed above - solvent vapor. In addition, it is reasonable to assume that photolysis and diffusion to the catalyst surface are less efficient in bulk quantities, leading again to low yields.

Significant quantities of H_2 have been isolated from systems which were photolyzed for long intervals while being stirred with catalyst. No calculations were made for those trials, however, since the number of moles of $Pq^{+\cdot}$ was undetermined.

II. Glass Studies

A. Adsorption of Reagents

1. Determination of the Number of Cavities/g Glass

The number of cavities/g of glass was determined to be $1.2 + 0.3 \times 10^{18}$ from measurements, outlined in IV-B-2a, on approximately 40 pieces of clean dry glass. The uncertainty in this value is consistent with the claimed deviation of 30% in the cavity size (96,97).

2. Adsorption of Reagents

To prepare glasses containing reagents, a clean dry glass was placed in an aqueous or non-aqueous solution of the reagent. Solvents ranging in polarity from water to cyclohexane were used. The rates of adsorption, calculated from spectral analysis of the soaking solution, for several species are depicted in Figures 33-34. The effect of ionic charge on adsorption rates and total adsorption is striking. Only 3% of the negatively charged tris-bathophenanthroline Ru(II) $^{4-}$ was adsorbed from 10 ml of an aqueous solution 10^{-4} M in reagent. 84% of a neutral species, $Ru(bpy)_2(CN)_2$, and 100% of a cationic complex, $Ru(bpy)_3^{2+}$, were adsorbed under the same conditions. Increasing the ionic strength of the soaking solutions by the addition of KCl increased the adsorption of the anionic species to 22% but caused a drop in the adsorption of cations

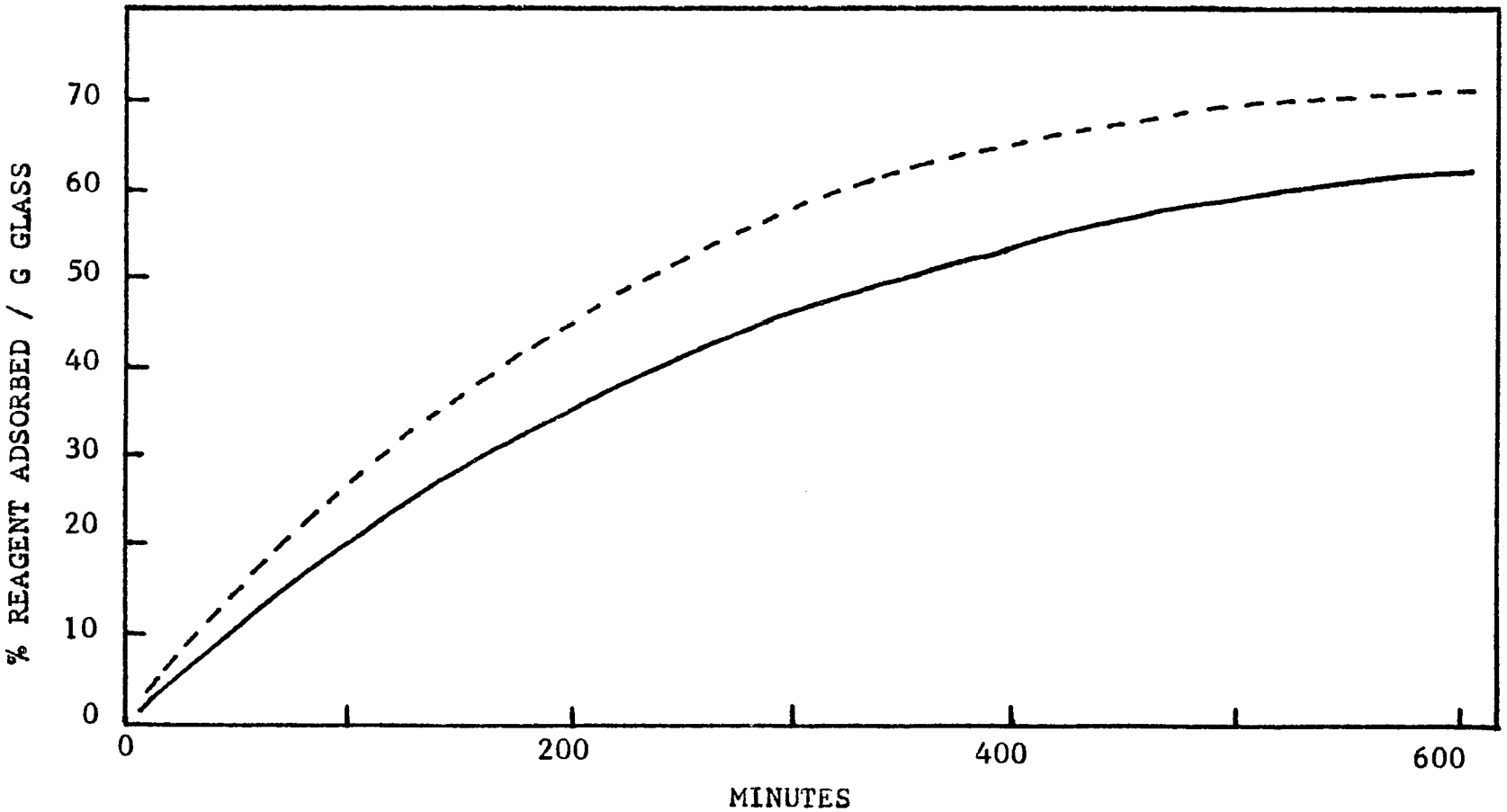

Figure 33. Adsorption Rates of : $Ru(bpy)_3^{2+}$ ——— and Pq^{2+} - - - - -.

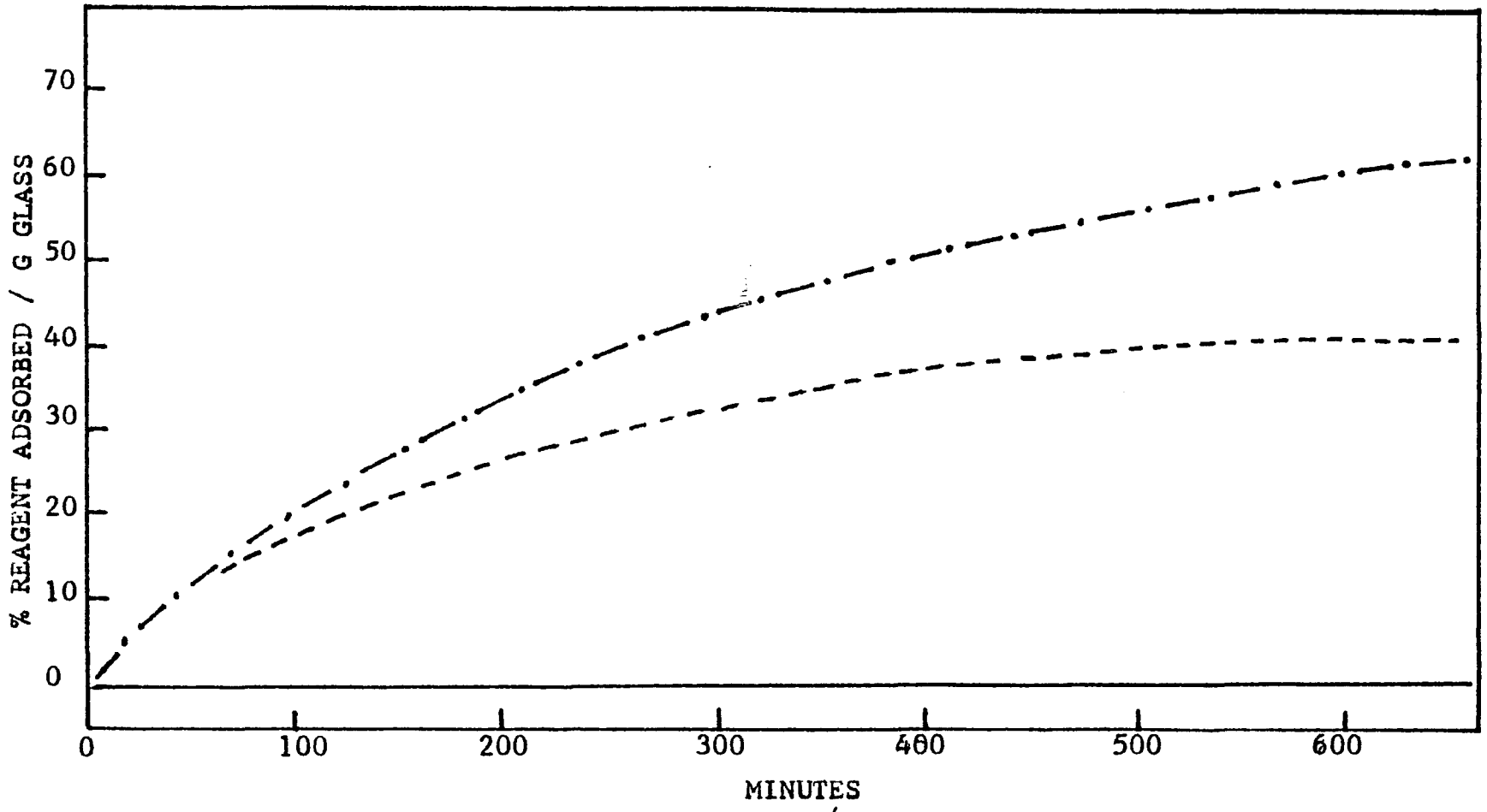

Figure 34. Adsorption Rates of: $Ru(bathophen)_3^{4-}$ ————, $Ru(bpy)_2(CN)_2$ – – – – , and $Ru(bpy)_3^{2+}$ —·—·— .

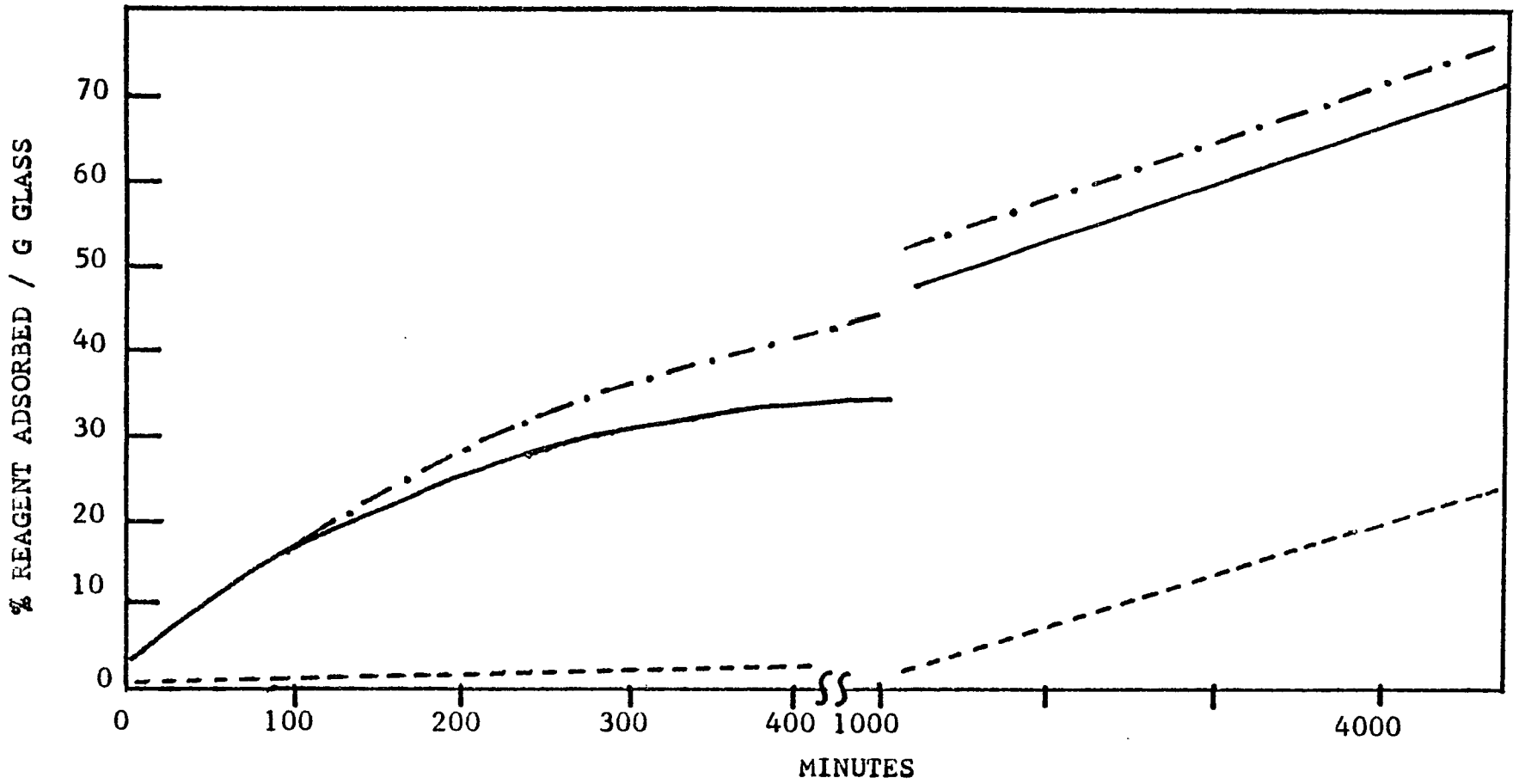

Figure 35. Effect of Increased Ionic Strength (0.1M KCl) on the Adsorption of Reagents. $Ru(bathophen)_3^{4-}$ ------, $Ru(bpy)_3^{2+}$ ———, $Ru(bpy)_2(CN)_2$ —·—·—·—.

to 68% (Figure 35).

These results illustrated the importance of electrostatic interactions between the reagents and the glass. The reaction system $Ru(bpy)_3^{2+}$ / EDTA / Pq^{2+} is composed of two cations, which were readily adsorbed, and the EDTA anion. Samples containing this reaction mixture were prepared with soaking solutions which were 0.1 M in KCl to insure adsorption of the EDTA anion.

Competition for surface sites by reagents was examined by preparing samples in solutions that contained both $5x10^{-4}$ M $Ru(bpy)_3^{2+}$ and $5x10^{-4}$ Pq^{2+}. 93% of the Pq^{2+} and 98% of the $Ru(bpy)_3^{2+}$ were adsorbed.

In examining the adsorption of charged species, it was noted that a solution of $[Fe(CN)_6]^{3-}$ turned green when the glass was added. A second sample was prepared by soaking it in the dark and there was no color change. Controls, run in aqueous and acidic (0.1 N) solutions in the light and dark, indicated that the color change was due to an acid catalyzed photochemical reaction. The acidity of the glass was examined by monitoring the pH of a measured volume of water to which a clean, dry piece of glass of known weight was added. Several trials indicated that $\sim 5x10^{-5}$ moles of H^+/g of glass were released from the glass surface into solution. Loss of these protons creates a negatively

charged surface covered with SiO^- groups.

Experiments were also performed to determine the relationship of the number of SiO^- sites created by proton loss to the adsorption of reagents. A weighed piece of glass was placed in a solution of $Fe(bpy)_3(ClO_4)_2$ and the adsorption of the complex and pH of the solution were monitored. At equilibrium, $6x10^{-5}$ moles of H^+ were released and $6x10^{-7}$ moles of complex were adsorbed per gram of the glass. This value for H^+ was in good agreement with that obtained above for distilled water, and suggests that the small amount of adsorbed complex does not affect the acid base properties of the glass.

For a complete characterization of the "reaction site" in a cavity, it was necessary to determine whether counterions were adsorbed by the glass. While tris-bathophenanthroline Ru(II) $^{4-}$ was not adsorbed to any significant extent, it was not certain if the smaller, less densely charged Cl^- was adsorbed. A glass sample was soaked in a solution containing $6.4x10^{-7}$ moles $Fe(bpy)_3Cl_2$. The concentration of the iron complex was monitored by the change in absorbance at 540 nm while the $[Cl^-]$ was measured with a specific ion electrode. Readings were taken over a 24 hr period and a standard solution of NaCl was used to insure the accuracy of the data. After 10^{-6} moles of

$Fe(bpy)_3^{2+}$ had been adsorbed, there was little change in the chloride concentration as can be seen in Figure 36.

3. Distribution of Reagents in the Glass

The total number of moles adsorbed/g glass was calculated from the decreased absorbance of the soaking solution. Correlation of these values with the absorption spectra of the glasses revealed a linear dependence, Figure 37. The distribution of reagents throughout the interconnected cavities of the glass however, was unknown. The effective concentration of reagents within the cavities was, therefore, also uncertain. Experiments were performed to determine the real concentrations of reagents. Following the procedure detailed in IV-B-2c, the number of $Ru(bpy)_3^{2+}$ / cavity was determined for several samples and the results can be seen in Figures 38-39. Reagents were concentrated at the surface of the glasses occupying only a fraction of the total pore volume. A plot of the moles of $Ru(bpy)_3^{2+}$ / moles of cavities versus the total number of moles adsorbed per gram of glass in Figure 40 is linear over a broad range. The initial deviation from linearity was due to inaccurate measurements of the sample thickness. The surface of the glass is irregular and the initial grinding process in removing the bumps, removes only a small volume of glass. It should be noted that the distribution of

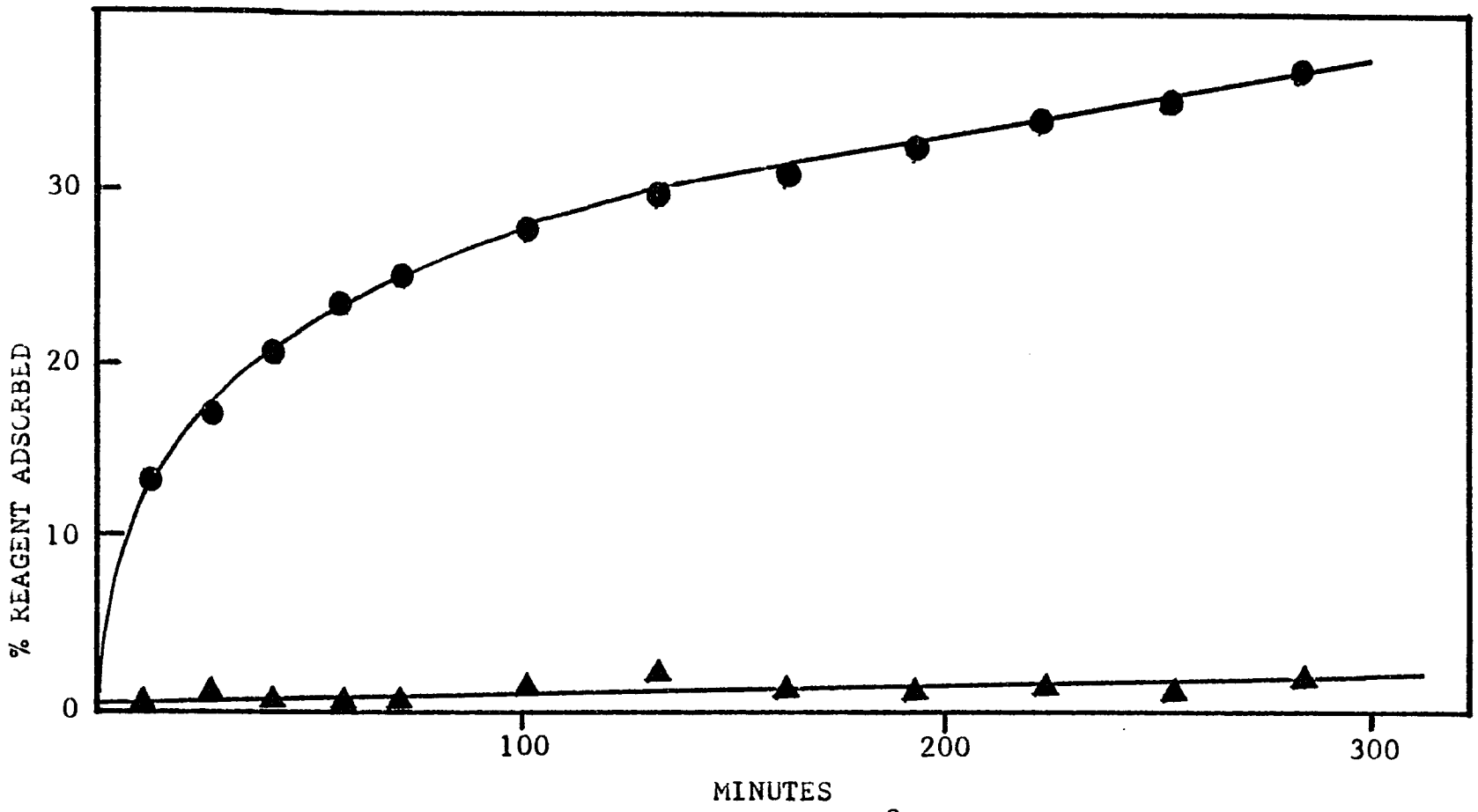

Figure 36. Relative Rates of Adsorption of $Fe(bpy)_3^{2+}$ and Cl^- onto Thirsty Glass from a Solution 1.03×10^{-4} M in $Fe(bpy)_3Cl_2$.

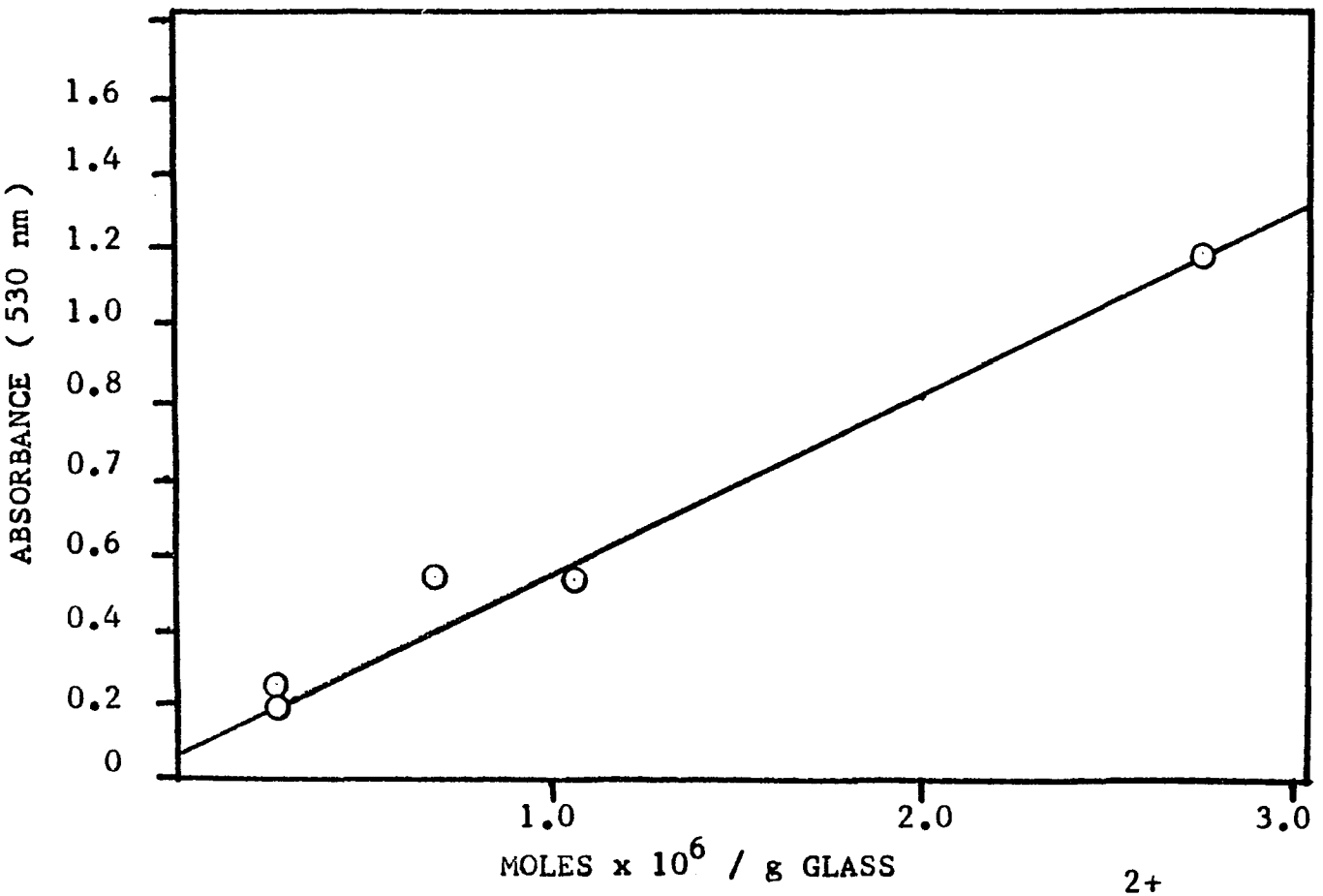

Figure 37. Absorbance of Glasses Containing $Ru(bpy)_3^{2+}$ as a Function of the Total Number of Moles Adsorbed / g Glass.

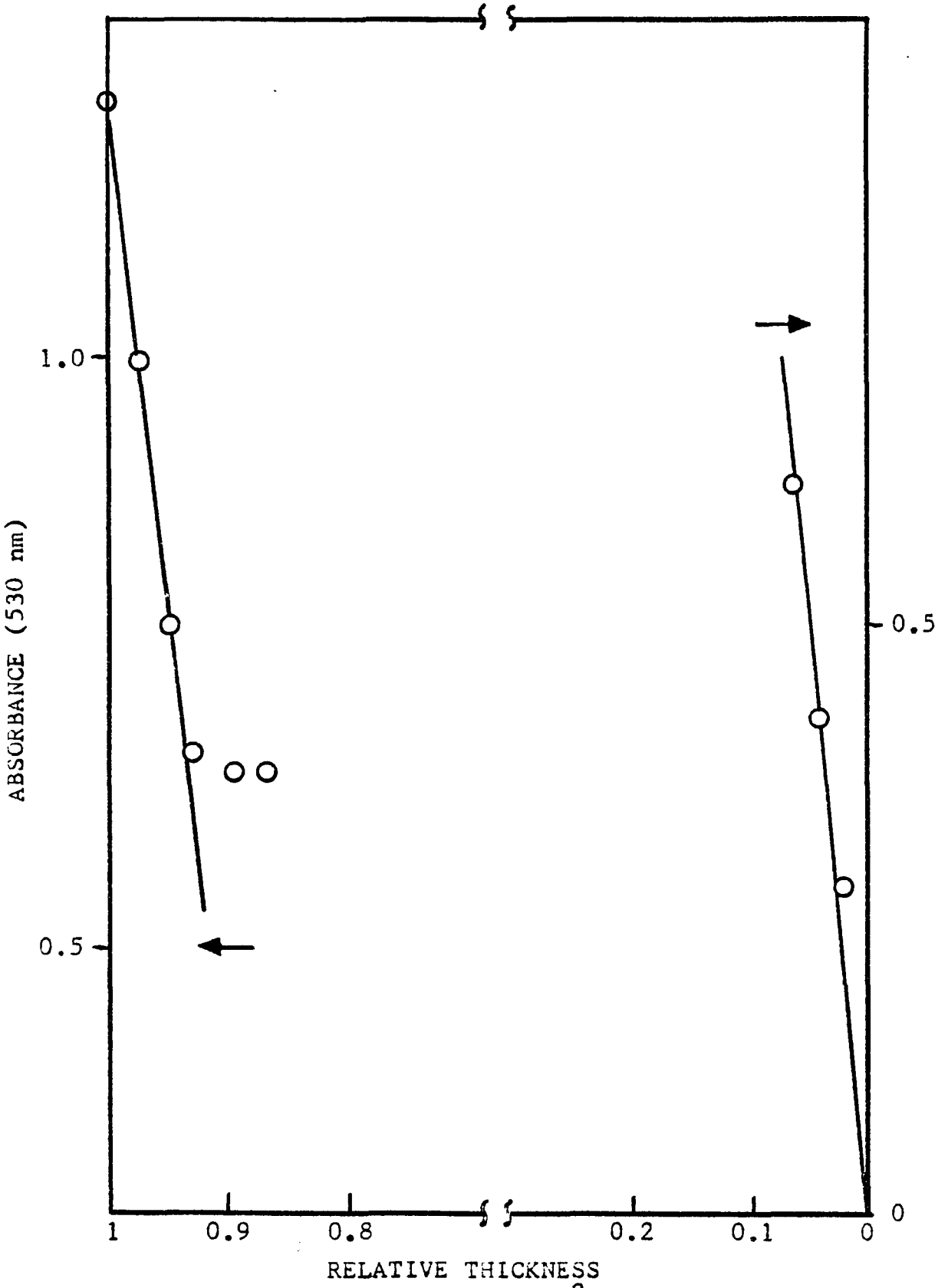

Figure 38. Distribution of $Ru(bpy)_3^{2+}$ as a Function of Sample Thickness. (1.08×10^{-6} moles/g glass, 3.84 molecules/cavity).

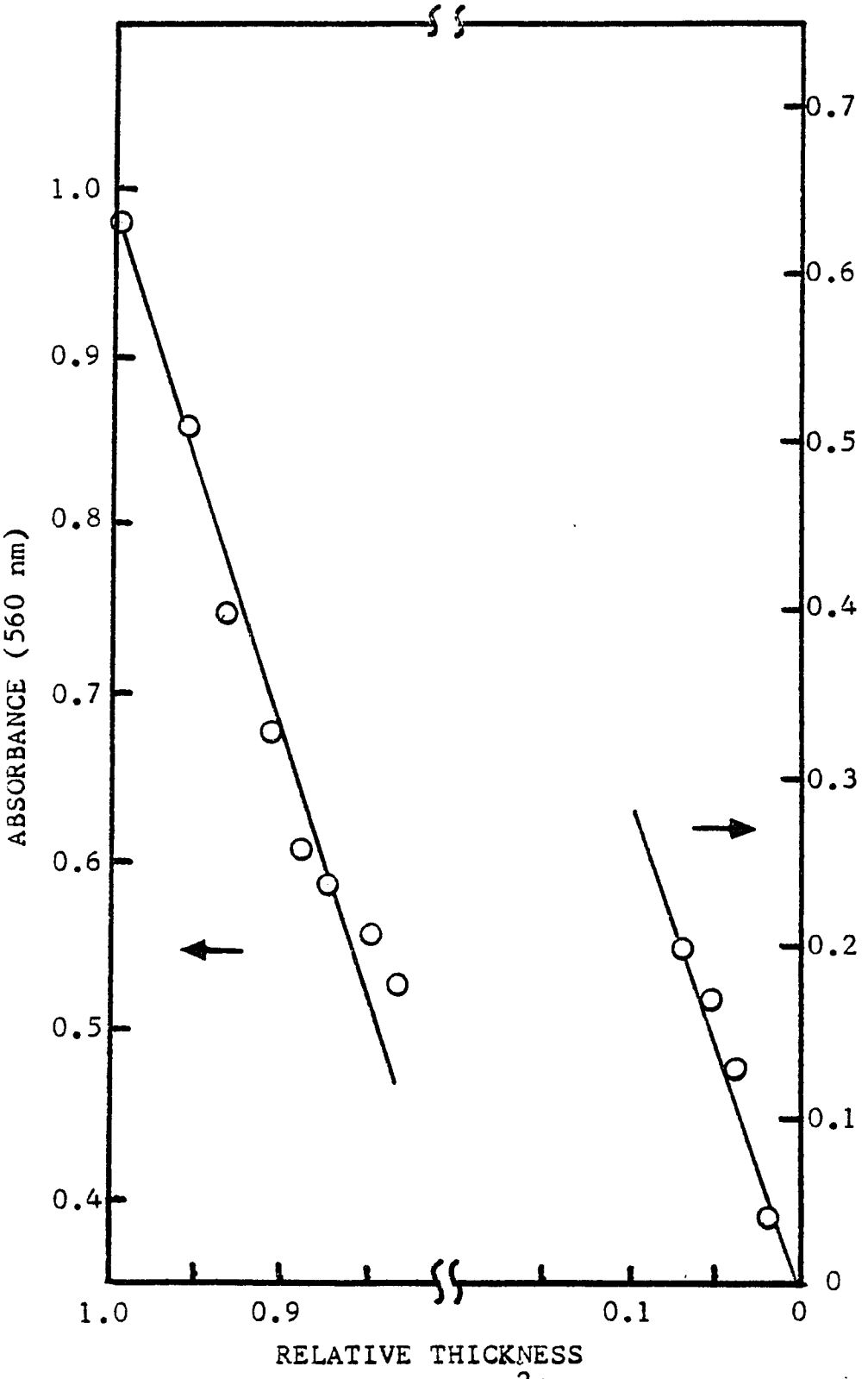

Figure 39. Distribution of $Ru(bpy)_3^{2+}$ as a Function of Sample Thickness. (7.7×10^{-6} moles/g glass, 14.54 molecules/cavity).

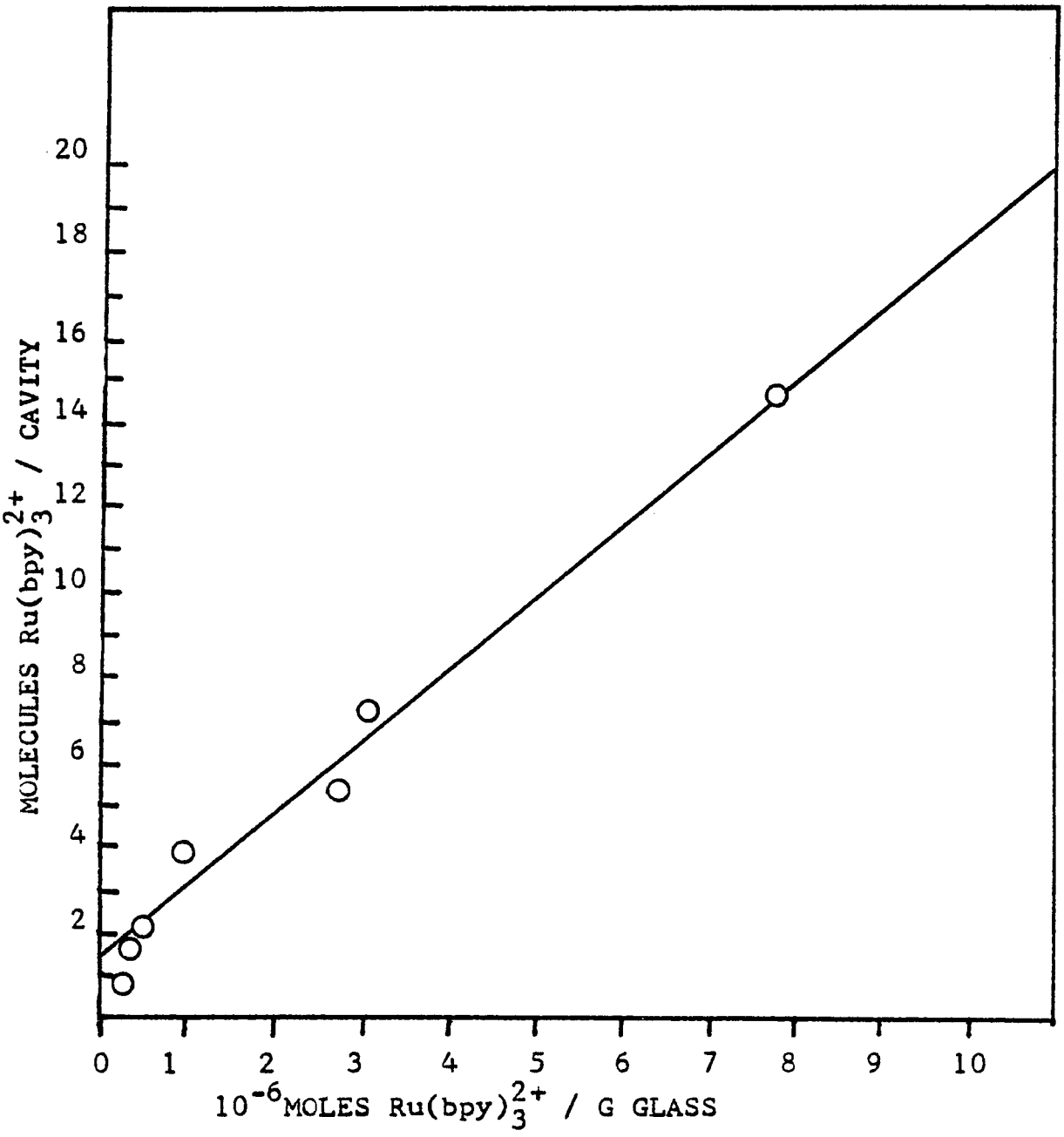

Figure 40. Distribution of $Ru(bpy)_3^{2+}$/ Cavity as a Function of the Total Concentration of $Ru(bpy)_3^{2+}$/ G Glass.

reagents in the glass is dependent of the length of the soaking period. 10^{-6} moles of $Ru(bpy)_3^{2+}$, adsorbed over a period of several hours, would have a distribution like those pictured in Figures 38 and 39. A sample prepared by soaking a glass for 9 months in a solution of the same concentration and volume in a sealed container had the uniform distribution depicted in Figure 41. In the first group of data, the reagents are concentrated in only 30% of the sample volume in a layer of$\sim$0.15 x sample thickness at each face regardless of the concentration of the soaking solution. This suggests that kinetics affect the initial distribution pattern. Before the adsorption of any $Ru(bpy)_3^{2+}$, the surface of the glass is negatively charged due to the presence of SiO^- groups. Cations in solution are coulombically attracted to this surface. As more of the Ru(II) complex is adsorbed, the effective charge of the surface decreases and $Ru(bpy)_3^{2+}$ still in solution is less strongly attracted. Redistribution of the adsorbate to the inner cavities which still have a large charge density takes time. In the interim the adsorbed $Ru(bpy)_3^{2+}$ limits adsorption at the surface and acts as a barrier to the inner cavities. At equilibrium, a uniform distribution, based on electrostatic attraction to the glass and repulsion of other complex cations, is achieved.

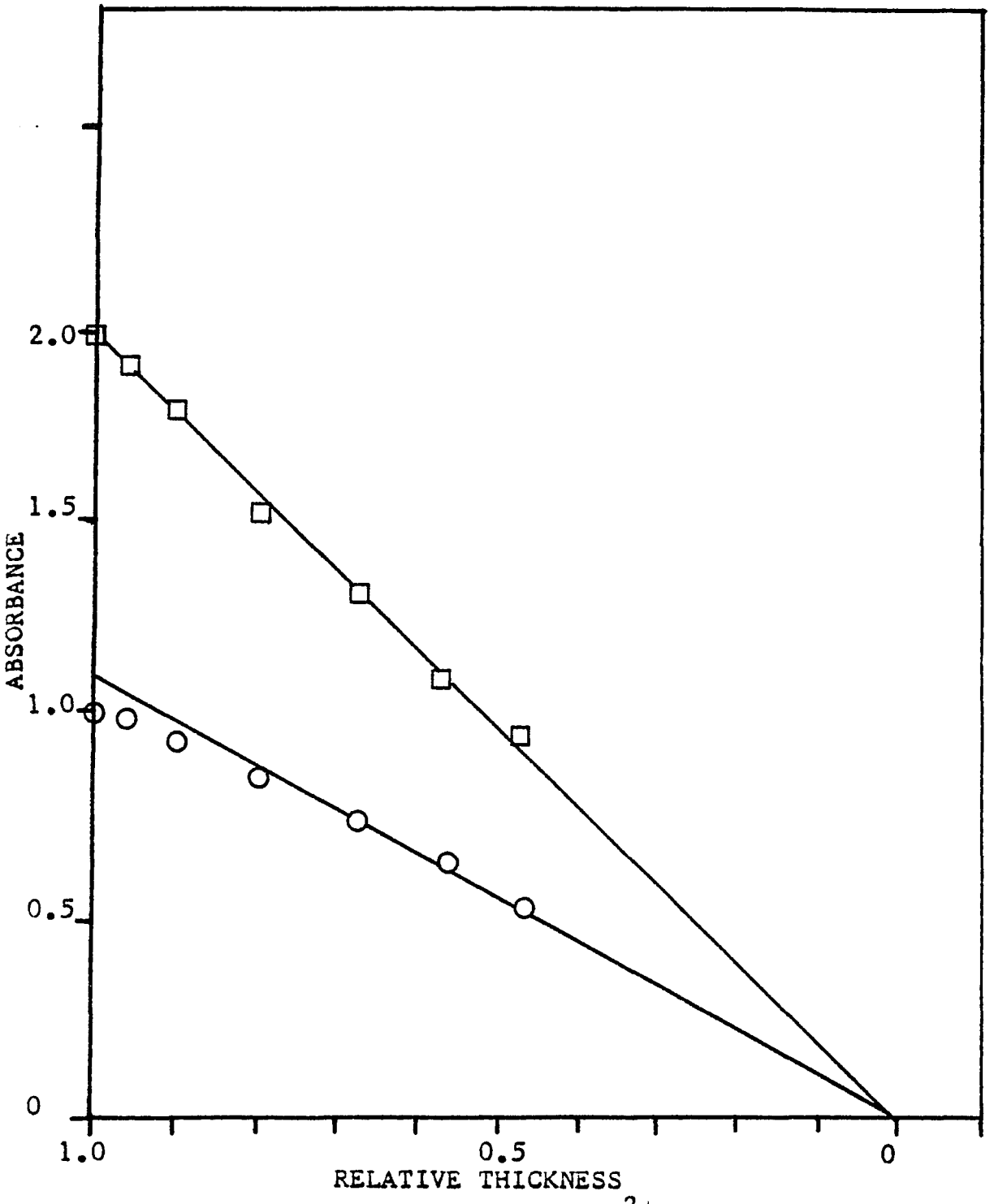

Figure 41. Distribution of $Ru(bpy)_3^{2+}$ in Glass. Absorbance measured at 530nm(□) and 550nm(○);3.44×10^{-6}moles/g of glass, 1.73 ± 0.6 molecules/cavity.

B. Spectra of $Ru(bpy)_3^{2+}$ in the Glass

Sample analysis by absorption spectroscopy is based on the molar extinction coefficient, ϵ, of a particular compound. ϵ is defined as the absorbance at a specific wavelength of a 1 M solution of sample with a 1 cm pathlength. Solutions are homogeneous by definition but the distribution of reagents in the glass was not. It was necessary to determine whether the glasses could be analyzed spectrally by calculating initial and changing concentrations of reactants from absorption spectra.

The definition of ϵ can be stated as:

$$\epsilon = \frac{A}{M\ cm} = \frac{A}{\frac{moles}{1} \times cm} = \frac{A}{\frac{moles}{103\ cm^3} \times cm} = \frac{A\ cm^2}{moles} \qquad (30)$$

A can be measured and the number of moles can be calculated from spectral analysis of the soaking solution. If cm^2 is defined as the surface area of the glass, calculated from the dimensions of height, width, and thickness, a value of ϵ_{glass} can be obtained. A plot of ϵ values over the range 350-550 nm for a 10^{-4} M solution of $Ru(bpy)_3Cl_2$ and for two glass samples containing 5.8×10^{-7} moles/g and 2.9×10^{-7} moles/g of $Ru(bpy)_3^{2+}$ can be seen in Figure 42. The good agreement of the solution and glass values suggests that absorption

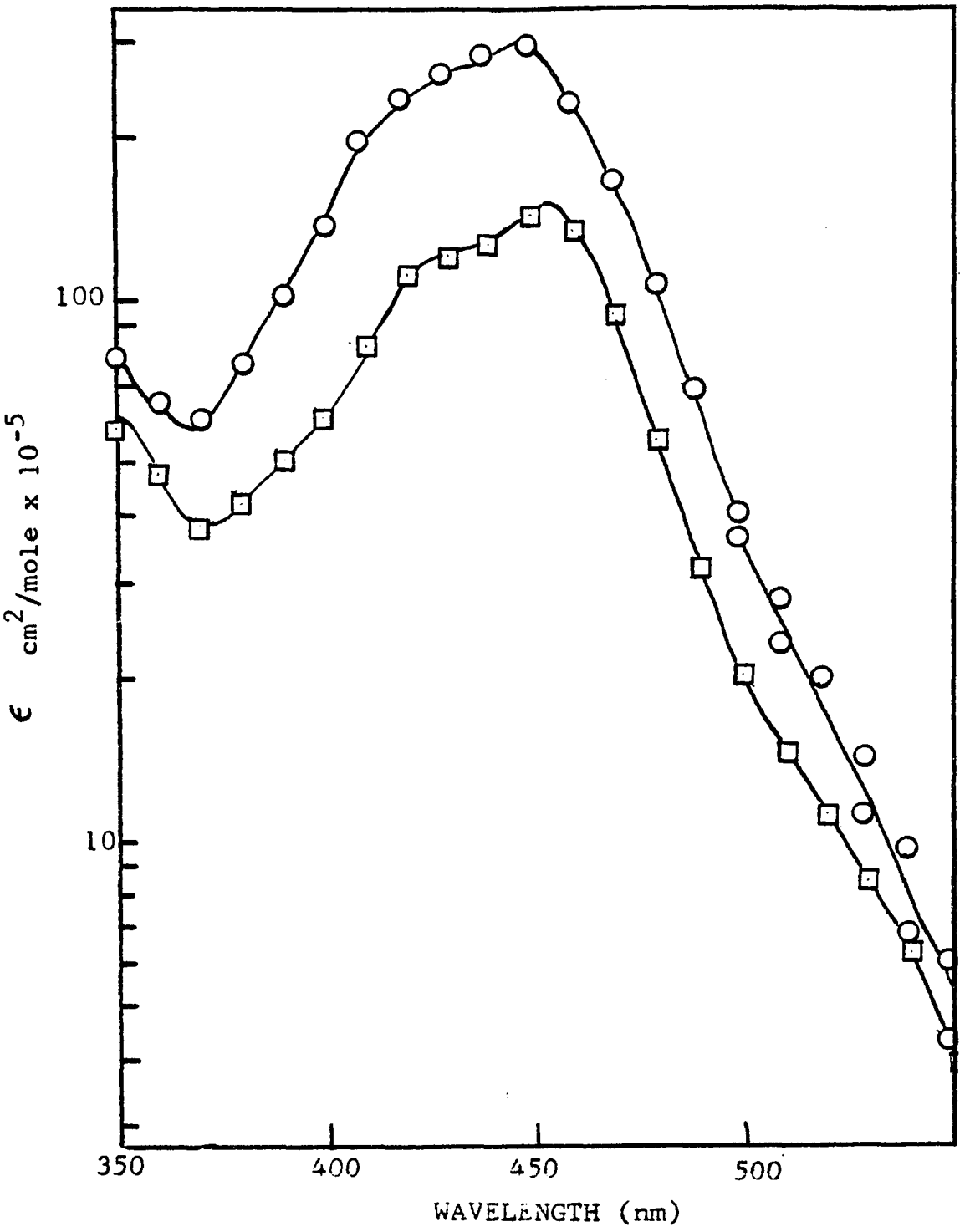

Figure 42. Relative Values of ϵ for $Ru(bpy)_3Cl_2$ in Aqueous Solution (□) and in Thirsty Glass (○).

spectroscopy is a valid method for analysis of reagents in the glass. The absorption and Raman spectra of $Ru(bpy)_3^{2+}$ in solution and in glasses, Figures 43 to 46, are essentially identical. There is, however, a slight red shift, Figures 47 to 48, in the emission maximum which is discussed below (53,82).

C. Photolysis of Glass Samples

Glasses containing $Ru(bpy)_3^{2+}$, EDTA, and Pq^{2+} were photolyzed with 457.9 nm light and a color change, a darkening of the irradiated area, was observed. Samples containing $Ru(bpy)_3^{2+}$ and Pq^{2+} but no EDTA were irradiated and the same darkening was observed. When glasses containing only $Ru(bpy)_3^{2+}$ were irratiated, the same color change was observed but qualitatively appeared darker than when Pq^{2+} was present. A more quantitative study of the photolysis of $Ru(bpy)_3^{2+}$ in the glass was performed and the difference spectra can be seen in Figure 49. Spectra were recorded against an unirradiated reference glass containing approximately the same amount of $Ru(bpy)_3^{2+}$. The non-zero base line, spectrum A, reflects the imperfect matching of sample and reference. The decrease in absorbance at 452 nm is indicative of a loss of $Ru(bpy)_3^{2+}$. The new absorbance at 510 nm, which increases with photolysis time, has been assigned by other workers to the $Ru(bpy)_3^{+}$ species (30a,53,82,83,91,120,121). Based on

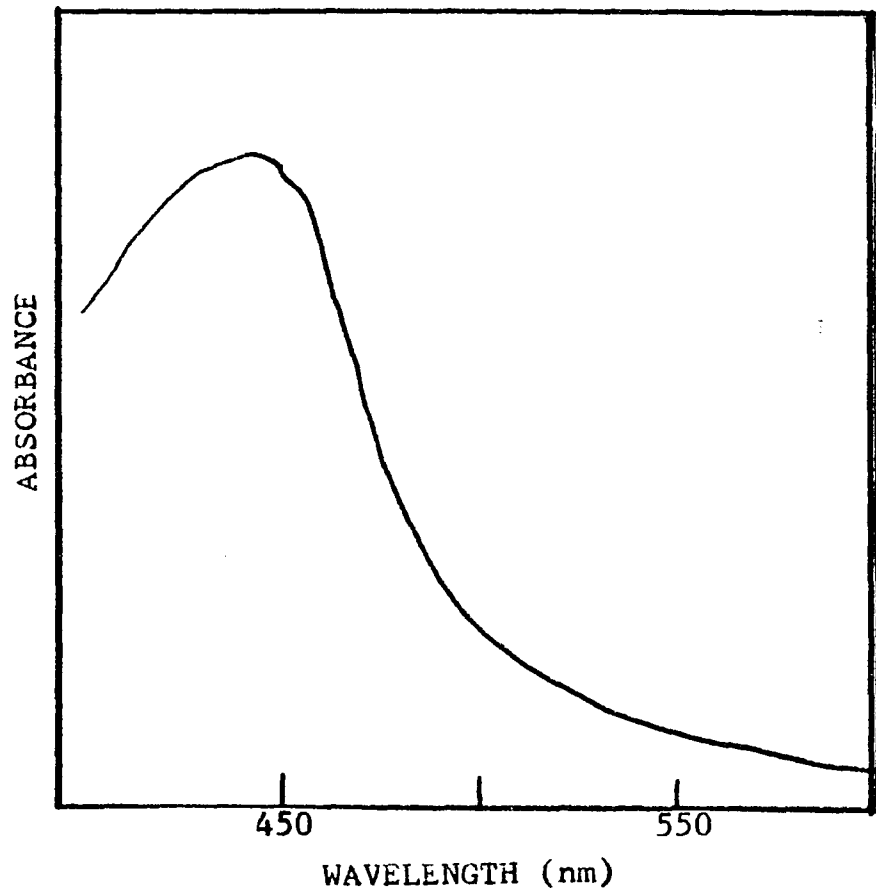

Figure 43. Absorption Spectrum of $Ru(bpy)_3Cl_2$ in Glass.

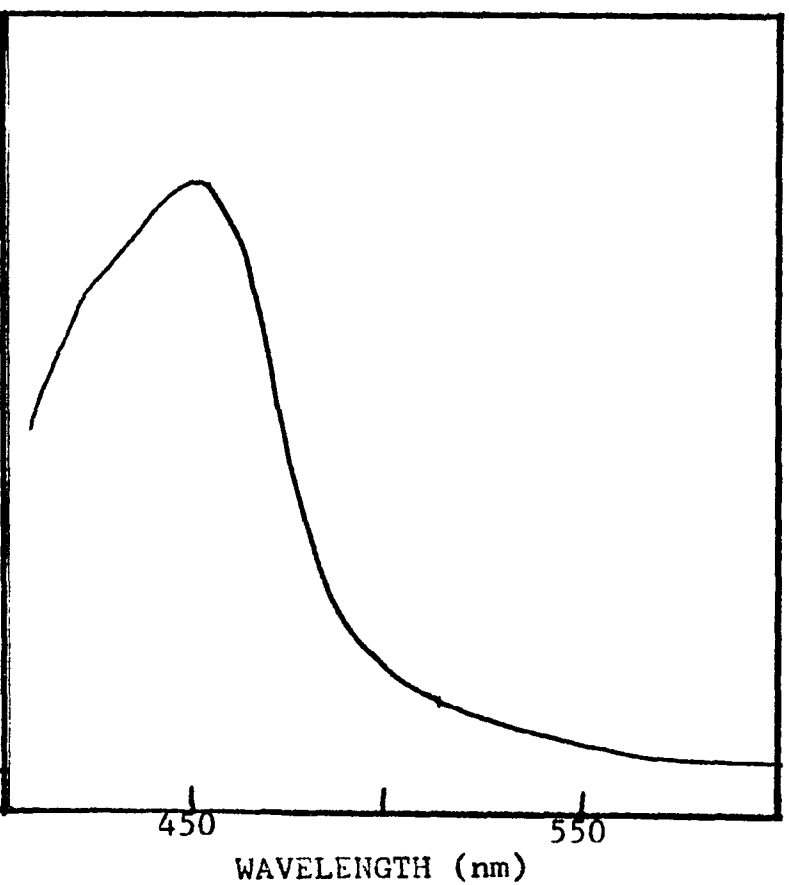

Figure 44. Absorption Spectrum of $Ru(bpy)_3Cl_2$ in Water.

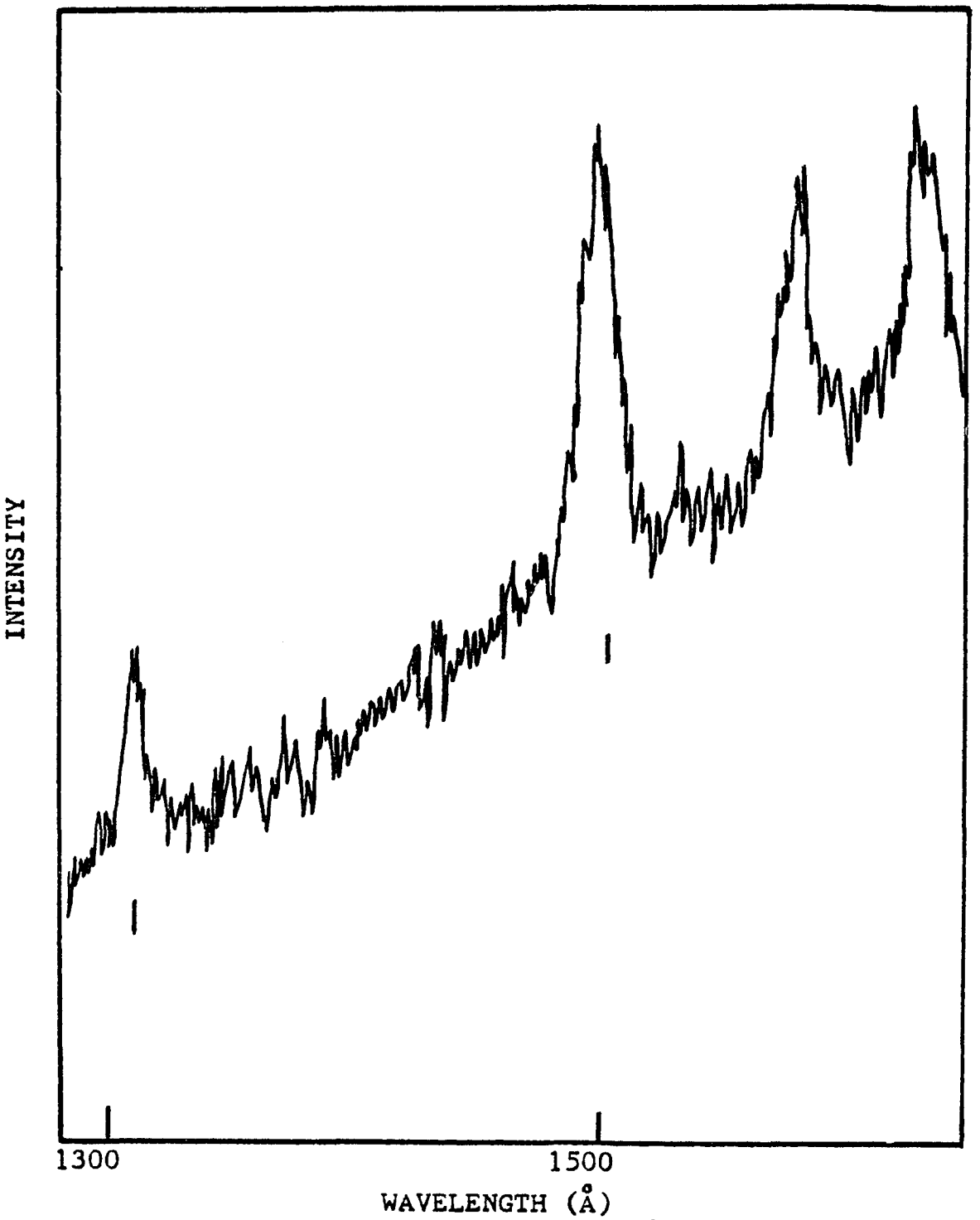

Figure 45. Raman Spectrum of $Ru(bpy)_3^{2+}$ Adsorbed onto Thirsty Glass (λ_{ex} = 4579 Å, 4880 Å spike filter).

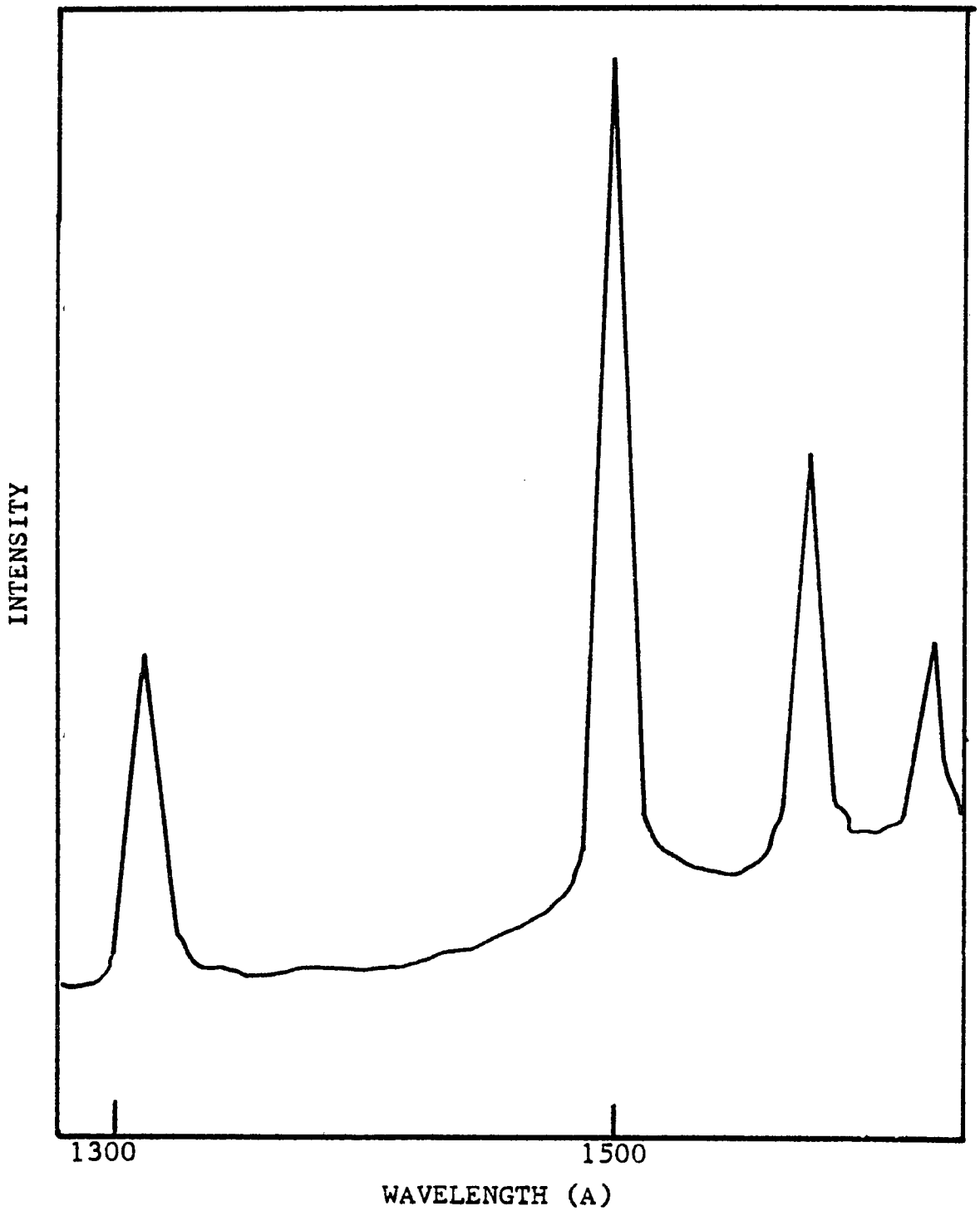

Figure 46. Raman Spectrum of $Ru(bpy)_3^{2+}$ in Aqueous Solution (10^{-3} M).

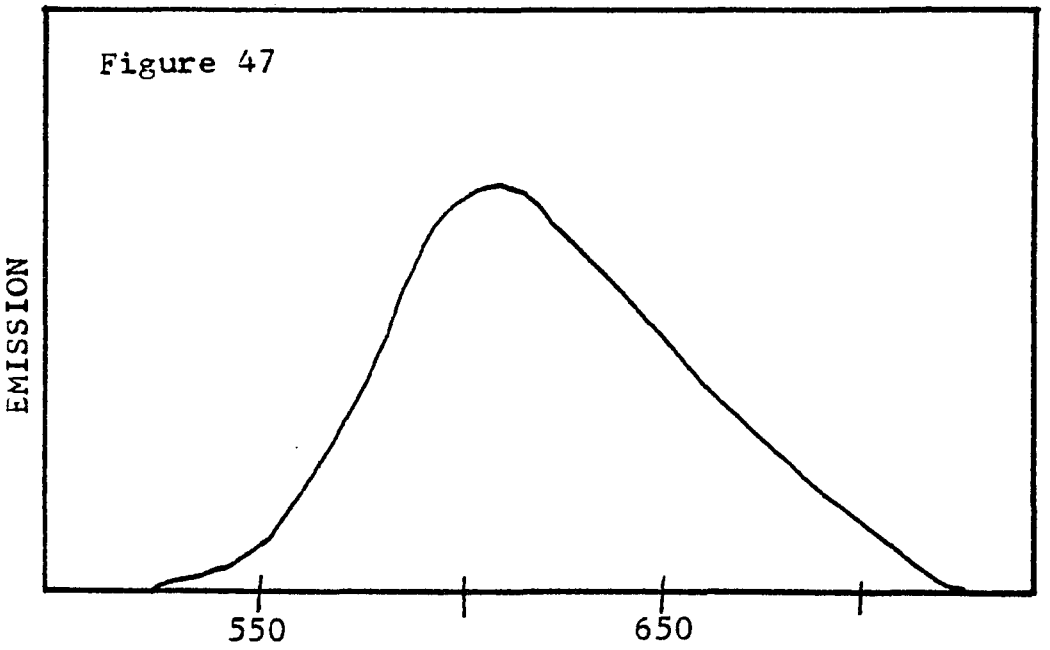

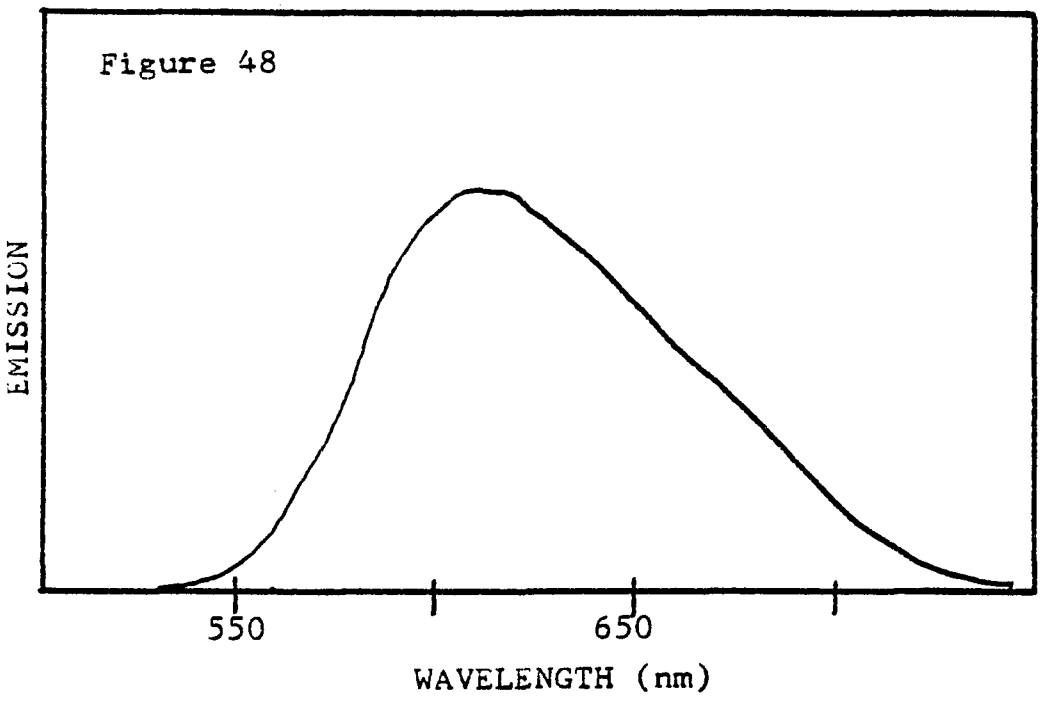

Figure 47. Emission Spectrum of $Ru(bpy)_3Cl_2$ in Glass.

Figure 48. Emission Spectrum of $Ru(bpy)_3Cl_2$ in Water.

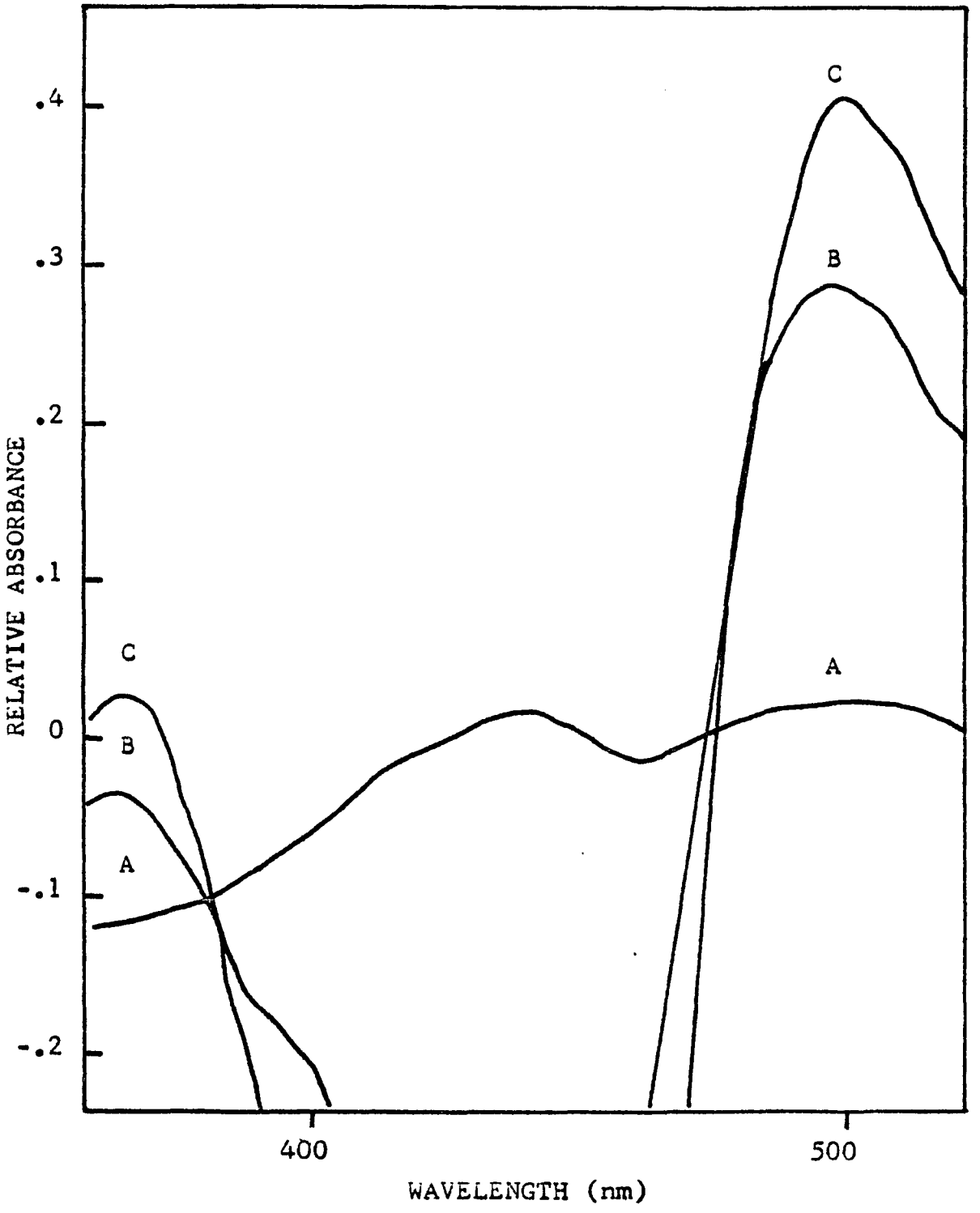

Figure 49. Absorbance Changes Induced by 457.9 nm Irradiation of $Ru(bpy)_3^{2+}$ in Glass Matrix. Laser power = 0.05 watts;irradiation times: A=0, B=30min, C=90min; 10^{-6}moles $Ru(bpy)_3^{2+}$/g glass.

a value of $\epsilon_{510} = 1.2 \times 10^4\ M^{-1}\ cm^{-1}$ for $Ru(bpy)_3^+$ (120), a ratio of 0.48 ± 0.05 was calculated for the appearance of $Ru(bpy)_3^+$ to the disappearance $Ru(bpy)_3^{2+}$. This value was in good agreement with the ratio of 0.5 reported by Meisel and coworkers (91) from their work on the intense flash photolysis of aqueous solutions of $Ru(bpy)_3^{2+}$.

Disproportionation was reported to proceed via an e_{aq}^- intermediate in fluid solution (91). Experiments indicated, however, that disproportionation proceeds by a different mechanism in the glass. O_2 and $EuCl_3$ quench $*Ru(bpy)_3^{2+}$ in solution and in the glass and thus prevent the formation of $Ru(bpy)_3^+$ in both media. It was reported that CCl_4, acting as an electron scavenger, also inhibited the reaction in solution, but it had no effect on the production of $Ru(bpy)_3^+$ in the glass.

To be certain that CCl_4 was adsorbed into the cavities, a dry glass containing $Ru(bpy)_3^{2+}$ was weighed, soaked in CCl_4, and weighed again. Calculations of the pore volume and the volume of CCl_4 adsorbed indicated that the cavities were filled with CCl_4.

A glass containing $Ru(bpy)_3^{2+}$ was mounted in a cell and degassed on a vacuum line. After measuring the emission intensity of the evacuated sample, the cell was connected to a degassing bulb containing 10 ml of CCl_4.

The solvent was degassed and the unit was tipped so that the glass was immersed in CCl_4. After allowing time for adsorption of the solvent, another measurement of the emission intensity was made. Beyond experimental error, CCl_4 did not affect the emission intensity of $Ru(bpy)_3^{2+}$.

CCl_4 did not alter the rate of $Ru(bpy)_3^+$ formation by quenching $*Ru(bpy)_3^{2+}$ or electron scavenging. Formation of $Ru(bpy)_3^+$ by direct disproportionation, reaction 31, would be consistent with the data.

$$2*Ru(bpy)_3^{2+} \longrightarrow Ru(bpy)_3^+ + Ru(bpy)_3^{3+} \qquad (31)$$

Assignment of the 510 nm absorption to $Ru(bpy)_3^+$ was made by Baxendale and Fiti (120) based on pulse radiolysis experiments. They indentified the reduced complex as $\left[Ru(bpy)_2(bpy^{\cdot-})\right]^+$. Polarographic studies are also consistent with a coordinated bipyridine radical anion (121). To confirm that the product in the glass was $\left[Ru(bpy)_2(bpy^{\cdot-})\right]^+$, glass samples containing $Ru(bpy)_3^{2+}$ were irradiated within the cavity of an ESR spectrometer. Photolysis induced a signal which increased with irradiation time as seen in Figure 50. The g value of 2.0086 is consistent with the electron being localized on the ligand, $bpy^{\cdot-}$ (123).

In addition, $Ru(bpy)_3^+$ was generated in the glass

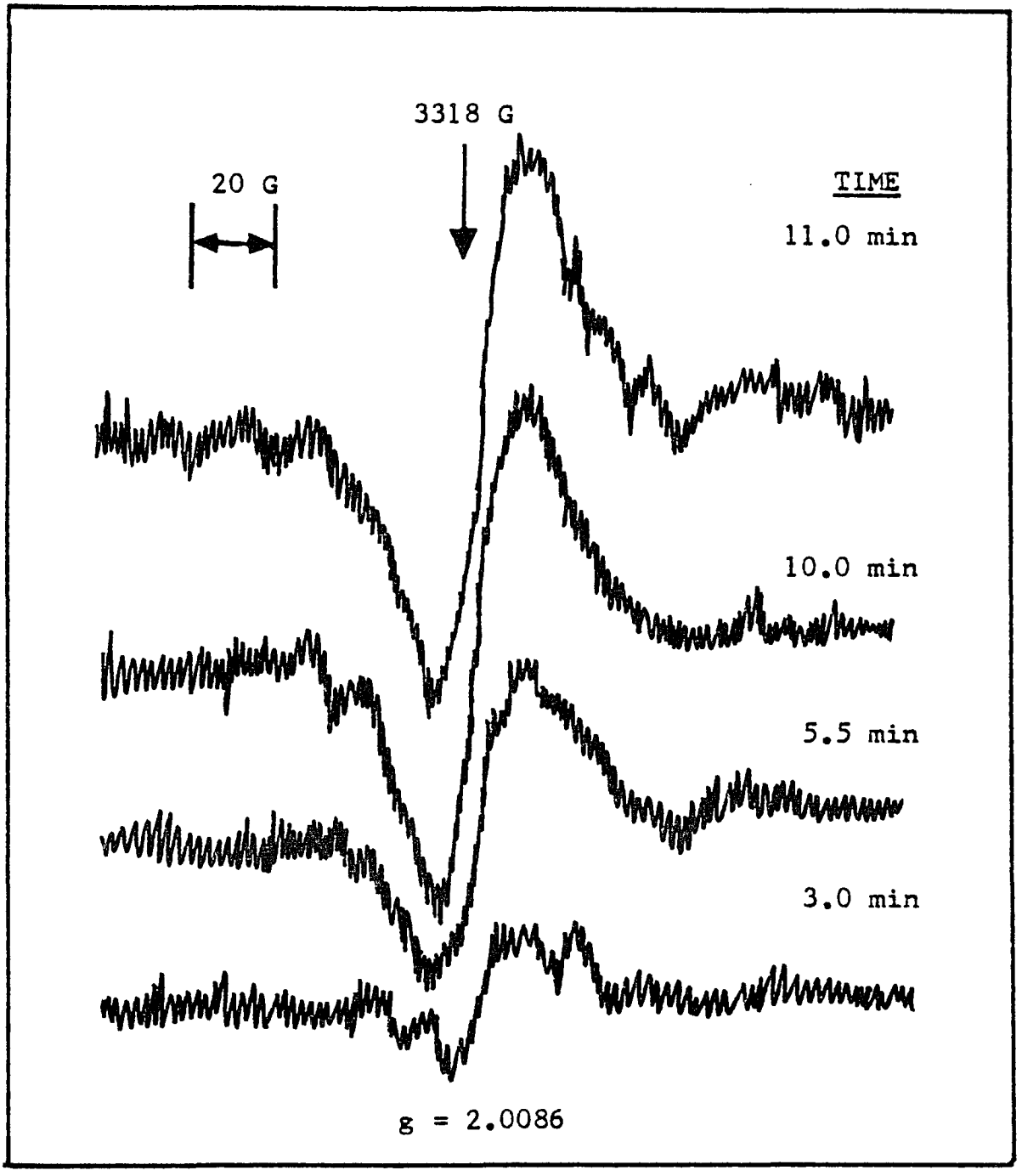

Figure 50. ESR Signal Generated by Photolysis of $Ru(bpy)_3^{2+}$ in Glass. Modulation amplitude = 5.0G; microwave power = 2 mW; microwave frequency = 9.238 GHz; H = 3320 G; T = 24°C; light source = 10^3W Hg arc.

by an alternative mechanism (30i,83) to establish that the absorbance at 510 nm was correctly assigned. Glasses containing $Ru(bpy)_3^{2+}$ were immersed in DMA, the sample cell was degassed by He bubbling, and photolyzed with visible light. The spectral changes at 510 nm, were identical to those obtained earlier. $^*Ru(bpy)_3^{2+}$ was not totally quenched by DMA even though the glass was immersed in 100% DMA. Formation of $Ru(bpy)_3^+$ was therefore due to both reductive quenching and disproportionation reactions. The $Ru(bpy)_3^+$ formed under these conditions was more stable than that formed by irradiation of dry glasses in vacuo. Leakage of air into the sample cells could have caused the decay of the 510 band in the dry glass. Keeping the sample immersed in DMA would limit the exposure to oxygen to the gas dissolved in the solvent. After eleven days, the 510 nm absorbance of a glass in DMA decreased only 6%. The lifetime of $Ru(bpy)_3^+$ under these conditions is $\geq 2.2 \times 10^3$ hr or ≥ 91 days.

Attempts to regenerate $Ru(bpy)_3^{2+}$ were unsuccessful. The 510 nm absorbance of $Ru(bpy)_3^+$ decayed but the absorption of $Ru(bpy)_3^{2+}$ at 452 nm was not restored. Preliminary experiments showed that the rate of decay of the 510 nm absorbance was accelerated by H_2O suggesting that $Ru(bpy)_3^+$ was reducing water. To detect the formation of H_2, glasses containing $Ru(bpy)_3^{2+}$

and Pt black were mounted in large cells which were attached to a degassing bulb containing water. The unit was degassed on a vacuum line and tipped to cover the glass with water. The sample was photolyzed with visible light for $\sim$ 2 hrs and then reattached to the vacuum line. All the liquid was isolated and frozen in the sidearm and the sample was analyzed for H_2. None was detected.

Direct disproportionation of $*Ru(bpy)_3^{2+}$ produces $Ru(bpy)_3^{3+}$ and $Ru(bpy)_3^{+}$ in equal amounts. The weak absorption spectrum of the $Ru(bpy)_3^{3+}$ complex, Figure 51, however,made quantitative measurement of this product difficult.

The quantum yield of $Ru(bpy)_3^{+}$ formation, ϕ_{Ru^+}, was determined from photolyses of dry glasses containing $Ru(bpy)_3^{2+}$ using the apparatus described in II-B. Glasses containing $4x10^{-7}$ moles/g of $Ru(bpy)_3^{2+}$ were mounted in the large cells and degassed on a vacuum line. A t_o absorbance reading at 510 nm was recorded and the sample was irradiated with 457.9 nm light. Additional spectra, were recorded periodically during the course of the photolyses. The increased absorbance is plotted as a fuction of irradiation time in Figures 52-54. A limiting value of $\phi_{Ru(bpy)_3^{+}}$ was calculated from a plot of

$$\log R = \log \phi + n \log I \qquad (32)$$

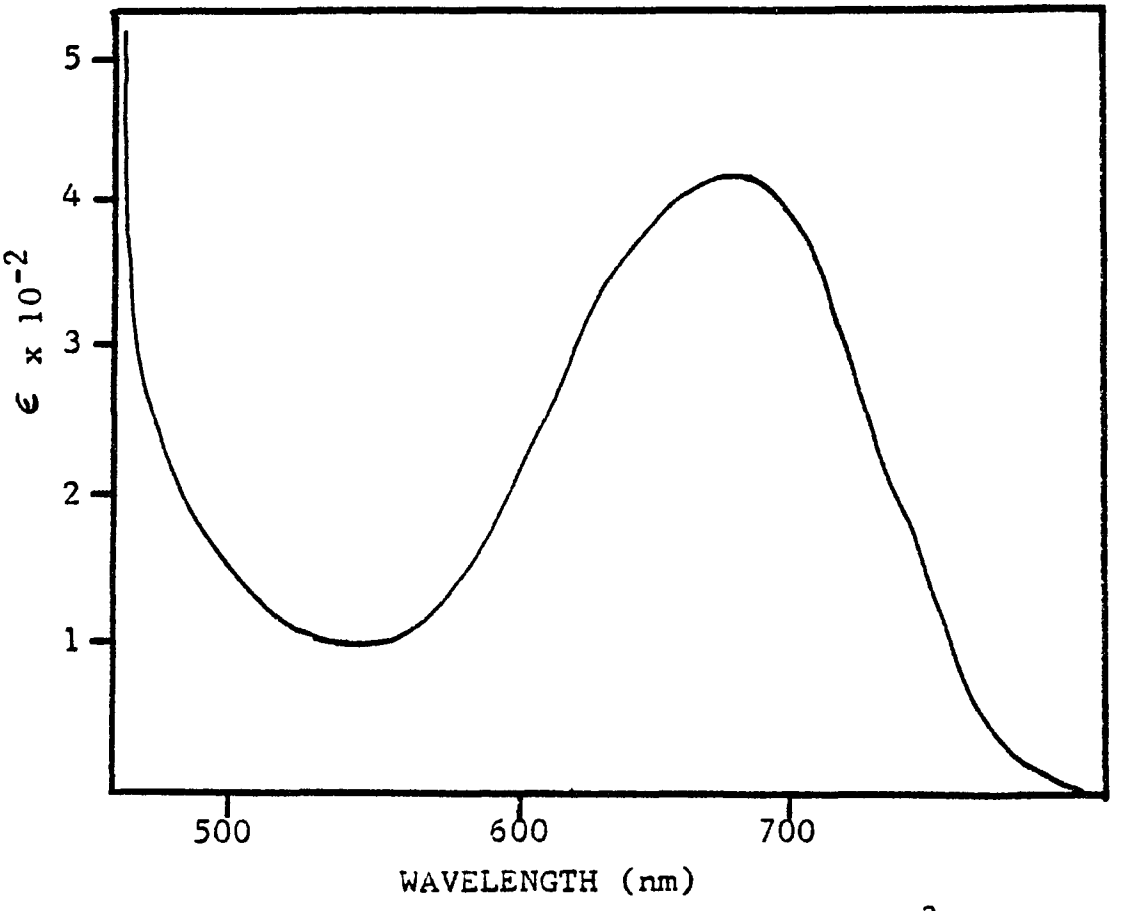

Figure 51. Absorption Spectrum of $Ru(bpy)_3^{3+}$.

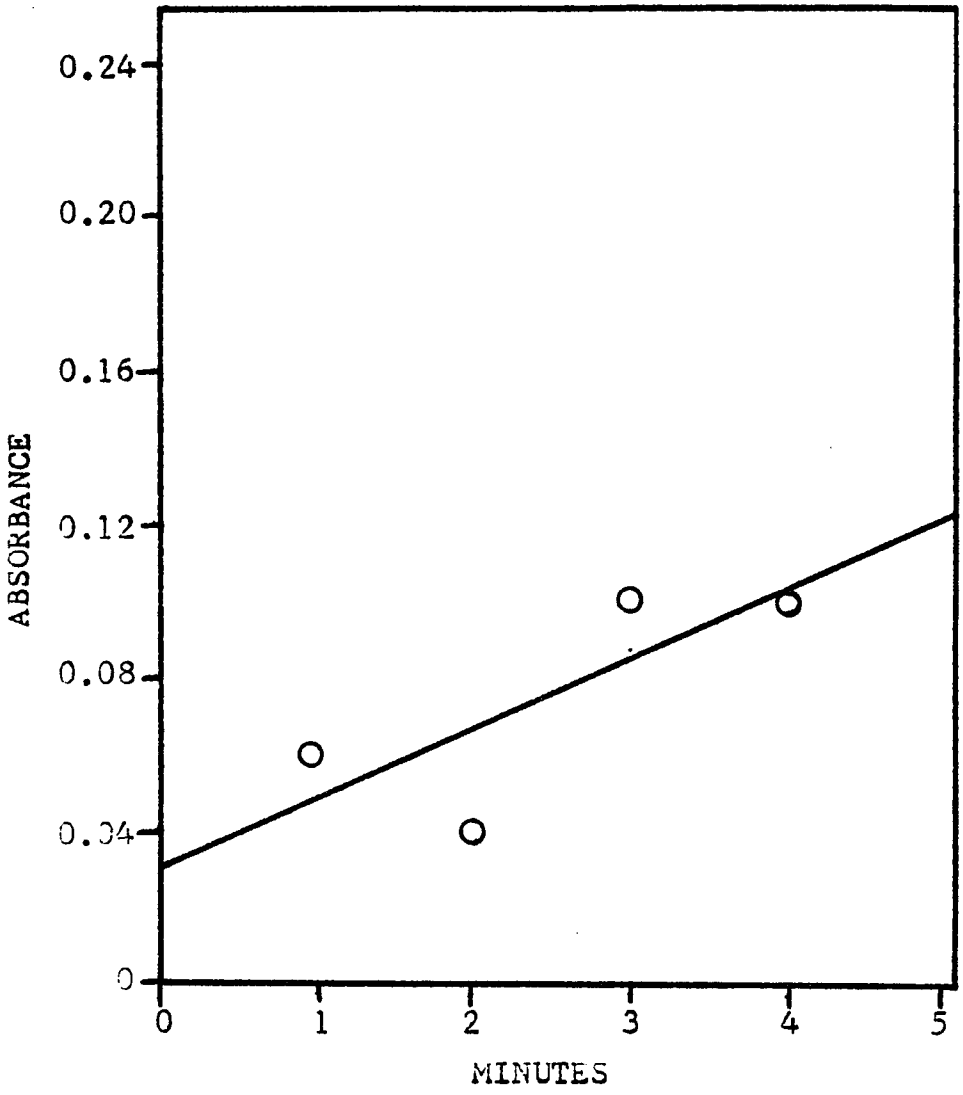

Figure 52. Rate of Formation of $Ru(bpy)_3^+$ (λ = 510nm, $\epsilon = 1.2 \times 10^4 M^{-1} cm^{-1}$). Laser light intensity = 0.046 watts.

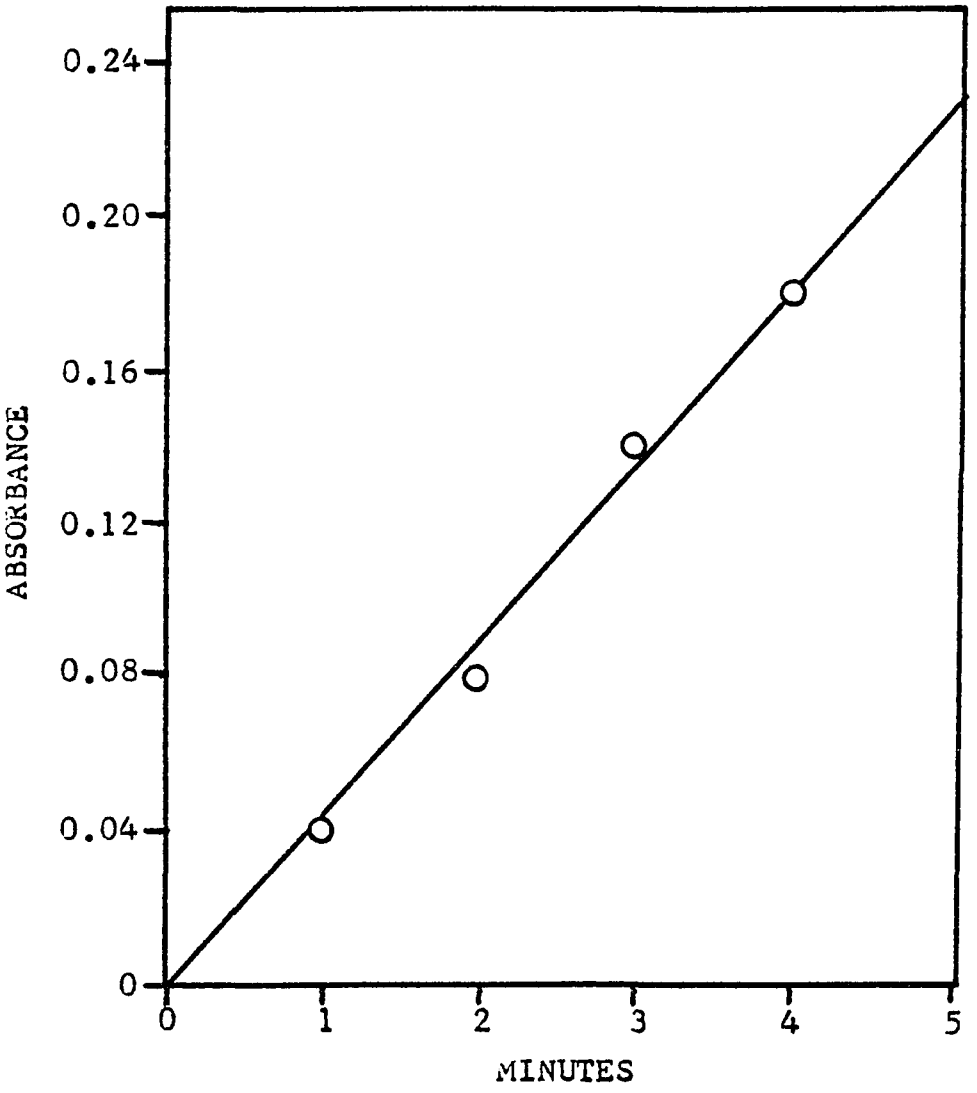

Figure 53. Rate of Formation of $Ru(bpy)_3^+$ (λ = 510nm, $\epsilon = 1.2 \times 10^4 M^{-1} cm^{-1}$). Laser light intensity = 0.095 watts.

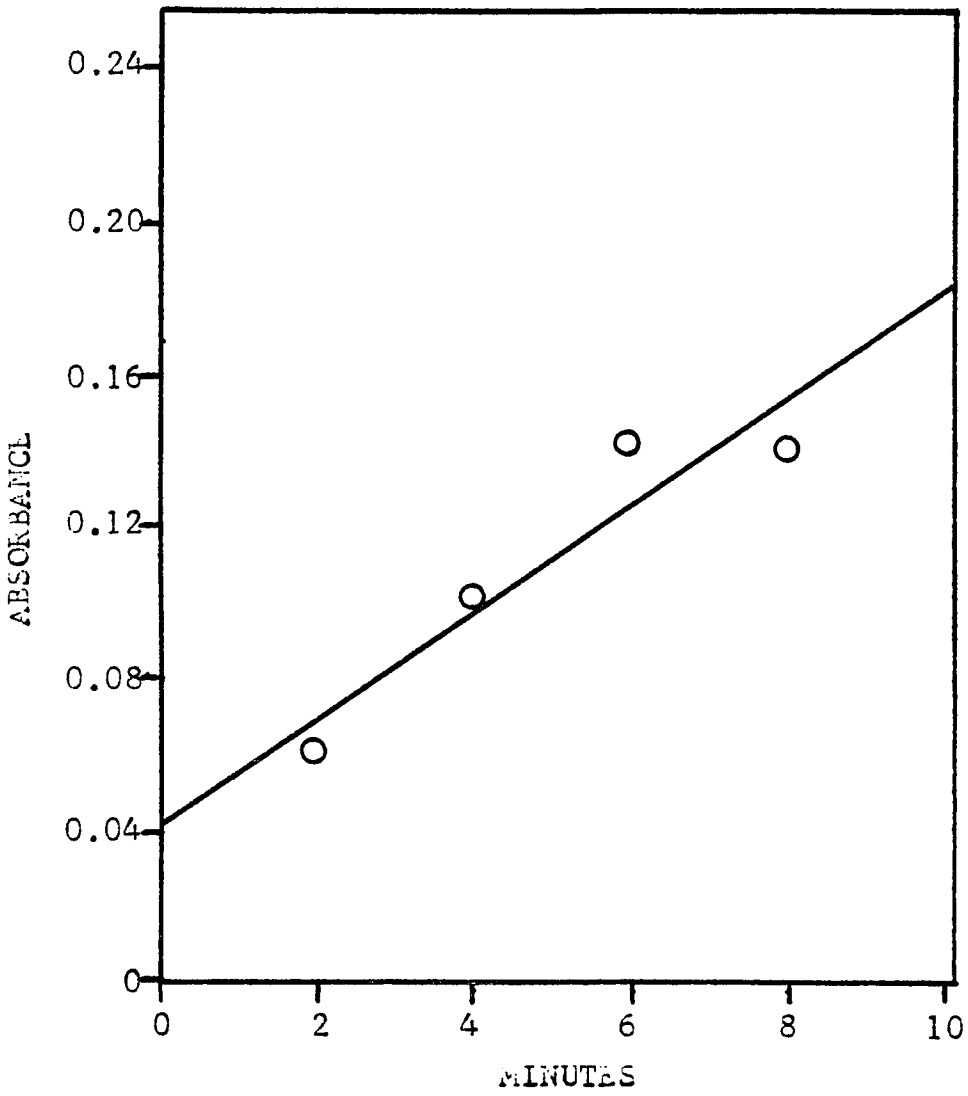

Figure 54. Rate of Formation of $Ru(bpy)_3^+$ (λ = 510nm, $\epsilon = 1.2 \times 10^4 M^{-1}cm^{-1}$). Laser light intensity = 0.18 watts.

where R = rate of formation of $Ru(bpy)_3^+$ and I = relative light intensity read from the power meter of the laser. Values of ϕ ranged from 6×10^{-12} to 9.9×10^{-9} (Figure 55). The same data were analyzed by plotting ϕ vs time and extrapolating to t=0 (Figures 56-58) to obtain $\phi_{initial} \sim 10^{-4}$. A plot of $\phi_{initial}$ versus I, Figure 59, shows that ϕ was inversely proportional to I. Large deviations in the data in Figure 55, the low value of ϕ, and the unexpected inverse dependence of ϕ on light intensity in Figure 59 prompted us to perform additional experiments, to evaluate $\phi_{Ru(bpy)_3^+}$.

The improper repositioning of the sample in the photolyzing light beam and in the light path of the spectrophotometer could account for some of the inconsistencies in the data (Table V). The time lapse between the removal of the sample from the light path and the measurement of the absorbance would also affect the results, if the reaction is reversible at low intensities and short irradiation times. There was qualitative evidence that this was the case. Many times, even when great care was taken in aligning the sample, no change in absorbance was measured even when a color change was visible to the eye when the sample was first removed from the photolysis apparatus. Additional evaluations of ϕ were made using the

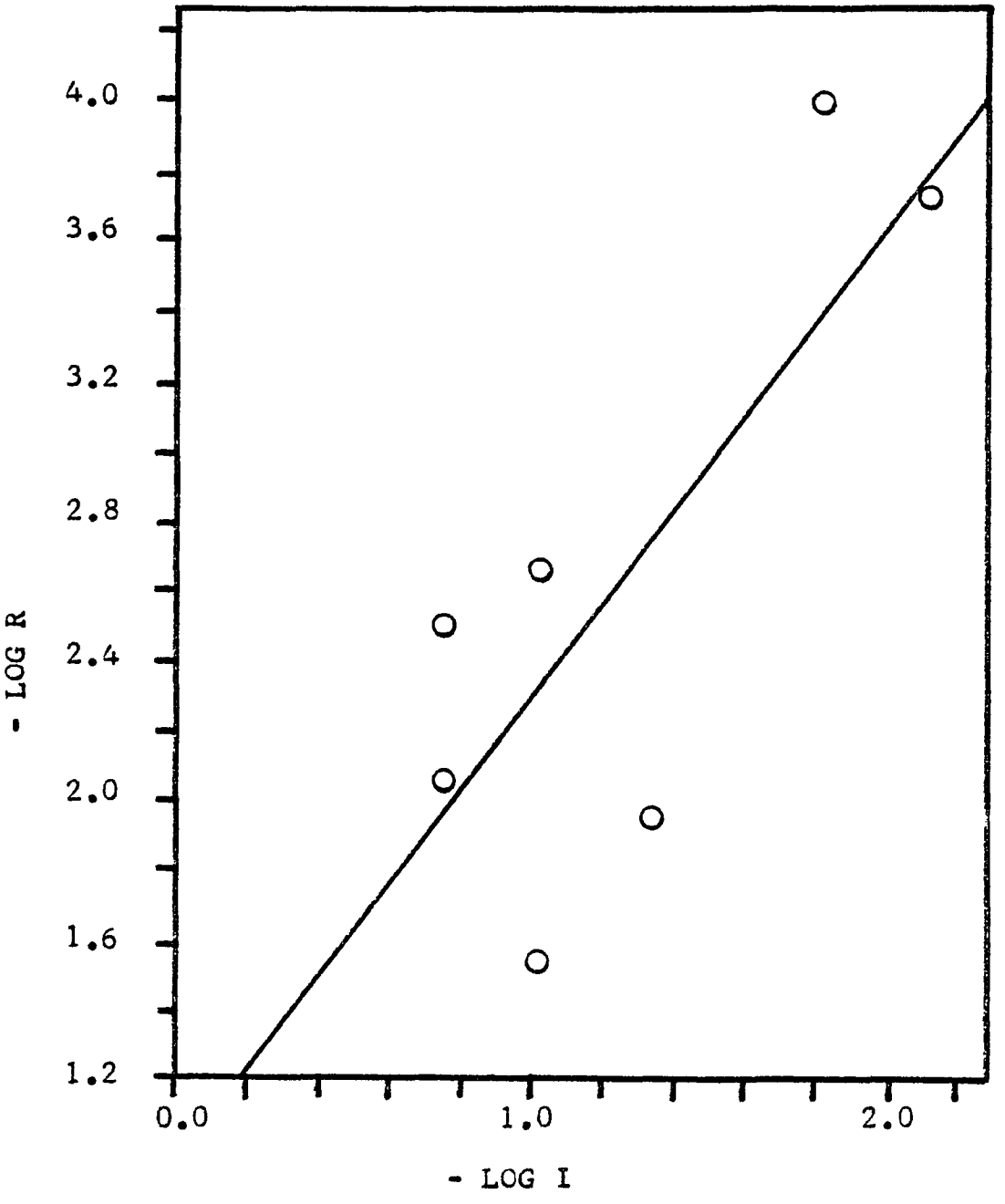

Figure 55. Plot of Log r = Log Ø + n Log I
(R is the slope of absorbance at 510 nm and
I is the laser intensity in watts).

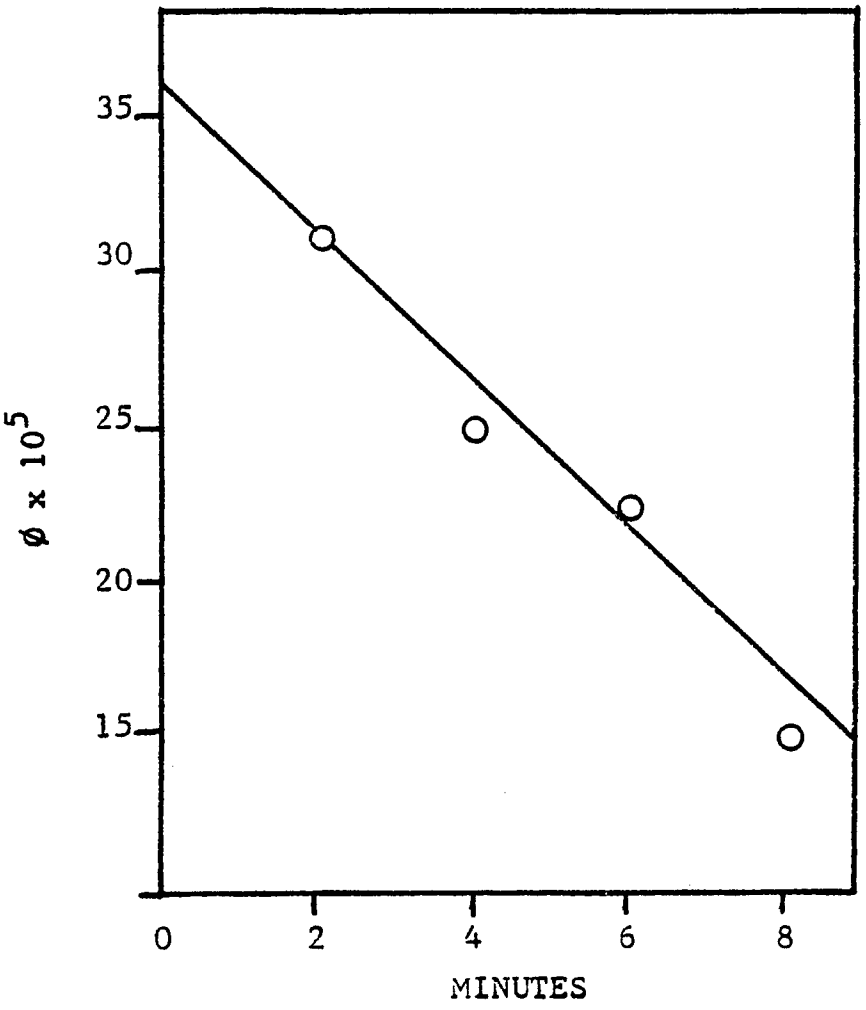

Figure 56. Time Dependence of the Quantum Yield of $Ru(bpy)_3^{\tau}$. Laser light intensity = 0.18 watts, $\phi_{limit} = 3.5 \times 10^{-4}$.

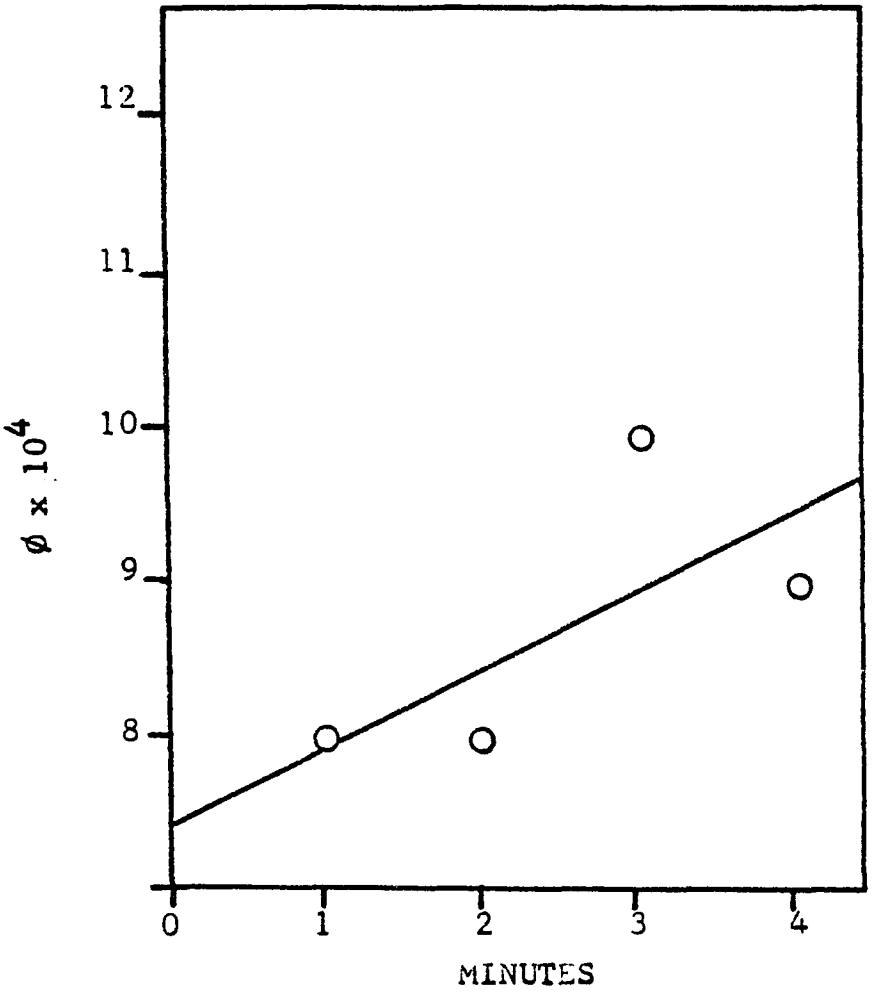

Figure 57. Time Dependence of the Quantum Yield of $Ru(bpy)_3^+$. Laser light intensity = 0.095 watts, $\phi_{limit} = 7.5 \times 10^{-4}$.

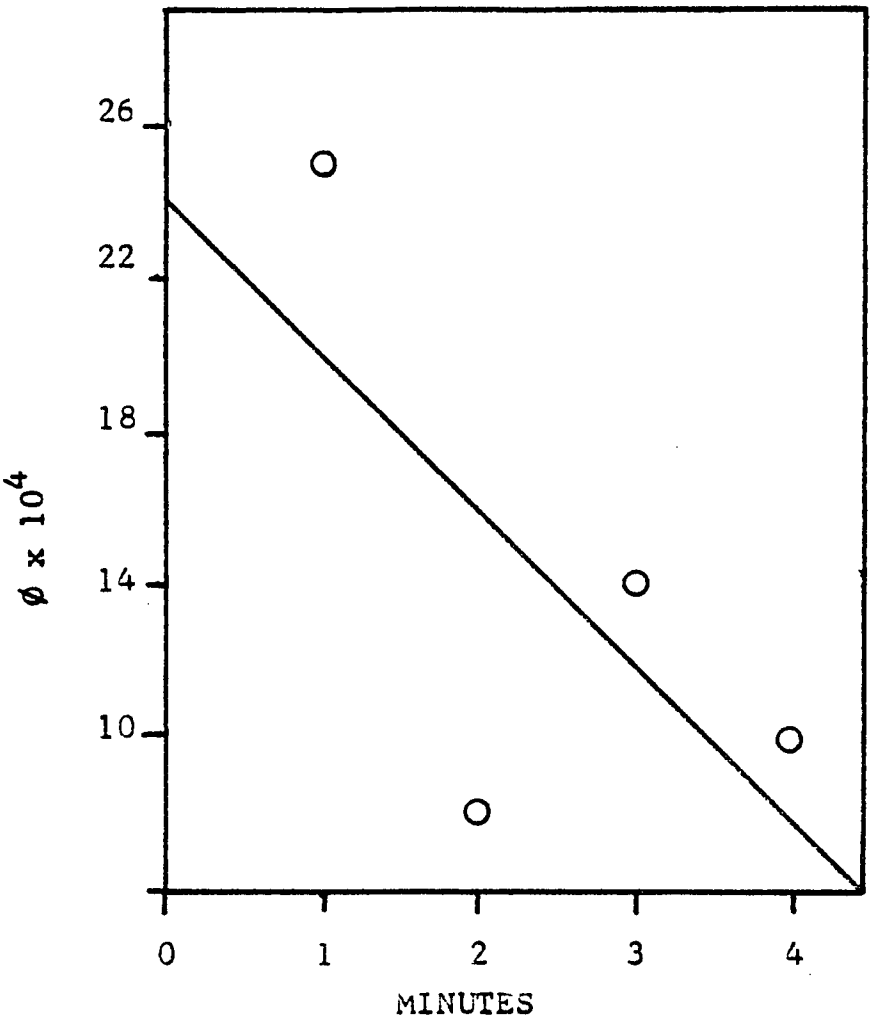

Figure 58. Time Dependence of the Quantum Yield of $Ru(bpy)_3^{+}$. Laser light intensity = 0.046 watts, $\phi_{limit} = 2.4 \times 10^{-4}$.

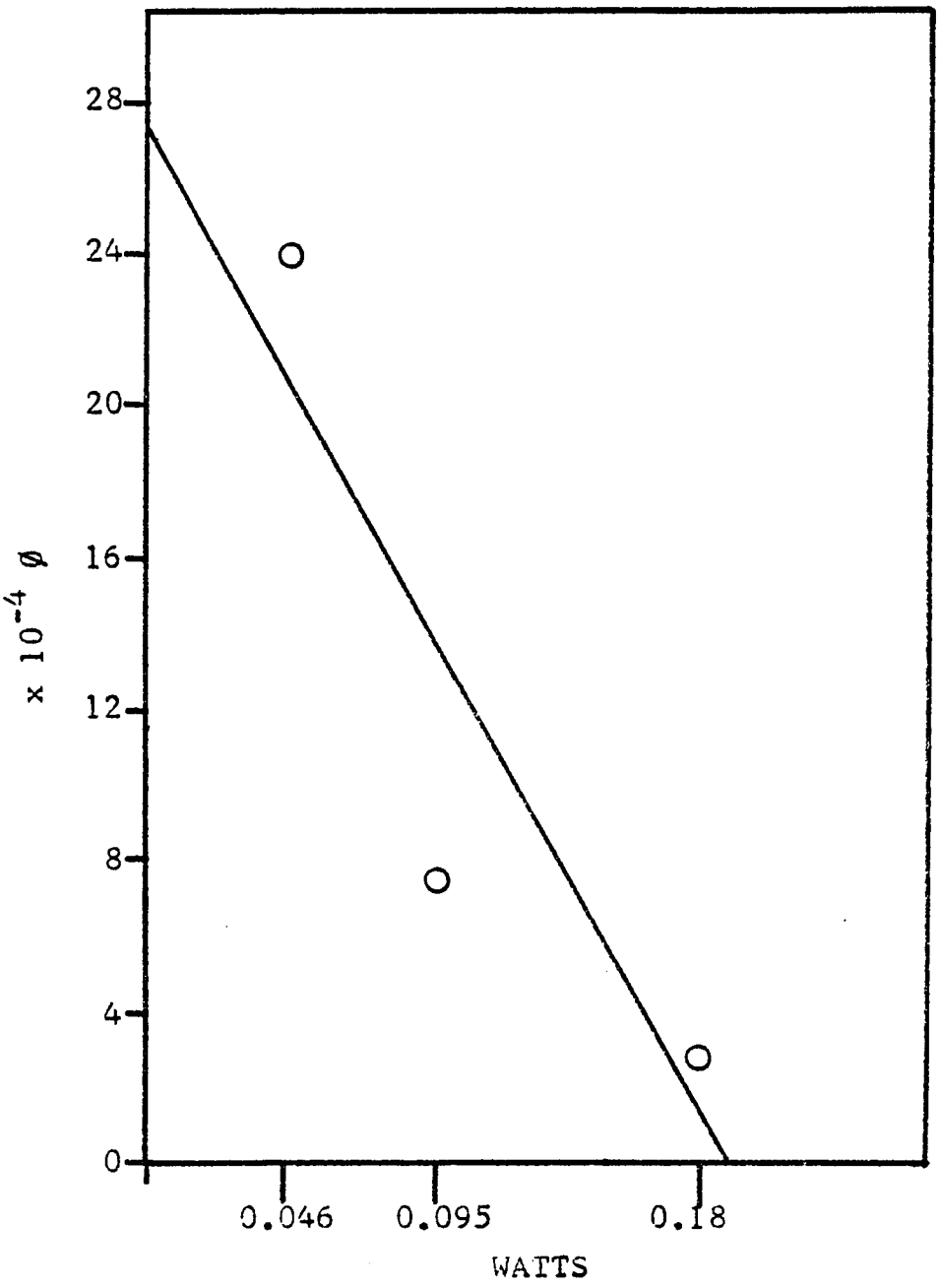

Figure 59. Intensity Dependence of the Quantum Yield of $Ru(bpy)_3^+$.

Table V. Visible Photolysis of Glasses Containing $Ru(bpy)_3^{2+*}$ (λ=457.9 nm).

I = 0.095 watts $\quad \phi = 7.5 \times 10^{-4}$

t (min)	A(510 nm)	$\phi \times 10^4$
1	0.04	7.8
2	0.08	7.8
3	0.14	9.2
4	0.18	8.9

I = 0.095 watts $\quad \phi = 1.9 \times 10^{-4}$

t (min)	A(510 nm)	$\phi \times 10^4$
2	0.02	1.9
4	0.02	0.9
6	0.03	0.9
8	0.04	1.0

I = 0.016 watts $\quad \phi = 6 \times 10^{-12}$

t (min)	A(510 nm)	$\phi \times 10^{12}$
5	0.005	9.0
10	0.005	4.7
15	0.005	3.0
105	0.025	2.0

apparatus described in II-B-2, in which the absorbance at 510 nm was monitored continuously during the photolysis. Ferric oxalate actinometry was used to measure the light intensity.

Formation of $Ru(bpy)_3^+$ was monitored by the change in absorbance at 510 nm (Figures 60-62). Values of $\phi^o \sim 10^{-3}$ were obtained by extrapolating plots of ϕ versus irradiation time to $t=0$ (Figures 63-65). ϕ^o was linearly dependent on I, as seen in Figure 66. A bimolecular reaction such as the disproportionation of $*Ru(bpy)_3^{2+}$ would be expected to show a square dependence on irradiation intensity. The value of the slope, 2.18, is consistent with such a mechanism.

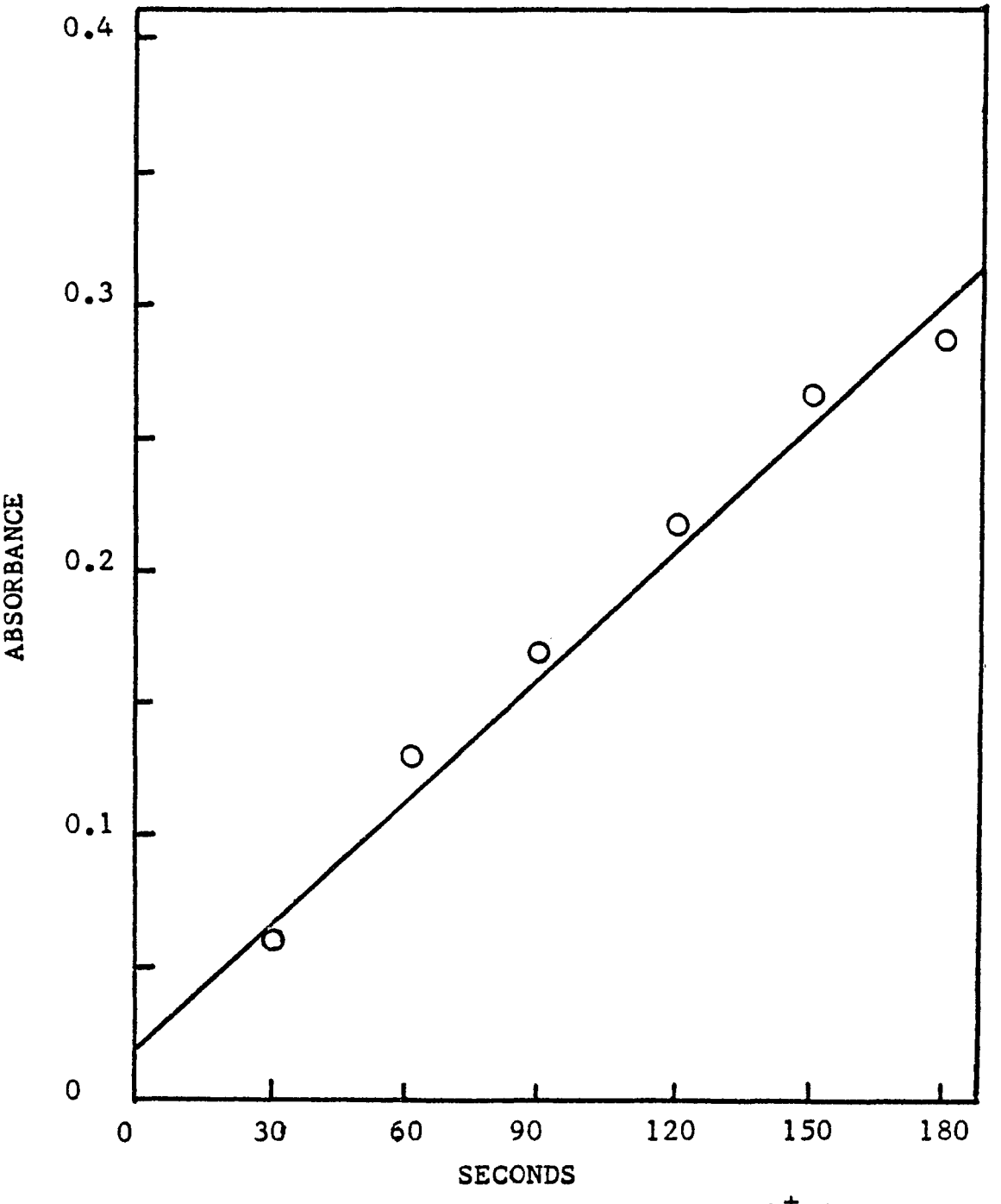

Figure 60. Rate of Formation of $Ru(bpy)_3^+$ (λ = 510nm, $\epsilon = 1.2 \times 10^4\ M^{-1}cm^{-1}$). Relative light intensity = 1.

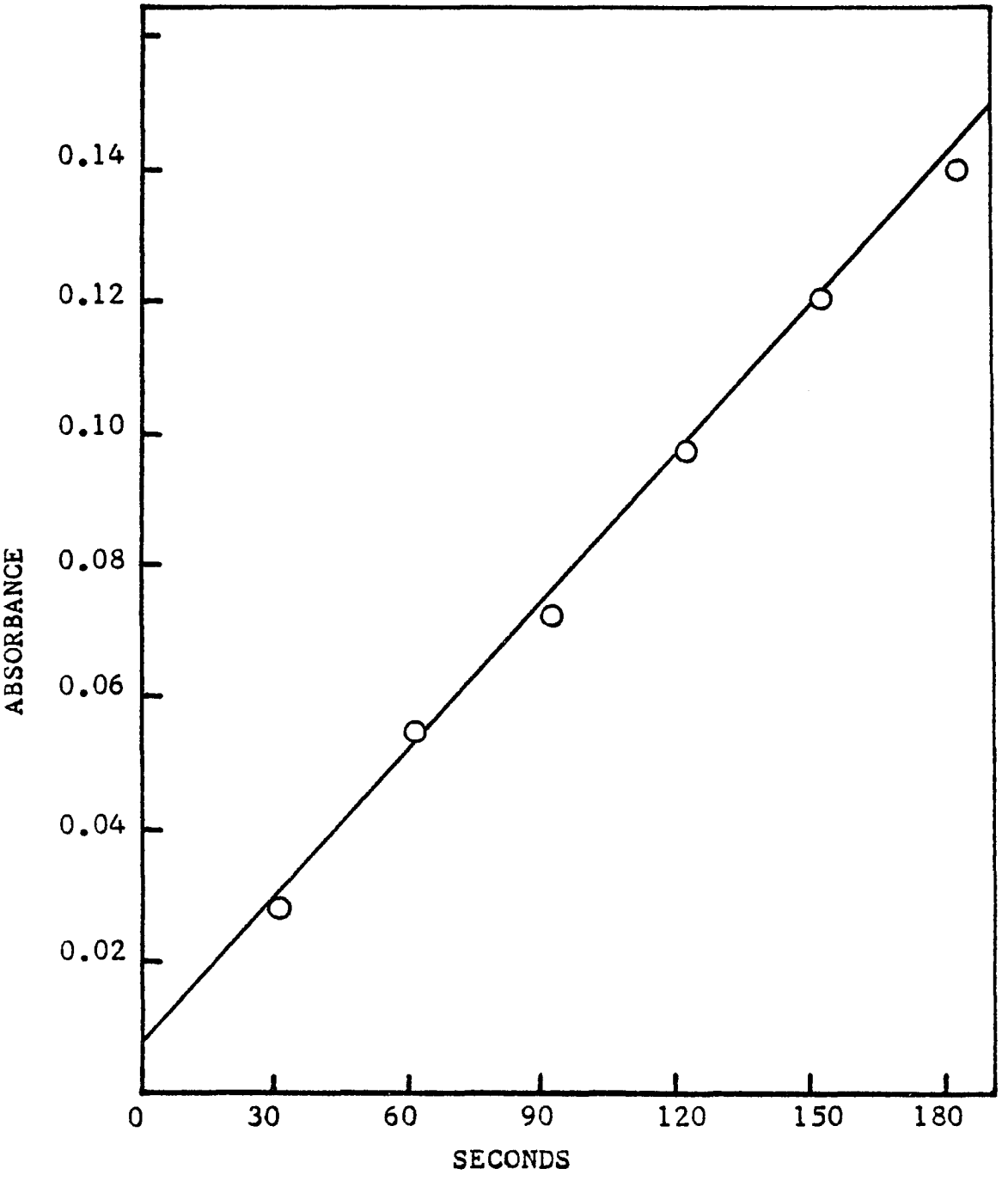

Figure 61. Rate of Formation of $Ru(bpy)_3^+$ (λ=510nm, $\epsilon = 1.2 \times 10^4 M^{-1} cm^{-1}$). Relative light intensity = 0.5.

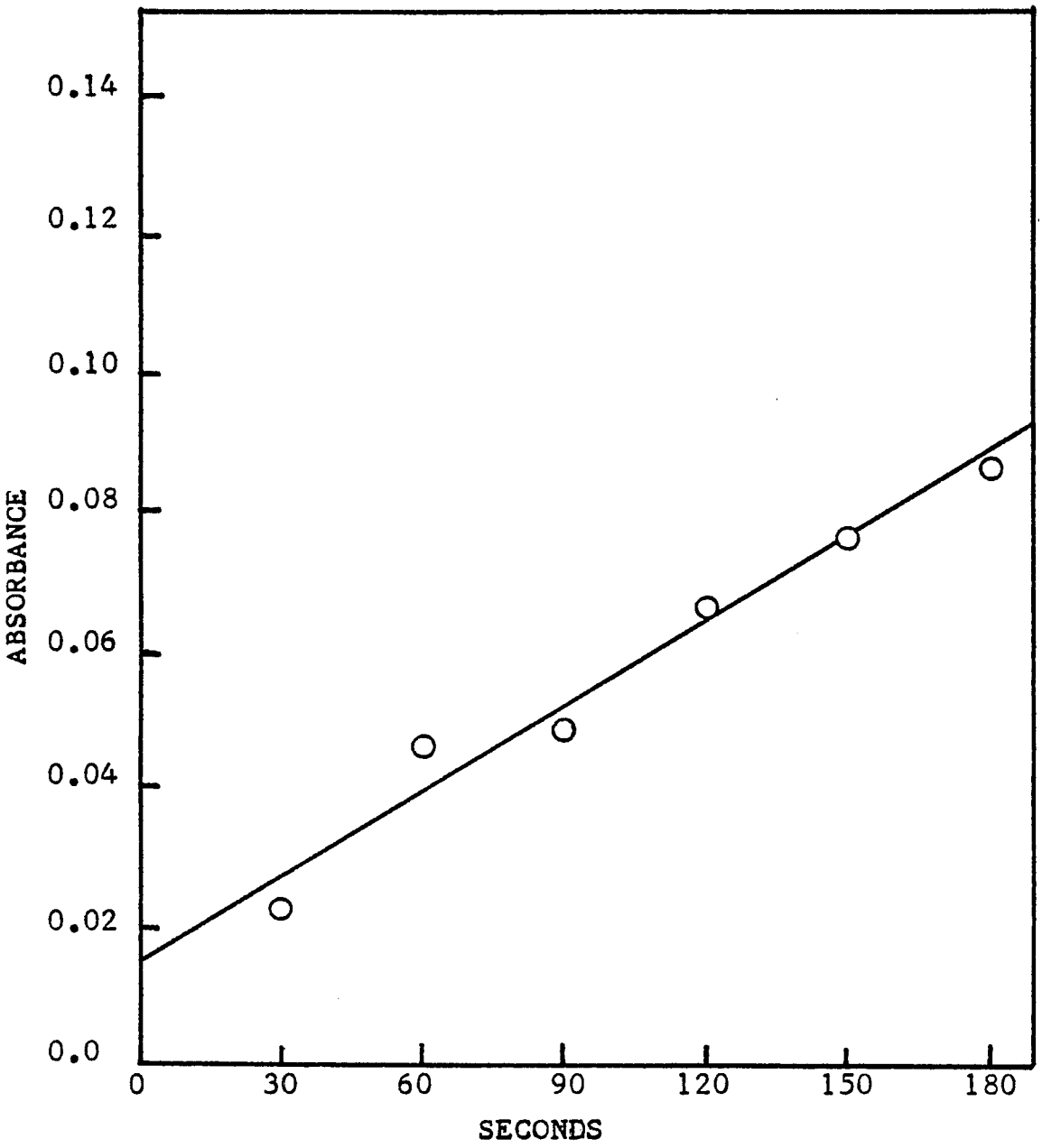

Figure 62. Rate of Formation of $Ru(bpy)_3^+$ (λ =510nm, $\epsilon = 1.2 \times 10^4 M^{-1} cm^{-1}$). Relative light intensity = 0.25.

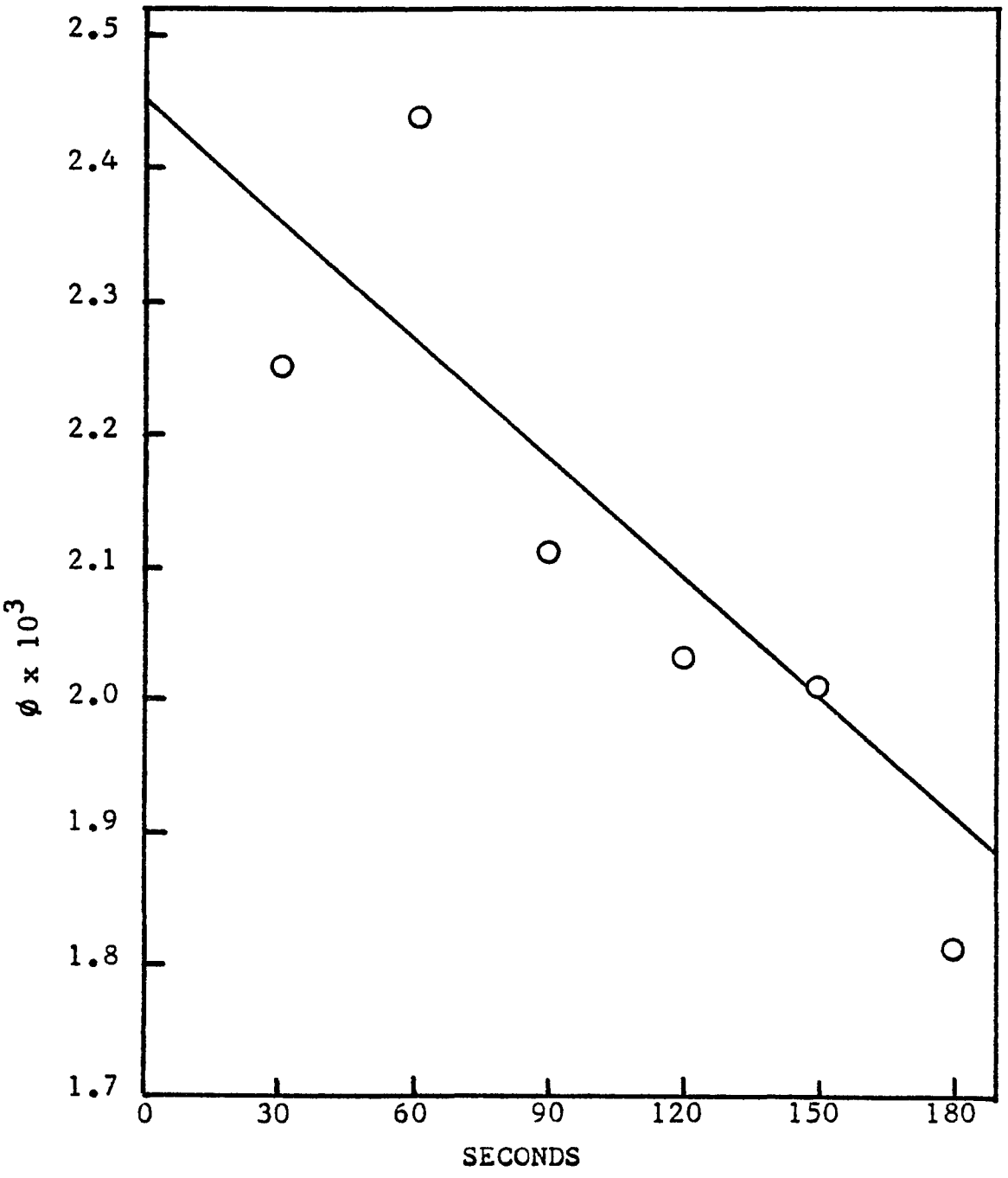

Figure 6 3. Time Dependence of the Quantum Yield of $Ru(bpy)_3^+$. Relative light intensity = 1, $\phi_{limit} = 2.45 \times 10^{-3}$.

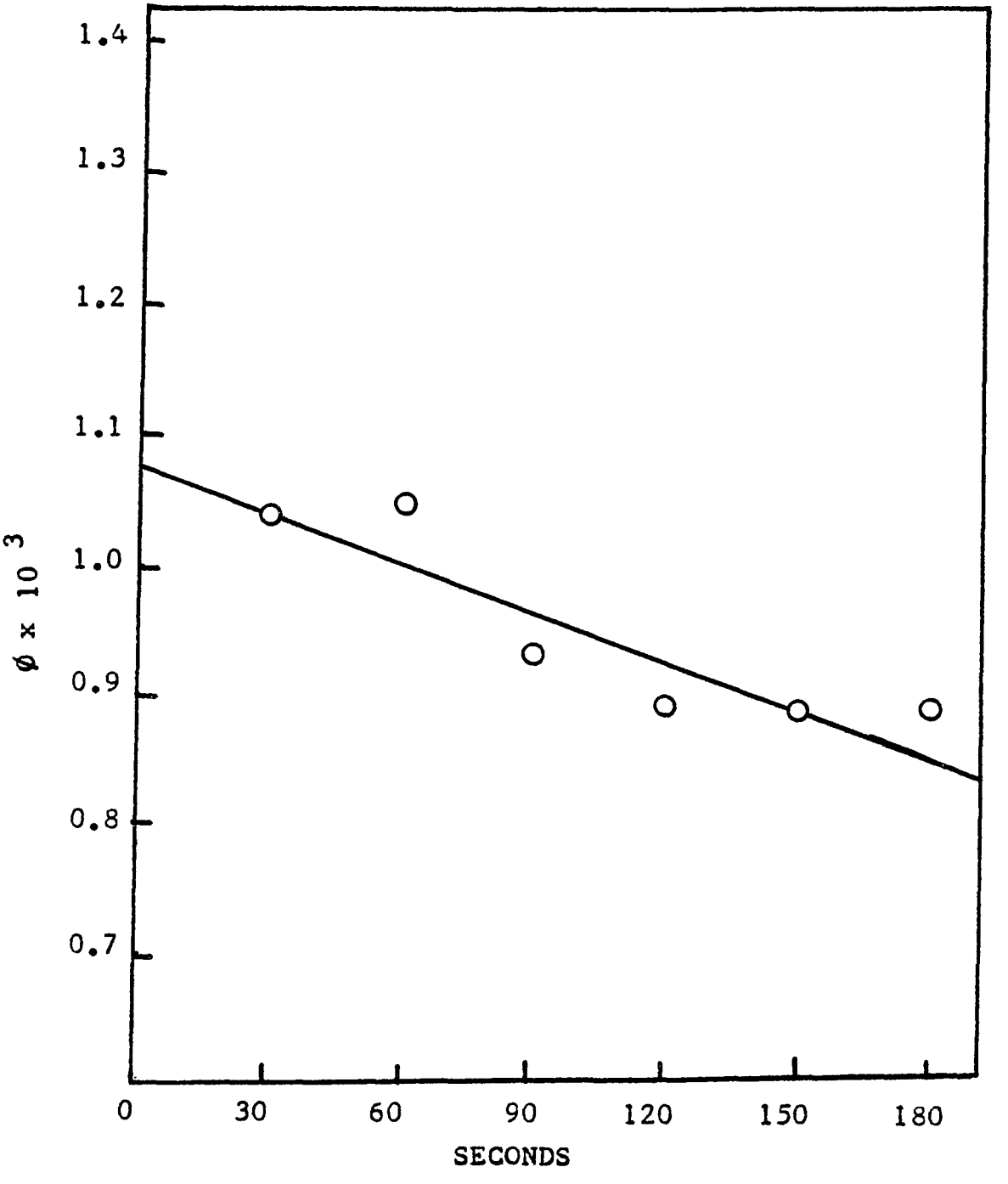

Figure 64. Time Dependence of the Quantum Yield of $Ru(bpy)_3^+$. Relative light intensity = 0.5, $\phi_{limit} = 1.07 \times 10^{-3}$.

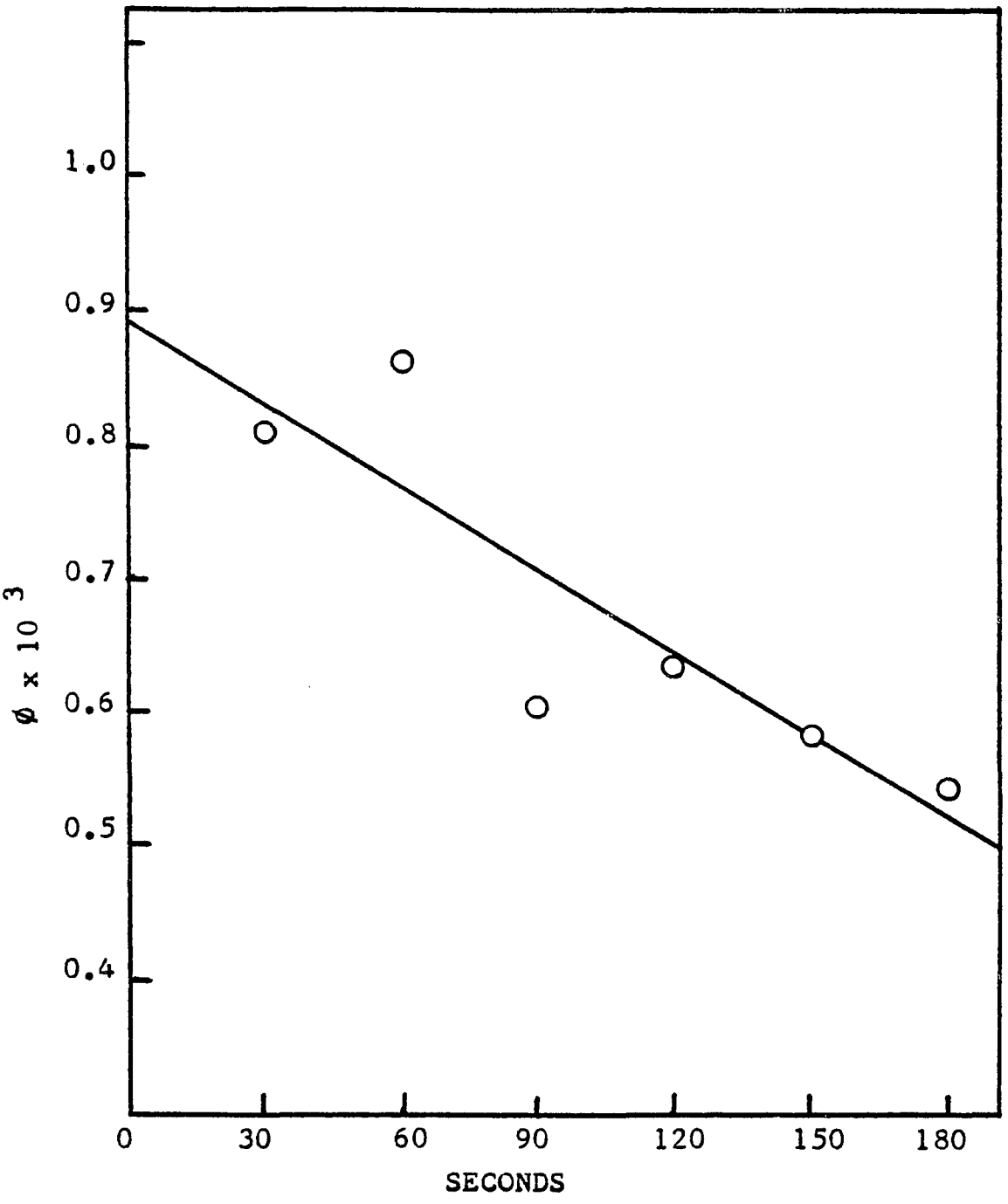

Figure 65. Time Dependence of the Quantum Yield of $Ru(bpy)_3^+$. Relative light intensity =0.25, $\phi_{limit} = .89 \times 10^{-3}$.

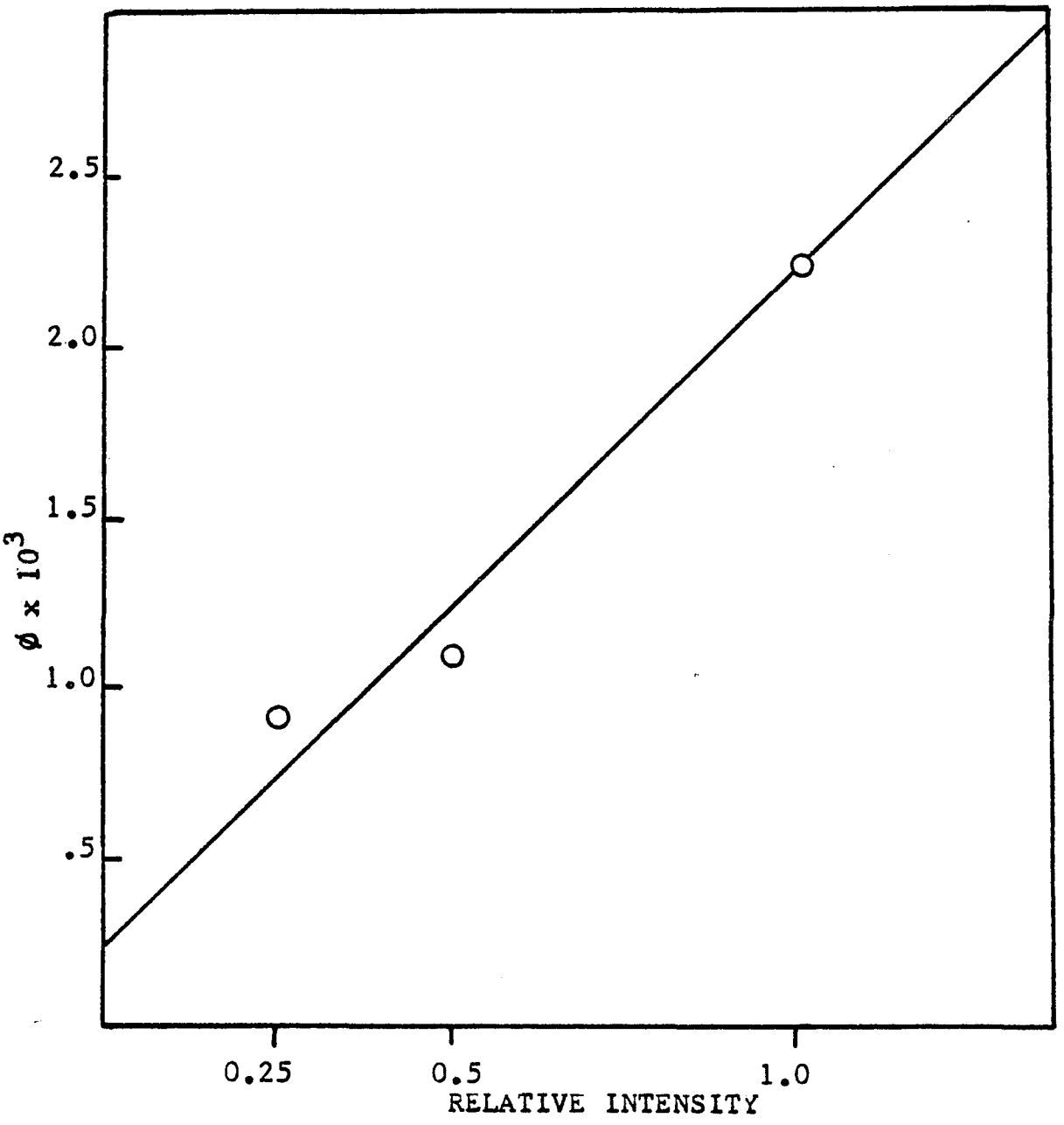

Figure 66. $\phi_{Ru(bpy)_3^+}$ as a Function of Light Intensity. Slope = 2.18.

CHAPTER 4

Discussion

Paraquat is widely used as a redox indicator (45-49). The dramatic color change which coincides with the one electron reduction, $Pq^{2+} + e^- \longrightarrow Pq^{+\cdot}$, makes it easy to monitor (46,50). The fact that it also has sufficient potential to reduce water at pH=7 accounts for its use in solar energy conversion systems.

In the $Ru(bpy)_3^{2+}$ / EDTA / Pq^{2+} / Pt system (42,51), energy storage makes the energy content of the products higher than the ground state reactants. The backreaction to to the starting materials is thermodynamically favored.

$$Ru(bpy)_3^{3+} + Pq^{+\cdot} \longrightarrow Ru(bpy)_3^{2+} + Pq^{2+} \qquad E = 1.7\ V \qquad (33)$$

Energy dissipation via this unproductive reaction is the major obstacle to be overcome in the development of these systems. The initial step in this energy storage process is the production of $Pq^{+\cdot}$ by an electron transfer mechanism (11). $Pq^{+\cdot}$ then reduces water to hydrogen in the presence of a catalyst. The efficiency of this first step obviously limits the overall process. A comparison of the yields of $Pq^{+\cdot}$ for different systems,

therefore, should be a good indication of their relative efficiencies. To evaluate the influence that incorporation of a reaction system into a glass matrix will have on the reaction rates, the ϕ_{Pq^+} in the glass could be compared to ϕ_{Pq^+} in solution. However, solution quantum yields for Pq^+ published in the literature range from 0.02 ($5x10^{-5}$ M $Ru(bpy)_3^{2+}$, $5x10^{-4}$ M Pq^{2+}, 10^{-3} M EDTA) (56) to 0.6 ($2x10^{-5}$ M proflavine, $4x10^{-4}$ M Pq^{2+}, $4x10^{-2}$ M EDTA) (53) in aqueous systems and from 0.07 (55) to 0.4 (16) in acetonitrile solutions. A determination of ϕ_{Pq^+} for the particular set of conditions we would be using seemed necessary.

A limiting value of $\phi_{Pq^+} = 0.04$ was obtained with the concentrations used in these experiments (Table VI). This low value did not bode well for a conversion system based on this reaction. Calculations based on the quenching of $*Ru(bpy)_3^{2+}$ emission by Pq^{2+} suggested that the limit of ϕ_{Pq^+} was approximately 0.1-0.25 (42). More than half of that energy was being lost. The back reaction of $Ru(bpy)_3^{3+}$ and Pq^+ has a driving force of 1.7 V but several observations made during these experiments led us to believe that the energy loss was not due solely to this reaction. A study of the solution reaction system was undertaken in the hope that the information obtained would enable us to optimize the yield of Pq^+, and ultimately the

Table VI. Determination of ϕ_{Pq^+} in Aqueous Solution (10^{-4}M $Ru(bpy)_3^{2+}$, 10^{-2}M EDTA, 10^{-1}M KCl, and 10^{-3} - 10^{-2}M Pq^{2+}).

a Pq^{2+}	ϕ_{Pq^+}	b Pq^{2+}	ϕ_{Pq^+}
10^{-3}	5.9×10^{-3}	$\times 10^{-3}$	6.7×10^{-2}
2×10^{-3}	5.6×10^{-3}	2.5×10^{-3}	7.9×10^{-2}
4×10^{-3}	3.0×10^{-3}	5.0×10^{-3}	3.9×10^{-2}
6×10^{-3}	3.3×10^{-3}	6.0×10^{-3}	4.8×10^{-2}
8×10^{-3}	3.9×10^{-3}	8.0×10^{-3}	5.6×10^{-2}
10^{-2}	6.6×10^{-3}	10^{-2}	7.2×10^{-2}

Measurement were made using the apparatus depicted in a)Figure 3 and b)Figure 4.

yield of H_2.

Two observations suggested that other mechanisms, in addition to the back reaction, were limiting the yield of $Pq^{\dagger}$. These were the existence of a variable induction period and the partial loss of $Pq^{\dagger}$ when photolysis was discontinued.

The induction period may be attributable to traces of O_2 and other oxidants. The sensitivity of $Pq^{\dagger}$ to O_2 is the basis of a scheme developed by Sweetser for detection of trace levels of O_2 (0-35 ppm) in gases (52). If oxygen was present in the reaction container no $Pq^{\dagger}$ would be detected until all the O_2 was scavenged by $Pq^{\dagger}$ and the system was clean. Even closed samples which were not degassed turn blue after a long induction period. Shaking these samples caused the color to disappear but it could be regenerated when the dissolved O_2 was all reacted. All samples were degassed by three successive freeze-thaw cycles in an effort to eliminate this problem, but this was only partially successful. The difference in the quantum yields obtained when the solution was mixed (4.0×10^{-3}) and when the solution was still (4×10^{-2}) was further indication that the oxidants were still present. Oxidizing impurities in the reagents were a possibility, but reaction samples were prepared from stock solutions and some consistency in the results

should have emerged if this were the case.

The thermal reaction of $Pq^{+\cdot}$ with oxidized EDTA ($EDTA_{ox}$), or its decomposition products might account for the partial loss of $Pq^{+\cdot}$ depicted in Figure 19. Kalyanasundaram and coworkers (42) have shown that the oxidized donor, $TEOA^+$, reacts with $Pq^{+\cdot}$, abstracting an electron. This reaction is favored by a potential

$$TEOA^+ + Pq^{+\cdot} \longrightarrow TEOA + Pq^{2+} \qquad (34)$$

of 1.26 V. Buffering the system prevented the reaction going to completion and the loss of all the energy. At high pH, the acid-base equilibrium of this species even promotes the thermal formation of $Pq^{+\cdot}$. The complex role of the electron donor, TEOA, in this system, prompted us to examine the role of EDTA in $Pq^{+\cdot}$ formation.

All attempts to produce $Pq^{+\cdot}$ by the photolysis of solutions containing only $Ru(bpy)_3^{2+}$ and Pq^{2+} have been unsuccessful. The presence of an electron donor is required for the net production of $Pq^{+\cdot}$. We knew from quenching studies that EDTA reduced the Ru complex after the electron transfer event (43), but we did not know how this reaction competed with the favored back reaction, which has a rate constant of $k = 2.4 \times 10^9\ M^{-1}\ s^{-1}$ (42). Whitten (55) described the scavenging of $Ru(bpy)_3^{3+}$

as "remarkable". When one thinks of the donor and quencher in a solvent cage, within a reaction radius and the strong driving force of the back reaction, this seems an apt description. The probability of the EDTA diffusing to and reducing the $Ru(bpy)_3^{3+}$ before the geminate recombination of the ions is not high. The probability of the reduction would be much higher if the diffusion step could be eliminated. A two component reaction, between one species and an EDTA modified compound, is more likely. Evidence for the existence of this new modified compound in the reaction solution was sought.

Spectra provided no indication of ligand substitution or outer-sphere complexes but the spectra of the ion-pair may not be very different from that of the unpaired complex (124). Conductivity measurements also did not detect any new species. Quenching studies, however, supported the idea that EDTA was interacting with $Ru(bpy)_3^{2+}$ and Pq^{2+}.

An examination of the data in Table I reveals that the increase in the quenching rate constant, k_q, due to EDTA far exceeds that expected on the basis of ionic strength alone, 0.01 M $EDTA^{2-}$ (μ=0.03) has a $K_{sv} = 1.3 \times 10^3\ M^{-1}$, approximately double that of 0.1 M KCl, $K_{sv} = 0.67 \times 10^3\ M^{-1}$, which has a three-fold larger ionic strength, μ=0.1. It also suggests that

the influence of EDTA is exerted before the quenching encounter even though it does not reduce $Ru(bpy)_3^{3+}$ until after that event. If EDTA did not interact with the donor and quencher until after the electron transfer, an increase in stable Pq^+ would be expected but not a change in the quenching rate itself. Increasing ionic strength increases the quenching rate by facilitaing the encounter of the two dications. It is logical to assume that EDTA accelerates the quenching rate in the same manner but by a more specific interaction. The simplest way for EDTA to minimize the electrostatic repulsion would be to form an ion pair.

The theory of ion pair formation, by ions of opposite charge, was first formalized in 1926 by Bjerrum (125). The theory deals with large spherical ions and can be applied to interactions between a substitution inert complex and an anion. Simpler theories indicate that for systems with $|Z_1Z_2| > 3$ (where Z_1 and Z_2 are the ionic charges) ion pairing is readily detected in water (126). $Ru(bpy)_3^{2+}$ is a spherical inert complex, and $|Z_1Z_2| = 4$ for the $Ru(bpy)_3^{2+}$: EDTA couple.

The preexistence of a $Ru(bpy)_3^{2+}$: EDTA ion pair would eliminate the diffusion step in the reduction of $Ru(bpy)_3^{3+}$ by EDTA. Contained within the same

solvent cage, EDTA could compete with $Pq^{+\cdot}$. Ordering the reactants within a reaction volume would act to increase the product yield in two ways; by decreasing the coulombic repulsion, ion pairing increases the quenching rate and, by having the e^- donor within the reaction volume, reduction of $Ru(bpy)_3^{3+}$ is competitive with the energy degrading back reaction.

The confinement of these reagents to a solvent cage could also explain the initial limited loss of $Pq^{+\cdot}$ when photolysis is stopped. Following reduction of $Ru(bpy)_3^{3+}$, $|Z_1Z_2| = 2$ for the $Ru(bpy)_3^{2+}$: $EDTA_{ox}$ couple and the ion pair will be more loosely bound. In addition, $EDTA_{ox}$ decomposes (51) to CO_2, H_2CO, and ethylenediaminetriacetic acid, which will further disrupt the ion pair. For a brief interval, however, $EDTA_{ox}$ and $Pq^{+\cdot}$ are within a solvent cage and may react (42). The stability of the remainder of the $Pq^{+\cdot}$ may be attributable to the rapid rates of dissociation of the ion pair and decomposition of $EDTA_{ox}$.

Additional evidence of the role of ion pairs in preventing the back reaction was sought in the experiments in which ion pair formation was inhibited by protonation or complexation. It was suggested that, even though $Ru(bpy)_3^{3+}$ was readily reduced by EDTA in 1.0 N H_2SO_4, the pH dependence of the potential of EDTA made the results of the first experiment

questionable and that a test of the ion pair hypothesis at neutral pH would be more conclusive. At neutral pH, EDTA can be complexed to inhibit ion pair formation. In actuality, it is not possible to chemically alter EDTA without affecting its potential. Even at pH=7, bound EDTA will have a different potential than free EDTA. If the EDTA is bound in a metal : EDTA complex which is readily oxidized by $Ru(bpy)_3^{3+}$, however, it should be possible to separate the effects of ion pairing and redox potential on the formation of $Pq^{+\cdot}$. $FeEDTA^{2-}$ ($FeEDTA^{2-/1-}$, E=0.117V) (117) is oxidized by $Ru(bpy)_3^{3+}$ ($Ru(bpy)_3^{3+/2+}$, E=1.3 V) but no $Pq^{+\cdot}$ was formed when solutions of $Ru(bpy)_3^{2+}$, Pq^{2+}, and the iron complex were photolyzed. If EDTA was acting only as a reducing agent, then $FeEDTA^{2-}$ should have the same effect. If the ion pair is non-specific, based only on electrostatic attraction, then again the anionic $FeEDTA^{2-}$ should have sufficed.

The choice of Fe^{2+} complicated the interpretation of these results. $FeEDTA^{2-}$ quenches $*Ru(bpy)_3^{2+}$, $K_{sv} = 6x10^4\ M^{-1}$ (127), at approximately the same rate as Pq^{2+} does, $K_{sv} = 6.7x10^4\ M^{-1}$. Competition between these two quenchers results in the formation of $Ru(bpy)_3^{3+}$ and $Ru(bpy)_3^{+}$ in essentially equal amounts, and

$FeEDTA^-$ oxidizes some of the $Pq^{+\cdot}$ formed.

$$FeEDTA^- + Pq^{+\cdot} \longrightarrow FeEDTA^{2-} + Pq^{2+}$$
$$E = 0.323\ V \qquad (35)$$

A look at equations 33-37 will reveal the problem.

$$FeEDTA^{2-} + {}^*Ru(bpy)_3^{2+} \longrightarrow FeEDTA^{-1} + Ru(bpy)_3^{+} \qquad (36)$$
$$Pq^{2+} + {}^*Ru(bpy)_3^{2+} \longrightarrow Pq^{+\cdot} + Ru(bpy)_3^{3+} \qquad (37)$$
$$Pq^{2+} + Ru(bpy)_3^{+} \longrightarrow Pq^{+\cdot} + Ru(bpy)_3^{2+} \qquad (38)$$
$$Pq^{+\cdot} + FeEDTA^{-1} \longrightarrow Pq^{2+} + FeEDTA^{2-} \qquad (39)$$
$$Ru(bpy)_3^{+} + Ru(bpy)_3^{3+} \longrightarrow 2Ru(bpy)_3^{2+} \qquad (40)$$

If equation 36-39 are representative of the solution reactions, then we would expect to see $Pq^{+\cdot}$ at about half the yield if ion pairing was not important. The absence of any $Pq^{+\cdot}$ would then suggest that ion pairing was essential. However, if the disproportionation products recombine, equation 40, then reaction 38 will not occur. In this case, the overall reaction would result in no $Pq^{+\cdot}$ formation. We do not know which of these mechanisms occurs in solution and so we can not draw any conclusions from this experiment.

The quenching data and NMR experiments are strong evidence for the formation of a pre-equilibrium ion pair between $Ru(bpy)_3^{2+}$ and EDTA. In fact, a careful

$[Ru(bpy)_2(bpy^-)(glass)]^0$. If reaction with the glass is responsible for the stability of the $Ru(bpy)_3^+$ species, this reaction must be rapid. The stability of ESR and absorption spectra for several hours following the termination of photolysis indicate that any reaction must have already occurred. Bonding to the glass may stabilize $Ru(bpy)_3^+$ by altering the redox potential of the complex and thus reducing the driving force of the recombination reaction of the disproportionation products. The photoanation products of $Ru(bpy)_3^{2+}$ in aqueous media are stable enough to permit separation of the products by chromatography (124).

Despite the potential of $*Ru(bpy)_3^{2+}$ to mediate the photolysis of water, no reaction between the excited complex and water has been detected. Formation of the disproportionation products, which do react with water, has been suggested as an alternative method for applying the photoredox chemistry of $Ru(bpy)_3^{2+}$ to solar conversion systems. Strong evidence that $Ru(bpy)_3^+$ and $Ru(bpy)_3^{3+}$ are formed in the glass has been presented in this thesis. However, photolysis of glasses containing $Ru(bpy)_3^+$ did not lead to the formation of detectable quantities of H_2. If 10^{14} radicals were generated, only $5x10^{13}$ H_2 molecules would be formed at 100% efficiency. The instrumentation used in these experiments were not capable of detecting 10^{-9} moles of H_2. Cycling of the

the glass. It was also noted that the concentration of stable radicals in the glass, $10^{14}/m^2$, was relatively uniform from sample to sample. This could be interpreted as further support of the idea that the radicals reacted with the glass, which would have some fixed number of reaction sites. In a typical photolysis experiment , $\sim 10^{-8}$ moles of $Ru(bpy)_3^+$ were generated in a 4 g $Ru(bpy)_3^{2+}$ glass sample. Assuming the reagent occupies 30% of the pore volume, this corresponds to a concentration of $6 \pm 1 \times 10^{13}$ radicals / m^2. This is in good agreement with Melamud's observation.

How does $Ru(bpy)_3^+$ react with the glass? One possibility is that the radical complex hydrogen bonds to the glass. Bpy^- is rapidly protonated at the N atom in solution. $[Ru(bpy)_2(bpy^-)]^+$ may H-bond with Si-OH groups on the glass surface to form $[Ru(bpy)_2$ $(bpy\ HO\text{-}Si\ glass^-)]^+$. Another possibility would be photoanation to the glass. Prolonged photolysis of of $Ru(bpy)_3^{2+}$ in aqueous and non-aqueous media leads to ligand substitution and the formation of a monodentate bpy ligand (36,124). Ion pairs have been implicated in the formation of $[Ru(bpy)_2 bpy\ OH]^+$ in solution due to its rapid rate of formation. The electrostatically adsorbed $Ru(bpy)_3^{2+}$ may be considered to be part of a complex : glass ion pair. $[Ru(bpy)_2(bpy^-)]^+$ may react with SiO^- groups on the glass surface to form

mechanistic data detailed above, the proposal of a direct $*Ru(bpy)_3^{2+}$--$*Ru(bpy)_3^{2+}$ disproportionation in the glass seems reasonable.

The recombination of the disproportionation products is favored by 2.6 V. In fluid media,

$$Ru(bpy)_3^{+} + Ru(bpy)_3^{3+} \longrightarrow 2Ru(bpy)_3^{2+} \qquad (44)$$

$Ru(bpy)_3^{+}$ has only been identified as a transient species with a lifetime of 2 ± 0.6 msec (128) to 5 sec (122). A surfactant $Ru(bpy)_3^{+}$ species prepared by Whitten had a lifetime on the order of a few days (16). $Ru(bpy)_3^{+}$ in the glass has a lifetime $\geq$ 91 days. Considering the strong driving force of the recombination reaction and the physical closeness of the complex ions, which facilitated the disproportionation reaction, the stability of $Ru(bpy)_3^{+}$ in the glass is striking.

Other workers have noted that transient species were stabilized in Thirsty Glass (101,102). When alkylated glasses were photolyzed, $\cdot CH_2$ radicals with lifetimes ranging up to 12 months were detected (101). ESR spectra of radicals in solution and in the glass indicated that the bond angles in $\cdot CH_2$ and the rotation of $\cdot C(CH_3)_3$ were altered in the glass. Melamud (101) therefore proposed that a reaction with the glass was responsible for the longer lifetimes of the radicals in

were subjected to intense flash photolysis. They postulated that a biphotonic process, involving an e^-_{aq} intermediate, led to the formation of $Ru(bpy)^+_3$. In O_2 free solutions, the halflife of $Ru(bpy)^+_3$ was

$$Ru(bpy)^{2+}_3 \longrightarrow *Ru(bpy)^{2+}_3 \quad (41)$$

$$*Ru(bpy)^{2+}_3 \longrightarrow Ru(bpy)^{3+}_3 + e^-_{aq} \quad (42)$$

$$e^-_{aq} + Ru(bpy)^{2+}_3 \longrightarrow Ru(bpy)^+_3 \quad (43)$$

2 ± 0.6 nsec.

While the stoichiometry, absorption spectra, and ESR data establish a photochemical reaction which is essentially identical to that previously observed in fluid solution, the reaction mechanism within the two media differ. In fluid solution, disproportionation proceeds via an e^-_{aq} intermediate (128), but postulating a similar mechanism within the glass is not supported by the experimental data. In the glass, as in solution, O_2 and $EuCl_3$ quench $*Ru(bpy)^{2+}_3$ and prevent the formation of $Ru(bpy)^+_3$ (128). CCl_4, acting as an e^-_{aq} scavenger, is also an inhibitor in solution (128), but was found to have no effect on the production of $Ru(bpy)^+_3$ in the glass. The formation of $Ru(bpy)^+_3$ is dependent on the square of the irradiation intensity (Figure 66). This is consistent with a bimolecular reaction between two photo-excited species. In conjunction with the other

and the similarity of the slower exponential decay, $\tau = 680 \pm 20$ nsec, with that previously observed in water, $\tau = 600 \pm 20$ nsec, suggests that the environment within the glass resembles that in aqueous or alcoholic solution. Like that reported in SDS micelles, however, there is a nonhomogeneous distribution of the complex within the glass.

Glasses containing 10^{-5} moles of $Ru(bpy)_3^{2+}$ / g glass exhibited only the fast, $\tau = 60$ nsec, decay. Assuming a distribution similar to those in Figures 38 and 39, these samples had ~ 16.7 $Ru(bpy)_3^{2+}$ / cavity near the surface. An upper limit for the number of $Ru(bpy)_3^{2+}$ / cavity was calculated to be 16.8 after making the following assumptions: 1) cavities are spherical with r = 35 Å; 2) $Ru(bpy)_3^{2+}$ is a sphere of r = 6.24 Å; and 3) adsorbed $Ru(bpy)_3^{2+}$ ions are arranged in a monolayer at the glass surface. The uncanny agreement of these two values suggests that the physical proximity of the $*Ru(bpy)_3^{2+}$ complex ions promotes the bimolecular reaction. No unimolecular decay was observed. A number of photochemical experiments were performed to determine the products of this reaction.

Photolysis of $Ru(bpy)_3^{2+}$ in the glass produces a new species which absorbed at 510 nm. Meisel and coworkers (128) observed a transient increase in absorbance at 510 nm when aqueous solutions of $Ru(bpy)_3^{2+}$

the number of $Ru(bpy)_3^{2+}$ / micelle suggests that an intramicellar $*Ru(bpy)_3^{2+}$--$*Ru(bpy)_3^{2+}$ annihilation competes with the unimolecular decay. A similar two component decay was found when $Ru(bpy)_3^{2+}$ was adsorbed on Thirsty Glass and irradiated. A relatively fast $\tau \sim 60$ nsec nonexponential decay was followed by an exponential $\tau = 680 \pm 20$ nsec decay (129).

Although the complex is adsorbed to the glass, attributing the two decay rates to differences caused by the adsorption of the complex to the glass is not supported by the experimental data. Both the surface of glass itself and the surface of the cavities within the glass are composed of Si-OH units (96). Therefore, the enviroment either within the cavity or on the surface would be similar and, a priori, might be expected to resemble that in aqueous or alcoholic solutions. As proviously reported, the absorption and Raman spectra of the complex within the glass is essentially identical to that recorded in aqueous solution (Figures 43-46). There is a 10 to 15-nm red shift in the emission maximum, Figures 47and 48, but this is similar to the red shift previously observed in SDS micelles and alcoholic solutions (53,82). The absence of significant spectral changes, which would be expected to reflect significant differences due to adsorption, suggests that this is not the cause of the two decay rates. Rather, these results

examination of the NMR data in Table IV shows that the two proton groups were shifted to different degrees. The carboxymethylene protons are shifted to a greater degree. This would be consistent with the approach of the positively charged Ru(II) complex to the CH_2COO^- group in the formation of the ion-pair. Further examination of the ion pairing hypothesis is warranted. Additional experiments will be carried out with a more carefully selected metal complex.

If the assumption of the ion pair is correct, then the arrangement of the reactants, $Ru(bpy)_3^{2+}$: EDTA and Pq^{2+}, within a reaction volume is responsible for the stabilization of $Pq^{+\cdot}$, which is a transient species in the absence of EDTA. If a degree of order beyond the solvent cage : ion pair can be achieved in the glass, it may be possible to improve the efficiency of this conversion reaction.

Photolysis of $Ru(bpy)_3^{2+}$ in a porous glass matrix produced the same spectral changes observed in aqueous (128) and micellar (82) solutions. The non-homogeneous distribution of $Ru(bpy)_3^{2+}$ in anionic SDS micelles enhanced the radiative decay of $*Ru(bpy)_3^{2+}$ (82). When the number of $Ru(bpy)_3^{2+}$ ions per micelle was high, a fast, $\tau \leq 5$ nsec, nonexponential decay was followed by a slower exponential decay, $\tau = 800 \pm 80$ nsec. A qualitative relationship between these decay rates and

catalyst is necessary to generate more H_2. The formation of $[Ru(bpy)_2bpy\ X]^{2+}$ is reversible in non-aqueous solution but we did not observe the regeneration of $Ru(bpy)_3^{2+}$ in the glasses. This is a major difficulty to be overcome if these systems are to have practical applications. Access to the catalyst could also lower the yield but we do not have any data on this aspect of the problem yet. Another problem which must be dealt with before these systems can be used on a large scale is the accessibility of reagents in the cavities to reagents in bulk solution. Flow systems would deliver fresh substrate and remove products from the surface of the glass, but these reagents must be able to get into and out of the reaction sites in the cavities. Preliminary experiments indicated that while gaseous products readily diffused out of the glass, exchange of reagents in solution between the bulk solvent and the glass was slow. Since the glass is functioning as 1) a support for the redox catalyst and 2) an adsorbent which permits the buildup of high local concentrations of $Ru(bpy)_3^{2+}$ and hence $*Ru(bpy)_3^{2+}$, using thinner pieces of glass should not affect the function of the glass but would increase the accessibility to adsorbed reagents. Incorporation of thin plates of treated glass into a flow system might make the reaction of $Ru(bpy)_3^{+}$ and $Ru(bpy)_3^{3+}$ with water competitive with the secondary reactions which

lead to loss of the catalytic form of the complex.

REFERENCES

1. Wrighton, M.S. Chem. and Eng. News. 1979, 57, 29.
2. Balzani, V.; Moggi, L.; Manfrin, M.F.; Bolletta, F.; and Gleria, M. Science. 1975, 189, 852 and references there in.
3. Kirch, M.; Lehn, J.-M.; and Sauvage, J.-P. Helv. Chim. Acta. 1979, 62, 1345 and references there in.
4. Scharf, H.-D.; Fleischhauer, J.; Leismann, H.; Ressler, I.; Schleker, W.; and Weitz, R. Angew. Chem. Int. Ed. Engl. 1979, 18, 652.
5. Almgren, M. Photochem. Photobiol. 1978, 27, 603.
6. Gafney, H.D. and Adamson, A.W. J. Am. Chem. Soc. 1972, 94, 8238.
7. Lin, C.-T. and Sutin, N. J. Phys. Chem. 1976, 80, 97.
8. Lin, C.-T.; Böttcher, W.; Chou, M.; Creutz, C.; and Sutin, N. J. Am. Chem. Soc. 1976, 98, 6536.
9. Hoselton, M.A.; Lin, C.-T.; Schartz, H.A.; and Sutin, N. ibid. 1978, 100, 2383.
10. Meyer, T.J. Israel J. Chem. 1976/1977, 15, 200.
11. Bock, C.R.; Meyer, J.T.; and Whitten, D.G. J. Am. Chem. Soc. 1974, 96, 4710.
12. Navon, G. and Sutin, N. Inorg. Chem. 1974, 13, 2159.
13. Bock, C.R.; Meyer, T.J.; and Whitten, D.G. J. Am. Chem. Soc. 1975, 97, 2909.
14. Creutz, C. Inorg. Chem. 1978, 17, 1046.

15. Creutz, C. and Sutin, N. ibid. 1976, 15, 496.

16. DeLaive, P.J.; Lee, J.T.; Sprintschnik, H.W.; Abruna, H.; Meyer, T.J.; and Whitten, D.G. J.Am. Chem. Soc. 1977, 99, 7094.

17. Young, R.C.; Meyer, T.J.; and Whitten, D.G. ibid. 1976, 98, 286.

18. Oishi, S. and Furuta, N. Chem. Lett. 1978, 45.

19. Sutin, N. J. Photochem. 1979, 10, 19.

20. Calvin, M. Science. 1974, 184, 375.

21. Kruck, T.; Sylvester, G.; and Kunau, I.P. Angew. Chem. Int. Ed. Engl. 1971, 10, 725.

22. Green, M.L.H.; Mitchard, L.C.; and Silverthorn, W.E. J. Chem. Soc. Dalton Trans. 1974, 1361.

23.a)Krogman, D.W. The Biochemistry of Green Plants, Prentice Hall, Englewood Cliffs, N.J., 1973.

b)Katz, J.J. Inorganic Biochemistry, Vol. II, G.L. Eichorn, ed., Elsevier, New York, N.Y., 1973.

24. Hong, F.T. Photochem. Photobiol. 1976, 24, 155.

25. Sprintschnik, G.; Sprintschnik, H.W.; Kirsch, P.P.; and Whitten, D.G. J. Am. Chem. Soc. 1976, 98, 2337.

26. Gaines, G.L.; Behnken, P.E.; and Valenty, S.J. ibid. 1978, 100, 6549.

27. Valenty, S.J. and Gaines, G.L. ibid. 1977, 99, 1285.

28. Sprintschnik, G.; Sprintschnik, H.W.; Kirsch, P.P.; and Whitten, D.G. ibid. 1977, 99, 4947.

29. Schumacher, E. Chimia. 1978, 32, 193.

30.a)Whitten, D.G. Acc. Chem. Res. 1980, 13, 83.

b)Huang, S.-M.Y. and Gafney, H.D. J. Phys. Chem. 1977, 81, 2602.

c)Ballardini, R.; Varani, G.; Scandola, F.; and Balzani, V. J. Am. Chem. Soc. 1976, 98, 7432.

d)Creutz, C. and Sutin, N. ibid. 1977, 99, 241.

e)Bensasson, R.V.; Salet, C.; and Balzani, V. C.R. Acad. Sc. Paris, Serie B. 1979, 289, 41.

f)Demas, J.N. and Addington, J.W. J. Am. Chem. Soc. 1976, 98, 5800.

g)Juris, A.; Manfrin, M.F.; Maestri, M.; and Serpone, N. Inorg. Chem. 1978, 17, 2258.

h)Bolletta, F.; Maestri, M.; and Maggi, L. J. Phys. Chem. 1973, 77, 861.

i)Anderson, C.P.; Meyer, T.J.; Salmon, D.J.; and Young, R.C. J. Am. Chem. Soc. 1977, 99, 1980.

31. Bolletta, F.; Maestri.; and Balzani, V. J. Phys. Chem. 1976, 80, 2499.

32. Demas, J.N. and Crosby, G.A. J. Am. Chem. Soc. 1971, 93, 2841.

33. Navon, G. and Sutin, N. Inorg. Chem. 1974, 13, 2976.

34. Demas, J.N. and Adamson, A.W. J. Am. Chem. Soc. 1973, 95, 5159.

35. Natarajan, P. and Endicott, J.F. ibid. 1973, 95, 2470.

36. Prolonged photolysis of aqueous solutions of $Ru(bpy)_3^{2+}$ at 95° C labilizes the bipyridine ligand.

Houten, J.V. and Watts, R.J. ibid. 1976, 98, 4853.

37. DeLaive, P.J.; Sullivan, B.P.; Meyer, T.J.; and Whitten, D.G. ibid. 1979, 101, 4007.

38. Brown, G.M.; Chan, S.-F.; Creutz, C.; Schwartz, H.A.; and Sutin, N. ibid. 1979, 101, 7638.

39. Gleria, M.; Minto, F.; Beggiato, G.; and Bortolus, P. J. Chem. Soc. Chem. Comm. 1978, 285.

40. Creutz, C. and Sutin, N. Proc. Nat. Acad. Sci. U.S.A. 1975, 72, 2858.

41. Lehn, J.-M. and Sauvage, J.-P. Nouv. J. Chim. 1977, 1, 449.

42. Kalyanasundaram, K.; Kiwi, J.; and Grätzel, M. Helv. Chim. Acta. 1978, 61, 2720.

43. Moradpour, A.; Amouyal, E.; Keller, P.; and Kagan, H. Nouv. J. Chim. 1978, 2, 547.

44. Brown, G.M.; Brunschwig, B.S.; Creutz, C.; Endicott, J.F.; and Sutin, N. J. Am. Chem. Soc. 1979, 101, 1298.

45. Krasnovskii, A.A. and Brin, G.P. Dokl. Akad. Nauk. S.S.S.R. 1965, 163, 761.

46. Michaellis, L. and Hill, E.S. J. Gen. Physiol. 1933, 16, 859.

47. Kramer, D.N.; Guilbault, G.G.; and Miller, F.M. J. Org. Chem. 1967, 32, 1163.

48. Naik, M.S. and Nicholas, D.J.J. Biochim. Biophys. Acta. 1967, 131, 204.

49. Naik, M.S. and Nicholas, D.J.J. ibid. 1966, 118, 195.

50. Michaelis, L. and Hill, E.S. J. Am. Chem. Soc. 1933, 55, 1481.

51. Krasna, A.I. Photochem. Photobiol. 1979, 29, 267.

52. Sweetser, P.B. Analyt. Chem. 1967, 39, 979.

53. Meisel, D.; Matheson, M.S.; and Rabani, J. J. Am. Chem. Soc. 1978, 100, 117.

54. Brugger, P.A. and Grätzel, M. J. Am. Chem. Soc. 1980, 102, 2461.

55. DeLaive, P.J.; Gianotti, C.; and Whitten, D.G. ibid. 1978, 100, 7413.

56. Takuma, K.; Shuto, Y.; and Matsuo, T. Chem. Lett. 1978, 983.

57. Kalyanasundaram, K. and Grätzel, M. Angew. Chem. Int. Ed. Engl. 1979, 18, 701.

58. Krasna, A.I. Photochem. Photobiol. 1980, 31, 75.

59. Other electron donors, e.g. dimethylaniline, react directly with the excited state. See reference 14.

59a. The formal charge of EDTA, ethylenediaminetetraacetic acid, is pH dependent. At neutral pH, the H_2Y^{2-} and HY^{3-} forms predominate. No designation of charge will be made except when necessary for clarity.

60. Kiwi, J. and Grätzel, M. J. Am. Chem. Soc. 1979, 101, 7214.

61. Kiwi, J. and Grätzel, M. Angew. Chem. Int. Ed. Engl. 1978, 17, 860.

62. Lee, K.-H. and deMayo, P. J. Chem. Soc. Chem. Comm. 1979, 493.

63. Greenbaum, E. Science. 1977, 196, 878.

64. Gibbs, M., ed. Structure and Function of Chloroplasts, Springer-Verlag, Berlin, 1971.

65. Calvin, M. J. Theoret. Biol. 1961, 1, 258.

66. Calvin, M. Acc.Chem. Res. 1978, 11, 369.

67. Hopf, F.R. and Whitten, D.G. J. Am. Chem. Soc. 1976, 98, 7424.

68.a)Zachariasse, K.A. and Whitten, D.G. Chem. Phys. Lett. 1973, 22, 527.

b)Hopf, F.R.; Mobius, D.; and Whitten, D.G. J. Am. Chem. Soc. 1976, 98, 1584.

69. Quina, F. and Whitten, D.G. ibid. 1977, 99, 877.

70. Parker, C.A. Photoluminesence of Solutions, Elsevier, New York, N.Y., 1968, p.144.

71. Escobi-Perez, J.R.; Nome, F.; Fendler, J.H. J. Am. Chem. Soc. 1977, 99, 7749.

72. Moroi, Y.; Infelta, P.P.; and Grätzel, M. ibid. 1979, 101, 573.

73. Moraczewski, J. and Geiger, Jr., W.E. ibid. 1978, 100, 7431.

74. Alkaitis, S.A. and Grätzel, M. ibid. 1975, 97, 5723.

75. Thomas, J.K. and Piciulo, P. ibid. 1978, 100, 3419.

76. Tsutsui, Y.; Takuma, K.; Nishijma, T.; and Matsuo, T. Chem. Lett. 1979, 617.

77. Alkaitis, S.A. and Grätzel, M. J. Am. Chem. Soc. 1976, 98, 3549.
78. Bunton, C.A.; Cerichelli, G.; Ihara, Y.; and Sepulveda, L. ibid. 1979, 101, 2429.
79. Schmehl, R.H. and Whitten, D.G. ibid. 1980, 102, 1938.
80. Katušin-Ražem, B.; Wong, M.; and Thomas, J.K. ibid. 1978, 100, 1679.
81. Takuma, K.; Kajiwara, M.; and Matsuo, T. Chem. Lett. 1977, 1199.
82. Lachish, U.; Ottolenghi, M.; and Rabani, J. J. Am. Chem. Soc. 1977, 99, 8062.
83. Nagle, J.K.; Young, R.C.; and Meyer, T.J. Inorg. Chem. 1977, 16, 3366.
84. Creutz, C. and Sutin, N. J. Am. Chem. Soc. 1976, 98, 6384.
85. Fendler, J.H. Acc. Chem. Res. 1976, 9, 153.
86. Kano, K.; Romero, A.; Djermouni, B.; Ache, H.J.; and Fendler, J.H. J. Am. Chem. Soc. 1979, 101, 4030.
87. Escobi-Perez, J.R.; Romero, A.; Lukac, S.; and Fendler, J.H. ibid. 1979, 101, 2231.
88. Infelta, P.P.; Grätzel, M.; and Fendler, J.H. ibid. 1980, 102, 1479.
89. Tran, C.D.; Klahn, P.L.; Romero, A.; and Fendler, J.H. ibid. 1978, 100, 1622.
90. Jonah, C.D.; Matheson, M.S.; and Meisel, D. J. Phys. Chem. 1979, 83, 257.

91. Meisel, D. and Matheson, M.S. J. Am. Chem. Soc. 1977, 99, 6577.

92.a)Taha, I. and Morawetz, H. J. Polym. Sci., Part A-2. 1971, 9, 1669.

b)Taha, I. and Morawetz, H. J. Am. Chem. Soc. 1971, 93, 829.

93. Clear, J.M.; Kelly, J.M.; Pepper, D.C.; and Vos, J.G. Inorg. Chim. Acta. 1979, 33, L 139.

94. Gafney, H.D. unpublished observations, 1974.

95. Elmer, T.H. and Felner, A. Corning Glass Co., private communication, 1977-1978.

96. Elmer, T.H.; Nordberg, M.E.; Carrier, G.B.; and Korda, E.J. J. Am. Ceram. Soc. 1970, 53, 171 and references there in.

97.a)Sakairo, T. Hyomen. 1971, 9, 115.

b)Pierce Chemical Co., General Catalogue, 1976-77, p.215, Pierce Chemical Co., Box 117, Rockford, Ill. 61105.

98. Spatorico, A.L. J. Appl. Polym. Sci. 1975, 12, 1601.

99. Burwell, Jr., R.L. Chemtech. 1974, 370.

100. Bazant, V.; Chvalovsky, V.; and Rathovsky, J. Organosilicon Compounds, Academic Press, New York, N.Y., 1965.

101. Melamud, E.; Reisner, M.G.; and Garbatski, U. J. Phys. Chem. 1973, 77, 1023.

102. Piciulo, P.L. and Sutherland, J.W. J. Am. Chem. Soc. 1979, 101, 3123.

103. Palmer, R.C. and Piper, T.S. Inorg. Chem. 1966, 5, 864.

104. Gafney, H.D. unpublished observation, 1974.

105. Vogel, A.I. Quantitative Inorganic Analysis, Third Ed. John Wiley and Sons, Inc., New York, N.Y., 1961, p.972.

106. Bricker, C.E. and Vail, W.A., Analyt. Chem. 1950, 22, 720.

107. Brauer, G., ed. Handbook of Preparitive Inorganic Chemistry, Vol II, Second Ed., Academic Press, New York, N.Y., 1965, p.1562.

108. Hipps, K.W. and Crosby, G.A. J. Am. Chem. Soc. 1975, 97, 7042.

109. Klassen, D.M. and Crosby, G.A. Chem. Phys. Lett. 1967, 1, 127.

110. Mayoh, B. and Day, P. Theoret. Chim. Acta. 1978, 49, 259.

111. Klassen, D.M. and Crosby, G.A. J. Chem. Phys. 1968, 48, 1853.

112. Hager, G.D. and Crosby, G.A. J. Am. Chem. Soc. 1975, 97, 7031.

113. The large spin orbit coupling of the Ru(II) ion, atomic number = 44, makes this assignment approximate but the term is used because these are the states to which it is correlated.

a)Crosby, G.A.; Hipps, K.W.; and Elfring, Jr., H.W. ibid. 1974, 96, 629.

b)Harrigan, R.W.; Hager, G.D.; and Crosby, G.A. Chem. Phys. Lett. 1973, 21, 487.

114. Basolo, F. and Pearson, R.G. Mechanisms of Inorganic Reactions, John Wiley and Sons, Inc., New York, N.Y., 1958, p.34 and references therein.

115. Gutowsky, H.S. and Saika, A. J. Chem. Phys. 1953, 21, 1688.

116. Olson, A.R. and Simonson, T.R. ibid. 1949, 17, 1167.

117. Schwartzenbach, G. and Heller, J. Helv. Chim. Acta. 1951, 34, 576.

118. Fischer, R.B. and Peters, D.G. Quantitative Chemical Analysis, W.B. Saunders Co., Philadelphia, 1968, p.416.

119.a)Kosower, E.M. and Cotter, J.F. J. Am. Chem. Soc. 1964, 86, 5524.

b)Corwin, A.H.; Arellano, R.R.; and Chivvis, A.B. Biochim. Biophys. Acta. 1968, 162, 533.

120. Baxendale, J.H. and Fiti, M. J. Chem. Soc. Dalton Trans. 1972, 1995.

121. Saji, T. and Aoyagui, S. Electroanalytical Chem. and Interfacial Chem. 1975, 58, 401.

122. Mulazzani, Q.G.; Emmi, S.; Fuochi, P.G.; Venturi, M.; and Hoffman, M.Z. J. Am. Chem. Soc. 1978, 100, 981.

123. Mahon, C. and Reynolds, W.L. Inorg. Chem. 1966, 5, 931.

124. Hoggard, P.E. and Porter, G.B. J. Am. Chem. Soc. 1978, 100, 1457.

125. Bjerrum, N. Kgl. Danske Videnskab. Selskab Mat. fys. Medd. 1926, 9, 7.

126. Denison, J.T. and Ramsay, J.B. J. Am. Chem. Soc. 1955, 77, 2615.

127. Gafney, H.D. unpublished observations, 1980.

128. Meisel, D.; Matheson, M.S.; Mulac, W.A.; and Rabani, J. J. Phys. Chem. 1977, 81, 1449.

129. Binder, M. and Gafney, H.D. unpublished observations, 1978.